



RC-1429, COG-I-95-150

**Verification and Validation of the ORIGEN-S  
Code and Nuclear Data Libraries**

I.C. Gauld, K.A. Litwin

**1995 August**

## **DISCLAIMER**

Copyright © 1995 Atomic Energy of Canada Limited

Atomic Energy of Canada Limited (AECL) has approved posting of this document on the Oak Ridge National Laboratory SCALE website with the understanding that it has not been edited for wide publication. This report is not to be listed in abstract journals. If it is cited as a reference, the source from which copies may be obtained should be given as: Scientific Document Distribution Office (SDDO), AECL, Chalk River, Ontario, Canada K0J 1J0.

RC-1429  
COG-I-95-150

AECL

VERIFICATION AND VALIDATION OF THE ORIGEN-S CODE  
AND NUCLEAR DATA LIBRARIES

by

I.C. Gauld and K.A. Litwin

This report is part of Work Package 2503 carried out under COG Working Party 25. The work was performed and archived in accordance with the Software Quality Assurance Policies and Procedures of the Research-Reactor Technology Branch described in RC-2000-063.

Research-Reactor Technology Branch  
Whiteshell Laboratories  
Pinawa, Manitoba R0E 1L0  
1995

AECL

VERIFICATION AND VALIDATION OF THE ORIGEN-S CODE  
AND NUCLEAR DATA LIBRARIES

by

I.C. Gauld and K.A. Litwin

ABSTRACT

This report documents a verification and validation study of the isotope generation and depletion code ORIGEN-S and its associated nuclear data libraries. The validation study covers the principal areas of code and nuclear data application: the prediction of 1) used-fuel nuclide inventories, 2) decay heat, and 3) neutron and gamma radiation source spectra. The validation study has made use of experimental data to benchmark the code and nuclear data, and includes a large number of measurements performed on irradiated CANDU reactor fuel. Where experimental data are not available for direct comparisons with predictions, calculations were compared against well-established standards, and against the validated results of independent codes and nuclear data. ORIGEN-S predicts the benchmark results, generally within the benchmark uncertainty, demonstrating that the code accurately models a broad spectrum of problems to which it is typically applied.

VALUE AND IMPLICATIONS

The Software Quality Assurance Standard CSA N286.7 is currently being implemented by the Canadian nuclear industry, and demonstrating conformance with the Standard will be a regulatory requirement. The Standard demands that rigorous procedures and documentation are in place that assures the software used in safety-related analyses for nuclear power plants is verified and validated for the range of applications for which it is intended. This document presents a series of benchmark calculations designed to verify and validate the ORIGEN-S code and associated nuclear data libraries for the types of applications routinely required by the industry. It is also designed to fulfil the documentation requirements established in CSA N286.7 for code validation and verification.



R.F. Lidstone  
Branch Manager

TABLE OF CONTENTS

1	INTRODUCTION	1
2	SUMMARY OF BENCHMARK STUDIES	3
3	ORIGEN-S NUCLEAR DATA LIBRARIES	3
4	ORNL AND LANL MULTICODE COMPARISONS	5
	4.1 Description of the Verification Benchmarks . . . . .	8
	4.2 Summary of Results . . . . .	8
5	NEA INTERNATIONAL CODE COMPARISON	9
	5.1 <sup>235</sup> U Fission Pulse . . . . .	11
	5.2 Extended <sup>235</sup> U Irradiation and Decay . . . . .	17
	5.3 Summary of Results . . . . .	24
6	USED-FUEL NUCLIDE INVENTORY BENCHMARK STUDIES	25
	6.1 NPD Reactor Fuel Study . . . . .	25
	6.1.1 Description of the Benchmark . . . . .	25
	6.1.2 Results . . . . .	27
	6.2 Bruce-A Reactor Fuel Study . . . . .	28
	6.2.1 Description of the Benchmark . . . . .	28
	6.2.2 Results . . . . .	28
	6.3 Pickering-A Reactor Fuel Study . . . . .	29
	6.3.1 Description of the Benchmark . . . . .	29
	6.3.2 Results . . . . .	32
	6.4 NEA Benchmark on PWR Isotopic Prediction . . . . .	36
	6.4.1 Description of the Benchmark . . . . .	36
	6.4.2 Results . . . . .	37
7	ANSI/ANS-5.1 DECAY HEAT CALCULATIONAL BENCHMARK	40
	7.1 Description of the Benchmark . . . . .	40
	7.2 Implementation of the ANS-5.1-1979 Standard . . . . .	41
	7.3 Results . . . . .	43
8	DOUGLAS POINT CANDU FUEL DECAY HEAT STUDY	49
	8.1 Description of the Douglas Point Fuel Measurements . . . . .	50
	8.2 Gamma Energy Leakage . . . . .	55
	8.3 Calculations using the ANSI/ANS-5.1-1979 Standard . . . . .	57
	8.4 Calculations using the ORIGEN-S Code . . . . .	57
	8.5 Summary of Douglas Point Fuel Decay Heat Study . . . . .	57
9	<sup>235</sup> U AND <sup>239</sup> Pu FISSION PRODUCT ENERGY RELEASE BENCHMARK	62
	9.1 Description of the ORR Experiments . . . . .	62
	9.2 <sup>235</sup> U Results . . . . .	63
	9.3 <sup>239</sup> Pu Results . . . . .	63

9.4 Summary of the Energy Release Studies . . . . .	72
10 RADIATION SOURCE SPECTRA BENCHMARK	72
10.1 Gamma Source Spectra . . . . .	73
10.2 Neutron Source Spectra . . . . .	77
10.3 Summary of Source Term Studies . . . . .	79
11 CONCLUSIONS	81
REFERENCES	81
DISTRIBUTION LIST	84

LIST OF FIGURES

1	Intercomparison of Total Decay Heat Predictions for the Extended $^{235}\text{U}$ Irradiation NEA Numerical Benchmark Problem. . . . .	23
2	The Maximum Correction Factor for Neutron Capture in Fission Products $G_{max}(t)$ as a Function of Cooling Time Since Irradiation as Prescribed by the ANSI/ANS-5.1-1979 Decay Heat Standard. . . . .	44
3	Comparison of Fission Product Decay Heat Predictions by ORIGEN-S and the ANS-5.1-1979 Standard for CANDU Reactor Fuel with a Low Burnup of 505 GJ/kgU. . . . .	45
4	Comparison of Fission Product Decay Heat Predictions by ORIGEN-S and the ANS-5.1-1979 Standard for CANDU Reactor Fuel with a Mid-Range Burnup of 685 GJ/kgU. . . . .	46
5	Comparison of Fission Product Decay Heat Predictions by ORIGEN-S and the ANS-5.1-1979 Standard for CANDU Reactor Fuel with a High Burnup of 1045 GJ/kgU. . . . .	47
6	Comparison of Fission Product, Actinide, and Total Decay Heat Predictions by ORIGEN-S with the ANS-5.1-1979 Standard for 685 GJ/kgU Burnup CANDU Reactor Fuel. . . . .	48
7	Comparison of the Measured and Calculated Decay Heat from Douglas Point Reactor Fuel. . . . .	61
8	Comparison of the Measured and Calculated Beta Energy Release Rates Following a Fission Pulse of $^{235}\text{U}$ . . . . .	66
9	Comparison of the Measured and Calculated Gamma Energy Release Rates Following a Fission Pulse of $^{235}\text{U}$ . . . . .	67
10	Comparison of the Measured and Calculated Beta Energy Release Rates Following a Fission Pulse of $^{239}\text{Pu}$ . . . . .	70
11	Comparison of the Measured and Calculated Gamma Energy Release Rates Following a Fission Pulse of $^{239}\text{Pu}$ . . . . .	71
12	Comparison of the Gamma Energy Spectra Calculated by ORIGEN-S, France using the Apollo Code, and UK-BNFL using the FISPIN Code, for PWR Fuel Assembly 5 At Mid-Height. . . . .	76

LIST OF TABLES

1	Description of the ORIGEN-S Benchmark Studies . . . . .	4
2	Summary of Nuclear Data Tested by Validation Studies . . . . .	5
3	Nuclide Inventory Benchmark Validation Matrix . . . . .	6
4	Sources of Multigroup Cross-Section Data . . . . .	7
5	List of Contributing Institutes in NEA Decay Heat Benchmark . . . . .	10
6	Total Decay Heat Results in MeV/s/fission for a <sup>235</sup> U Fission Pulse Given at Cooling Times from 1 to 10 <sup>13</sup> Seconds . . . . .	12
7	Beta Decay Heat Results in MeV/s/fission for a <sup>235</sup> U Fission Pulse Given at Cooling Times from 1 to 10 <sup>13</sup> Seconds . . . . .	13
8	Gamma Decay Heat Results in MeV/s/fission for a <sup>235</sup> U Fission Pulse Given at Cooling Times from 1 to 10 <sup>13</sup> Seconds . . . . .	14
9	Fission Product Contribution as a Percentage of the Total Decay Heat for a <sup>235</sup> U Fission Pulse After 10 Seconds . . . . .	15
10	Fission Product Contribution as a Percentage of the Total Decay Heat for a <sup>235</sup> U Fission Pulse After 10 <sup>6</sup> Seconds . . . . .	16
11	Fission Product Contribution as a Percentage of the Total Decay Heat for a <sup>235</sup> U Fission Pulse After 10 <sup>9</sup> Seconds . . . . .	16
12	Total Decay Heat Results in MeV/s/fission for a <sup>235</sup> U Irradiation Case Given at Cooling Times from 1 to 10 <sup>13</sup> Seconds . . . . .	18
13	Beta Decay Heat Results in MeV/s/fission for a <sup>235</sup> U Irradiation Case Given at Cooling Times from 1 to 10 <sup>13</sup> Seconds . . . . .	19
14	Gamma Decay Heat Results in MeV/s/fission for a <sup>235</sup> U Irradiation Case Given at Cooling Times from 1 to 10 <sup>13</sup> Seconds . . . . .	20
15	Fission Product Contribution as a Percentage of the Total Decay Heat for a <sup>235</sup> U Irradiation Case After 10 <sup>4</sup> Seconds . . . . .	21
16	Fission Product Contribution as a Percentage of the Total Decay Heat for a <sup>235</sup> U Irradiation Case After 10 <sup>8</sup> Seconds . . . . .	22
17	Specifications for the NPD Fuel Inventory Calculations . . . . .	26
18	Measured and Calculated Atom Ratios for NPD Fuel Study . . . . .	27
19	Experimental Fuel Analysis Results for Bruce-A Bundle F21037C . . . . .	29
20	Material and Lattice Specifications for the Bruce-A Fuel Inventory Calculations . . . . .	30
21	Specifications for the Bruce-A Bundle F21037C Bundle Irradiation History . . . . .	31
22	Measured and Calculated Atom Percents for Bruce-A Fuel Inventory Study . . . . .	31
23	Specifications for the Pickering-A Fuel Inventory Calculations . . . . .	33
24	Specifications for the Pickering-A Outer Fuel Element Irradiation History . . . . .	34
25	Measured and Calculated U and Pu Inventories in the Pickering-A Fuel Study . . . . .	34
26	Measured and Calculated Isotopic Activities in the Pickering-A Fuel Study . . . . .	35
27	Specifications for the ATM-104 PWR Fuel Inventory Calculations . . . . .	38
28	Specifications for the ATM-104 Assembly Irradiation History . . . . .	38
29	Comparison of Calculated and Reference PWR Fuel Inventories . . . . .	39
30	CANDU Reactor Fuel Fission Fractions . . . . .	42
31	Douglas Point Fuel Bundle Irradiation Histories . . . . .	51
32	Summary of Measured Decay Heat Data and Correction Factors . . . . .	56

33	ANS-5.1 Decay Heat Standard Results for Douglas Point Fuel . . . . .	58
34	Decay Heat for Douglas Point Fuel Calculated using ORIGEN-S . . . . .	59
35	Summary of Douglas Point Fuel Measured and Calculated Decay Heat . . . . .	60
36	$^{235}\text{U}$ Beta-ray Energy Release . . . . .	64
37	$^{235}\text{U}$ Gamma-ray Energy Release . . . . .	65
38	$^{239}\text{Pu}$ Beta-ray Energy Release . . . . .	68
39	$^{239}\text{Pu}$ Gamma-ray Energy Release . . . . .	69
40	Specifications for PWR Assembly Gamma Benchmark Calculations . . . . .	74
41	PWR Assembly Gamma Benchmark Irradiation History . . . . .	74
42	Calculated Gamma Source Spectra for Fuel Assembly 5 at Mid-Height with a Burnup of 19461 MWd/MgU. . . . .	75
43	Specifications for PWR Assembly used in Neutron Benchmark Calculations . . . . .	78
44	PWR Assembly Irradiation History used in Neutron Benchmark . . . . .	78
45	Calculated Neutron Source Terms for Fuel Assembly 12 at Mid-Height with a Burnup of 38893 MWd/MgU . . . . .	80
46	Calculated Actinide Content for Fuel Assembly 12 at Mid-Height with a Burnup of 38893 MWd/MgU . . . . .	80

## 1 INTRODUCTION

This report presents a series of benchmark calculations using the ORIGEN-S code [1] designed to assess the performance and the accuracy of the code and nuclear data libraries for use in routine applications within the Canadian nuclear industry. ORIGEN-S is an isotope generation and depletion code used in nuclear safety-related analyses to calculate time-dependent isotopic inventories in irradiated nuclear reactor fuel and activated components, and associated quantities including decay heat, and neutron and gamma radiation spectra. The code also provides methods that integrate time-dependent quantities such as source terms and decay heat, and includes methods that model fuel reprocessing.

Code and data benchmarking is becoming increasingly important within the nuclear industry, as analyses used in safety-related and design studies are increasingly reliant on computer software and software applications. The software quality assurance standards document CAN/CSA N286.7 [2], recently released by the Canadian Standards Association covering the development and use of safety-related computer programs for nuclear power plants, is currently being implemented within the Canadian nuclear industry. Demonstrating compliance with the new standard will be required by the Canadian nuclear regulatory agency, and will require upgrading code and data validation and documentation for a number of software applications.

Benchmarks provide a standard against which the performance and accuracy of a code and nuclear data libraries can be assessed. This study documents a series of both experimental and numerical (calculational) benchmarks aimed at demonstrating code verification and validation, as described in the CSA N286.7 Standard. Verification and validation pertain to:

- verifying that the numerical methods of the code perform correctly,
- verifying that the nuclear data used by the code are accurate, and
- verifying that the code and nuclear data predict accurate results over the range of applications and systems for which they are intended.

The ORIGEN-S code is a module of the larger SCALE [3] (Standardized Computer Analyses for Licensing Evaluations) computational system, developed and maintained under a configuration management plan [4] by Oak Ridge National Laboratory (ORNL). The code has been extensively validated and verified by the code developers and through years of international experience with the code in routine applications, analysis of measurements and benchmarks, and code comparison

studies. Improvements in the code and nuclear data libraries, combined with the requirement to produce software documentation with the traceability demanded by the new quality assurance procedures has led to a complete review, and for the most part, re-analysis of previously reported ORIGEN-S benchmarks using the new version of the code and nuclear data.

All calculations using ORIGEN-S presented in this document were performed with the version of the code and nuclear data libraries released with SCALE-4.2, designated and controlled by the Computing Applications Division (CAD) Nuclear Engineering Applications Section (NEAS) at ORNL. The calculations were performed on an IBM RS/6000 computer.

The verification studies involve comparisons of the ORIGEN-S results with a wide array of other codes that use both similar numerical methods, and codes that use independent methods including analytical solutions. Validation is performed with benchmarks involving either validated standards, experimental measurements, or other validated codes designed to perform similar types of analyses. Available benchmarks relevant to the pressurized heavy water CANDU<sup>1</sup> reactor system are also included. Nuclear data testing involved a combination of code and nuclear database comparisons, and benchmarking against experiments that test selected parts of the nuclear data libraries.

Many of the validation studies performed as part of this report involved the use of problem-dependent neutron cross sections to accurately represent the different nuclear systems during the fuel depletion (irradiation) analysis. Special cross-section libraries were generated for each specific benchmark using the WIMS-AECL transport code [5, 6], and a combination of ENDF/B-IV, -V, and VI evaluated nuclear data for over 200 isotopes. These ORIGEN-S libraries are not of general interest for production applications. The system used to create the ORIGEN-S libraries, and the sources of the nuclear data, are outlined in this report. The report does not address validation of the problem-dependent cross-section libraries that have been developed for specific systems (e.g., LWR or CANDU reactor specific libraries) that may be distributed with the code for production analyses. Validation of production cross-section libraries is documented in separate reports since the cross-section data will be different than those used in this study.

Nuclear data, including decay constants, branching fractions, fission product yields, and cross sections, are an integral part of the ORIGEN-S code as they determine the nuclide transition rates used in the equations that ORIGEN-S solves. Testing the code generally involves simultaneously testing the nuclear data libraries. The nuclear data validated in the present study include the problem-independent aspects of the library: 1) the decay data which includes decay constants, branching fractions, and energy release, 2) fission product yields, and 3) neutron and photon source term data. Also included are the cross sections for the isotopes not updated with problem-dependent sets. These data are generally common to all ORIGEN-S libraries.

The validation of any code is an ongoing process. This study is aimed at verifying the performance of the numerical aspects of the code, and validating the code and nuclear data over a range of applications for which it is typically subjected by the Canadian nuclear industry, using a series of benchmark problems. It is intended to serve as a baseline verification and validation document.

---

<sup>1</sup>CANada Deuterium Uranium, a registered trademark of Atomic Energy of Canada Ltd.

Validation of the code and data for applications that fall outside the range documented in this work is the responsibility of the code user. Further validation studies will be indicated where experimental or numerical benchmark quality data needs to be improved.

## 2 SUMMARY OF BENCHMARK STUDIES

The verification and validation of the ORIGEN-S code and nuclear data libraries is accomplished through a combination of intercode comparisons, comparisons of code results against well established standards, and benchmarking of calculated results against measurements. Table 1 gives an overview of the verification and validation benchmark studies performed or cited in this document, the type of system analyzed, and the principal quantities evaluated. The benchmarks involved numerical code and data comparisons, and comparisons against experimental data.

A list of the nuclear data in the ORIGEN-S libraries tested by each of the validation benchmark problems performed as part of this report is summarized in Table 2. A matrix of the nuclides covered in each of the nuclide inventory benchmarks (NPD, Bruce-A, Pickering-A, and PWR/NEA studies) is listed in Table 3.

## 3 ORIGEN-S NUCLEAR DATA LIBRARIES

The base ORIGEN-S nuclear decay data, cross sections and fission product yield libraries used in the present studies, unless indicated otherwise, are from the SCALE-4.2 system release and are described in detail elsewhere [7]. In summary, all fission product yields are derived from ENDF/B-V, nuclear decay and energy data is based mainly on ENDF/B-VI and ENSDF, and photon production data is from the Oak Ridge National Laboratory Master Photon Data Base and an ENDF/B-IV data base. The cross sections provided with the base library are largely based on ENDF/B-IV for the nuclides in that evaluation, with updating with ENDF/B-V cross sections for some important nuclides.

Accurate depletion analyses require that the standard cross sections in the ORIGEN-S library are updated with problem-dependent data that has been derived for the system being analyzed. In addition, it may be important to update the cross sections during the depletion analysis to account for changes in composition and neutron flux with burnup.

For the present benchmark calculations, problem- and burnup-dependent cross-section sets were generated using a code system [8] that couples the WIMS-AECL two-dimensional (2-D) transport code with the ORIGEN-S depletion code. Cross sections are compiled from two sources: 1) the AMPX format ENDF/B-IV 27-group burnup library used in SCALE, and 2) the WIMS-AECL 89-group library. Cross sections from WIMS-AECL are only available for fission, capture, and (n,2n) reactions. All other reaction types and processes were obtained from the AMPX 27-group library. The present study used a special hybrid WIMS-AECL cross-section library containing mainly

Table 1: Description of the ORIGEN-S Benchmark Studies

Problem Number	Type	Quantities Calculated	Description
1,2	Calculational (Cited)	Mass inventory, activity, decay heat, source terms, and energy spectra	A code verification study involving comparisons of ORIGEN-S, ORIGEN2, and CINDER-2 for decay-only and LWR fuel irradiations. Cited results only.
3	Calculational	Decay heat	An NEA <sup>†</sup> international code verification study involving ten different fuel depletion codes. All of the codes use an identical nuclear data base specified in the study.
4	Experimental	U and Pu inventories	Validation of code predictions against measured isotopics for NPD CANDU reactor fuel.
5	Experimental	U and Pu inventories	Validation of code predictions against measured isotopics for Bruce-A CANDU reactor fuel.
6	Experimental	Actinide and fission product inventories	Validation of nuclide inventory predictions in CANDU Pickering-A reactor fuel.
7	Experimental/ Calculational	Actinide and fission product inventories	Measurements in PWR fuel test material ATM-104, and calculated nuclide inventories in an NEA numerical code comparison.
8	Calculational	Decay heat	Validation against the ANS-5.1-1979 decay heat standard for times ranging from discharge to about 30 years.
9	Experimental	Decay heat	Measured data from Douglas Point CANDU fuel at intermediate cooling times (several years).
10	Experimental	Decay heat	Burst irradiation measurements of <sup>235</sup> U and <sup>239</sup> Pu at short cooling times (2 seconds to 4 hours).
11	Calculational/ Experimental	Source terms	Comparison of neutron and photon source terms and energy spectra for an irradiated PWR fuel assembly against validated predictions of other codes in an NEA shielding code benchmark.

<sup>†</sup> Nuclear Energy Agency.

Table 2: Summary of Nuclear Data Tested by Validation Studies<sup>†</sup>

Problem Number	Report Sect.	Cross Sections	Decay Data	F.P. Yields		Energy Release	Source Terms	
				<sup>235</sup> U	<sup>239</sup> Pu		Photon	Neutron
1	4	C	C	C	C	C		
2	4	C	C	C	C		C	C
3	5	X	X	X				
4	6	X	X	X	X			
5	6	X	X	X	X			
6	6	X	X	X	X			
7	6	X	X	X	X			
8	7	X	X	X	X	X		
9	8	X	X	X		X		
10	9		X	X	X	X		
11	10	X	X	X	X		X	X

<sup>†</sup> Indicates results from present study (X) or cited (C) from other publications.

ENDF/B-V cross sections, supplemented with ENDF/B-VI cross sections for a number of nuclides not previously available with the ENDF/B-V library. In addition, ENDF/B-V cross sections for <sup>154</sup>Eu and <sup>155</sup>Eu were replaced with new ENDF/B-VI data which have been demonstrated to be yield better inventory predictions [9, 10]. A total of over 200 nuclides with multigroup cross sections were applied to ORIGEN-S library updating. The nuclides and the source of evaluated cross-section data are listed in Table 4.

The ORIGEN-S libraries used in all calculations contained the same nuclear decay data, fission product yields, and photon production libraries as the base ORIGEN-S libraries in SCALE-4.2. Updating of the library was only performed on the cross-section data in order that they more accurately reflect the specific nuclear systems being analyzed in the benchmark calculations.

#### 4 ORNL AND LANL MULTICODE COMPARISONS

Two separate code comparison studies were published in a cooperative effort between Oak Ridge National Laboratory (ORNL) and Los Alamos National Laboratory (LANL) involving multicode comparisons using ORIGEN-S, ORIGEN2 [11] and CINDER-2 [12]. The objective of these studies was to verify the predictive capabilities of the codes in terms of the numerical methods and the nuclear data used. The results of these verification studies are cited and summarized here.

Table 3: Nuclide Inventory Benchmark Validation Matrix<sup>†</sup>

Isotope	Bruce-A	NPD	Pickering-A	PWR/NEA
<sup>234</sup> U			X	X
<sup>235</sup> U	X	X	X	X
<sup>236</sup> U	X		X	X
<sup>238</sup> U	X	X	X	X
<sup>238</sup> Pu			X	X
<sup>239</sup> Pu	X	X	X	X
<sup>240</sup> Pu	X	X	X	X
<sup>241</sup> Pu	X	X	X	X
<sup>242</sup> Pu	X	X	X	X
<sup>3</sup> H			X	
<sup>79</sup> Se				X
<sup>90</sup> Sr			X	
<sup>95</sup> Mo				N
<sup>99</sup> Tc			X	X
<sup>103</sup> Ru				N
<sup>106</sup> Ru			X	
<sup>125</sup> Sb			X	X
<sup>126</sup> Sn				X
<sup>129</sup> I			X	
<sup>133</sup> Cs				X
<sup>134</sup> Cs			X	
<sup>135</sup> Cs				X
<sup>137</sup> Cs			X	X
<sup>143</sup> Nd				N
<sup>145</sup> Nd				N
<sup>147</sup> Sm				N
<sup>149</sup> Sm				N
<sup>150</sup> Sm				N
<sup>151</sup> Sm				N
<sup>152</sup> Sm				N
<sup>153</sup> Eu				N
<sup>154</sup> Eu			X	
<sup>155</sup> Eu			X	
<sup>155</sup> Gd				N
<sup>237</sup> Np			X	X
<sup>241</sup> Am			X	X
<sup>244</sup> Cm			X	

<sup>†</sup> Experimental (X) and numerical (N) comparisons are indicated.

Table 4: Sources of Multigroup Cross-Section Data

Isotope	ENDF/B Version								
CO-59	V	TC-99	V	TE-123	VI	ND-145	V	RE-185	VI
GE-72	IV	RU-99	IV	TE-124	VI	ND-146	V	RE-187	VI
GE-73	IV	RU-100	VI	TE-125	VI	ND-147	V	AU-197	V
GE-74	IV	RU-101	V	TE-126	VI	ND-148	V	TH-232	V
GE-76	IV	RU-102	VI	TE-127M	VI	ND-150	V	PA-233	V
AS-75	IV	RU-103	V	TE-128	VI	PM-147	V	U-233	V
SE-76	VI	RU-104	VI	TE-129M	VI	PM-148	V	U-234	V
SE-77	VI	RU-105	VI	TE-130	V	PM-149	V	U-235	V
SE-78	VI	RU-106	VI	TE-132	IV	PM-151	V	U-236	V
SE-80	VI	RH-103	V	I-127	V	SM-147	V	U-238	V
SE-82	VI	RH-105	V	I-129	VI	SM-148	V	NP-237	V
BR-79	IV	PD-104	VI	I-130	VI	SM-149	V	PU-238	V
BR-81	IV	PD-105	V	I-131	V	SM-150	V	PU-239	V
KR-80	VI	PD-106	VI	I-135	V	SM-151	V	PU-240	V
KR-82	VI	PD-107	VI	XE-128	VI	SM-152	V	PU-241	V
KR-83	V	PD-108	V	XE-129	VI	SM-153	V	PU-242	V
KR-84	V	PD-110	VI	XE-130	VI	SM-154	VI	AM-241	V
KR-85	VI	AG-107	IV	XE-131	V	EU-151	VI	AM-243	V
KR-86	VI	AG-109	V	XE-132	VI	EU-152	VI	CM-244	VI
RB-85	VI	AG-111	IV	XE-133	V	EU-153	VI		
RB-86	VI	CD-108	IV	XE-134	VI	EU-154	VI		
RB-87	VI	CD-110	IV	XE-135	V	EU-155	VI		
SR-86	VI	CD-111	IV	XE-136	VI	EU-156	VI		
SR-87	VI	CD-112	V	CS-133	V	EU-157	VI		
SR-88	VI	CD-113	V	CS-134	V	GD-154	VI		
SR-89	VI	CD-114	IV	CS-135	V	GD-155	V		
SR-90	VI	CD-115M	IV	CS-136	VI	GD-156	VI		
Y-89	VI	CD-116	IV	CS-137	VI	GD-157	V		
Y-90	VI	IN-113	VI	BA-134	IV	GD-158	VI		
Y-91	IV	IN-115	V	BA-135	IV	GD-160	VI		
ZR-90	IV	SN-115	VI	BA-136	IV	TB-159	VI		
ZR-91	IV	SN-116	VI	BA-137	IV	TB-160	VI		
ZR-92	IV	SN-117	VI	BA-138	IV	DY-160	V		
ZR-93	IV	SN-118	VI	BA-140	IV	DY-161	V		
ZR-94	IV	SN-119	VI	LA-139	V	DY-162	V		
ZR-95	IV	SN-120	VI	LA-140	VI	DY-163	V		
ZR-96	IV	SN-122	VI	CE-140	VI	DY-164	V		
NB-93	V	SN-123	VI	CE-141	VI	HO-165	V		
NB-94	IV	SN-124	VI	CE-142	VI	ER-166	V		
NB-95	IV	SN-125	VI	CE-143	VI	ER-167	V		
MO-94	VI	SN-126	VI	CE-144	VI	LU-175	IV		
MO-95	V	SB-121	VI	PR-141	VI	LU-176	V		
MO-96	VI	SB-123	VI	PR-142	VI	TA-181	V		
MO-97	VI	SB-124	VI	PR-143	VI	W-182	IV		
MO-98	V	SB-125	VI	ND-142	VI	W-183	IV		
MO-99	VI	SB-126	VI	ND-143	V	W-184	IV		
MO-100	IV	TE-122	VI	ND-144	V	W-186	IV		

## 4.1 Description of the Verification Benchmarks

The first published study [13] from the study reported the results of the code predictions of mass inventories, activity, and decay heat, for several Light Water Reactor (LWR) models involving fuel depletion, and a case that involved using the codes in a decay-only mode. Comparisons were performed for 52 nuclides (actinides and fission products) of importance to the assessment of criticality and long-term waste management of irradiated fuel, for cooling times ranging from 30 days to  $10^4$  years. All codes used identical input data, and each used its own nuclear decay data, neutron and photon production data, and cross-section libraries.

The second published study [14] compared the neutron and photon source terms using the same codes and models used in the first study. The study provided a verification of the nuclide inventories important to radiation source term calculations, and verification of the respective neutron and photon data bases themselves. Aggregate neutron and photon source terms were compared for cooling times between 30 days and 100 years, while source spectra were compared for times of 5 and 50 years. The aggregate photon source terms are compared separately for actinide and fission products, and neutron source terms are compared separately for the spontaneous fission and ( $\alpha, n$ ) components.

The objective of the studies was to test the data-base libraries and code methodologies used by each code to characterize irradiated fuel. Both ORIGEN-S and ORIGEN2 use a matrix exponential method to solve the rate processes. To prevent numerical instabilities caused by widely varying transition rates in the exponential matrix, the codes use the Bateman equations to solve for the inventories of the short-lived isotopes. The analytical methods applied by the CINDER codes use an explicit solution to the Bateman equations for each chain of nuclides coupled through the decay or neutron transmutation processes, and therefore represents an independent solution to the verification problems.

## 4.2 Summary of Results

A detailed presentation and discussion of the results of the studies has been published [13, 14]. The calculations were not repeated in this study, but the major results and conclusions are summarized from the original reports.

The average deviation of the results for the decay-only case were within 1% for all codes up to a cooling time of 100 years, and increased to between 2 and 6% for times up to  $10^4$  years. All differences are related to the nuclear data libraries. Many differences are due to the source of the decay data (mainly ENDF/B-IV, ENDF/B-V, or ENSDF), while the majority of other differences are due to missing decay chains in the CINDER-2 library. Small differences in the data are shown to lead to significant discrepancies between codes.

The irradiation cases showed larger discrepancies than the decay-only case, due to differences in cross-section data used during the irradiation. The decay heat calculated by all codes does not differ from the average by more than 6% for all times. Within the first 50 years the fission product heat varies from the average by less than 2%. The  $^{235}\text{U}$  and  $^{239}\text{Pu}$  inventories are all within 5 and 3% of the average, respectively. The inventory of  $^{244}\text{Cm}$ , a dominant neutron source and decay heat component, agrees to within about 15% of the average.

Differences in the irradiation cases are a result of the widely differing sources of nuclear data (as in the decay-only case), and the methods for generating the cross sections (described in Reference [13]). The different sources of cross-section data included ENDF/B-IV and -V, the Livermore Laboratory LENDL library, and Savannah River Laboratory data. Additional variations were introduced by differences in the fission product yield data.

A subsequent comparison of aggregate photon production rates [14] showed agreement between the two ORIGEN code results of about 1% for the decay-only case and 3% for the irradiation cases, for cooling times up to 100 years, the maximum time in the comparison. Differences of over a factor of two are observed between the CINDER-2 and both ORIGEN calculations as a result of the CINDER-2 libraries not containing bremsstrahlung radiation. A comparison of photon spectra shows the differences are mainly below about 400 keV. When bremsstrahlung was removed from the ORIGEN-S calculations, the agreement between the codes (total photons) is better than 9%.

Total neutron source terms were generally within about 10% up to 100 years cooling times. A comparison of the neutron spectra was limited to ORIGEN-S and CINDER-2 since there is no capability in ORIGEN2 to calculate neutron spectra. The spectral shapes were found to be nearly identical, with the small differences attributed mainly to the calculated inventories.

In summary, aggregate quantities such as decay heat and total source terms, are in excellent agreement among all codes. Individual nuclides demonstrated larger discrepancies due primarily to the different nuclear data used by the codes, and not in the different numerical methods. The code intercomparison is useful in determining overall performance of the numerical methods and accuracy of the nuclear data libraries, and has provided a verification of the methods of the ORIGEN-S code and nuclear data libraries for typical applications. The use of widely different data sets in the calculations however makes it virtually impossible to separate the effects of the numerical methods from differences in the nuclear data. Numerical comparison problems also suffer from the lack of definitive values with which to compare the calculations and therefore evaluate the accuracy of the difference sources of data, underlining the importance of supplementing code comparisons with experimental benchmarks.

## 5 NEA INTERNATIONAL CODE COMPARISON

The Nuclear Energy Agency (NEA) Committee on Reactor Physics (CRP) and the NEA Nuclear Data Committee (NDC) initiated a decay heat code comparison in 1987 to compare the computational methods used by different codes that solve the generalized Bateman equations which describe

Table 5: List of Contributing Institutes in NEA Decay Heat Benchmark

Code	Method	Institute
AFPA	A	Moscow Engineering Physics Institute, USSR
CINDER-10	A	Los Alamos National Laboratory, USA
CINDER	A	Chinese Nuclear Data Center, China
DCHAIN	A	Japan Atomic Energy Research Institute, Japan
FISP6	A	National Power Nuclear, Berkeley, UK
INVENT	A	Studsvik Neutron Research Laboratory, Sweden
PEPIN	A	CEN Saclay, France
FISPIN	N	AEA Winfrith, UK
KORIGEN	N	Kernforschungszentrum Karlsruhe, Fed. Rep. of Germany
MECCYCO	N	CEA/CEN Cadarache, France
ORIGEN-S	N	Atomic Energy of Canada Ltd., Canada

nuclide generation and depletion during irradiation and cooling [15]. The objective of the computational benchmark was to verify that differences in the decay heat rates predicted by different codes were a result of differences observed in the nuclear data libraries used in the calculations and not the computational methods used by the codes.

In order to meet the objective, all fission product yields, capture cross sections, and nuclear decay data were specified in the benchmark for all calculations. The comparison is therefore a valuable verification of the computational aspects of isotope generation and depletion codes, and is independent of the differences in nuclear data used by the codes since common nuclear data was provided.

Two benchmark problems were specified for the study; 1) a  $^{235}\text{U}$  fission pulse (all results normalized to one fission) followed by decay for cooling times ranging from 1 to  $10^{13}$  seconds in decade increments, and 2) a long irradiation of  $^{235}\text{U}$  ( $3 \times 10^7$  seconds) followed by decay for the same cooling times used in the first benchmark. The first benchmark therefore tests the ability of the codes to use the fission product yield data and correctly treat the mass decay-chain algorithms. The second benchmark problem tests the ability of the codes to represent simultaneously neutron capture processes, production via fission yields, and nuclear decay processes.

Solutions to the benchmark problems are presented in the original report [15] for 11 different codes, 7 of which can be classed as analytical solutions to the Bateman equations, and 4 of which are numerical (summation) solutions. The contributing institutes are listed in Table 5, with the solution type (Aanalytical or Numerical) of the codes. Note that ORNL contributed results using an older version of ORIGEN-S. These are not included in this comparison, but have been replaced with the results generated during this study using the newer version of the code from the SCALE-4.2 code system.

Nuclear data for the benchmark was provided as a truncated set of 94 fission product nuclides in the heavy mass peak ( $A = 131 - 140$ ) of the  $^{235}\text{U}$  fission product yield curve. Decay data and

fission product yield data were derived from the Evaluated Nuclear Structure Data File (ENSDF) and provided in the format of the Evaluated Nuclear Data Files (ENDF). This data included half-lives, decay modes and branching fractions, and decay energies. Delayed neutron data (neutron production following beta decay) was also provided. Fission product yields were provided for the 94 fission products in ENDF format, and average one-group neutron capture cross sections were provided in a separate file.

The decay, fission product yield, and cross-section data were processed and reformatted into two ASCII files in the standard ORIGEN-S library formats [7]. Significant effort was put into ensuring that the five digit accuracy of the the fission yield and cross-section data in the benchmark library was retained in the ORIGEN-S libraries. A number of stable nuclei not specified in the benchmark had to be added to the library.

Calculated results are presented for the two benchmarks for beta (electron plus positron), gamma, and total heating as a function of cooling time. Only the heating from fission products (i.e. no actinide heating) was considered in the benchmark.

## 5.1 $^{235}\text{U}$ Fission Pulse

The fission pulse benchmark involved a burst irradiation of pure  $^{235}\text{U}$  followed by cooling up to  $10^{13}$  seconds. All results are normalized to one fission event. The ORIGEN-S fission product beta decay heat was calculated from the difference in the total heat and gamma heat. Since there are no alpha transitions in the benchmark database, this is a accurate assumption.

The total, beta, and gamma heating rate results are presented in Tables 6–8. The fission product nuclides contributing more than 1% of the total heating rate are also compared at cooling times of 10,  $10^5$ , and  $10^9$  seconds in Tables 9–11 respectively.

The agreement between the present ORIGEN-S results for the  $^{235}\text{U}$  fission pulse and the other code results reported in the benchmark is extremely good. All results are within  $\pm 0.1\%$  (the numerical accuracy of the ORIGEN-S methods [1]) of the average of the other code results. The contributions to the total decay heating by nuclide are in similarly good agreement with the other codes. The results have not been graphed since the differences between most of the codes results is so small.

The benchmark provides a rigorous verification of the code, and demonstrates that the numerical methods of ORIGEN-S produce results that are in agreement with other codes using similar and independent numerical methods for problems involving fission product yield and decay processes.

Table 6: Total Decay Heat Results in MeV/s/fission for a  $^{235}\text{U}$  Fission Pulse Given at Cooling Times from 1 to  $10^{13}$  Seconds

Code	Cooling Time (s)						
	1	10	$10^2$	$10^3$	$10^4$	$10^5$	$10^6$
AFPA	5.090-2 <sup>†</sup>	1.904-2	3.882-3	2.597-4	2.589-5	1.004-6	1.167-7
CINDER10	5.100-2	1.903-2	3.884-3	2.592-4	2.587-5	1.011-6	1.172-7
DCHAIN	5.093-2	1.903-2	3.883-3	2.591-4	2.587-5	1.004-6	1.167-7
FISP6	5.093-2	1.903-2	3.883-3	2.591-4	2.586-5	1.003-6	1.167-7
FISPIN	5.093-2	1.903-2	3.883-3	2.591-4	2.587-5	1.004-6	1.167-7
INVENT	5.094-2	1.906-2	3.890-3	2.596-4	2.591-5	1.006-6	1.169-7
KORIGEN	5.093-2	1.904-2	3.885-3	2.593-4	2.590-5	1.008-6	1.173-7
MECCYCO	5.093-2	1.903-2	3.882-3	2.591-4	2.586-5	1.004-6	1.166-7
PEPIN	5.093-2	1.903-2	3.883-3	2.591-4	2.587-5	1.004-6	1.167-7
ORIGEN-S	5.092-2	1.903-2	3.882-3	2.591-4	2.586-5	1.003-6	1.167-7

<sup>†</sup> Read as  $5.090 \times 10^{-2}$

Code	Cooling Time (s)						
	$10^7$	$10^8$	$10^9$	$10^{10}$	$10^{11}$	$10^{12}$	$10^{13}$
AFPA	3.095-10	3.403-11	1.761-11	2.424-14	3.555-17	3.525-17	3.234-17
CINDER10	3.095-10	3.403-11	1.761-11	2.424-14	3.555-17	3.525-17	3.234-17
DCHAIN	3.095-10	3.403-11	1.761-11	2.424-14	3.555-17	3.525-17	3.234-17
FISP6	3.096-10	3.400-11	1.759-11	2.423-14	3.552-17	3.522-17	3.231-17
FISPIN	3.096-10	3.403-11	1.761-11	2.424-14	3.555-17	3.525-17	3.234-17
INVENT	3.105-10	3.409-11	1.764-11	2.432-14	3.562-17	3.532-17	3.241-17
KORIGEN	3.101-10	3.414-11	1.766-11	2.432-14	3.556-17	3.526-17	3.235-17
MECCYCO	3.095-10	3.403-11	1.761-11	2.424-14	3.554-17	3.524-17	3.234-17
PEPIN	3.095-10	3.403-11	1.761-11	2.424-14	3.555-17	3.525-17	3.234-17
ORIGEN-S	3.094-10	3.402-11	1.760-11	2.424-14	3.556-17	3.525-17	3.235-17

Table 7: Beta Decay Heat Results in MeV/s/fission for a  $^{235}\text{U}$  Fission Pulse Given at Cooling Times from 1 to  $10^{13}$  Seconds

Code	Cooling Time (s)						
	1	10	$10^2$	$10^3$	$10^4$	$10^5$	$10^6$
AFPA	3.358-2	1.073-2	1.958-3	1.253-4	8.224-6	3.282-7	3.017-8
CINDER10	3.366-2	1.073-2	1.958-3	1.250-4	8.220-6	3.349-7	3.072-8
DCHAIN	3.359-2	1.073-2	1.958-3	1.249-4	8.198-6	3.282-7	3.017-8
FISP6	3.359-2	1.073-2	1.958-3	1.249-4	8.197-6	3.281-7	3.017-8
FISPIN	3.359-2	1.073-2	1.958-3	1.249-4	8.198-6	3.282-7	3.017-8
INVENT	3.359-2	1.074-2	1.962-3	1.252-4	8.216-6	3.289-7	3.023-8
KORIGEN	3.359-2	1.073-2	1.959-3	1.251-4	8.227-6	3.290-7	3.032-8
MECCYCO	3.359-2	1.072-2	1.957-3	1.249-4	8.197-6	3.282-7	3.016-8
PEPIN	3.359-2	1.073-2	1.958-3	1.249-4	8.198-6	3.282-7	3.017-8
ORIGEN-S	3.358-2	1.072-2	1.958-3	1.250-4	8.191-6	3.281-7	3.019-8

Code	Cooling Time (s)						
	$10^7$	$10^8$	$10^9$	$10^{10}$	$10^{11}$	$10^{12}$	$10^{13}$
AFPA	7.776-11	1.034-11	5.351-12	7.393-15	3.555-17	3.525-17	3.234-17
CINDER10	7.778-11	1.034-11	5.351-12	7.393-15	3.555-17	3.525-17	3.234-17
DCHAIN	7.778-11	1.034-11	5.351-12	7.393-15	3.555-17	3.525-17	3.234-17
FISP6	7.779-11	1.033-11	5.347-12	7.390-15	3.552-17	3.522-17	3.231-17
FISPIN	7.779-11	1.034-11	5.351-12	7.393-15	3.555-17	3.525-17	3.234-17
INVENT	7.772-11	1.036-11	5.361-12	7.416-15	3.548-17	3.532-17	3.241-17
KORIGEN	7.794-11	1.036-11	5.362-12	7.440-15	3.537-17	3.507-17	3.218-17
MECCYCO	7.777-11	1.034-11	5.351-12	7.393-15	3.554-17	3.524-17	3.234-17
PEPIN	7.778-11	1.034-11	5.351-12	7.393-15	3.555-17	3.525-17	3.234-17
ORIGEN-S	7.773-11	1.034-11	5.352-12	7.392-15	3.556-17	3.525-17	3.235-17

Table 8: Gamma Decay Heat Results in MeV/s/fission for a  $^{235}\text{U}$  Fission Pulse Given at Cooling Times from 1 to  $10^{13}$  Seconds

Code	Cooling Time (s)						
	1	10	$10^2$	$10^3$	$10^4$	$10^5$	$10^6$
AFPA	1.732-2	8.312-3	1.924-3	1.344-4	1.767-5	6.755-7	8.650-8
CINDER10	1.735-2	8.304-3	1.926-3	1.342-4	1.767-5	6.758-7	8.651-8
DCHAIN	1.734-2	8.303-3	1.925-3	1.342-4	1.767-5	6.756-7	8.650-8
FISP6	1.734-2	8.303-3	1.925-3	1.342-4	1.767-5	6.753-7	8.650-8
FISPIN	1.734-2	8.303-3	1.925-3	1.342-4	1.767-5	6.756-7	8.650-8
INVENT	1.735-2	8.320-3	1.929-3	1.344-4	1.770-5	6.769-7	8.664-8
KORIGEN	1.734-2	8.306-3	1.926-3	1.342-4	1.767-5	6.792-7	8.697-8
MECCYCO	1.734-2	8.301-3	1.925-3	1.342-4	1.767-5	6.755-7	8.647-8
PEPIN	1.734-2	8.303-3	1.925-3	1.342-4	1.767-5	6.756-7	8.650-8
ORIGEN-S	1.734-2	8.303-3	1.925-3	1.341-4	1.767-5	6.750-7	8.646-8

Code	Cooling Time (s)						
	$10^7$	$10^8$	$10^9$	$10^{10}$	$10^{11}$	$10^{12}$	$10^{13}$
AFPA	2.317-10	2.369-11	1.225-11	1.685-14	8.921-27	6.416-27	2.376-28
CINDER10	2.318-10	2.369-11	1.225-11	1.685-14	8.921-27	6.416-27	2.376-28
DCHAIN	2.318-10	2.369-11	1.225-11	1.685-14	8.921-27	6.416-27	2.376-28
FISP6	2.318-10	2.367-11	1.224-11	1.684-14	—	—	—
FISPIN	2.318-10	2.369-11	1.225-11	1.685-14	8.921-27	6.416-27	2.376-28
INVENT	2.325-10	2.373-11	1.228-11	1.690-14	—	—	—
KORIGEN	2.323-10	2.373-11	1.228-11	1.696-14	8.830-27	6.350-27	2.351-28
MECCYCO	2.317-10	2.368-11	1.225-11	1.685-14	8.921-27	—	—
PEPIN	2.318-10	2.369-11	1.226-11	1.685-14	8.921-27	6.416-27	2.376-28
ORIGEN-S	2.317-10	2.368-11	1.225-11	1.684-14	8.927-27	6.419-27	2.376-28

Table 9: Fission Product Contribution as a Percentage of the Total Decay Heat for a  $^{235}\text{U}$  Fission Pulse After 10 Seconds

Code	$^{131}\text{Sn}$	$^{132}\text{Sn}$	$^{132}\text{Sb}$	$^{133}\text{Sb}$	$^{134}\text{Sb}$	$^{135}\text{Te}$	$^{136}\text{Te}$	$^{137}\text{Te}$
AFPA	1.84	1.93	1.03	1.72	3.77	15.24	10.67	1.03
CINDER10	1.85	1.93	1.03	1.72	3.77	15.24	10.57	1.03
DCHAIN	1.84	1.93	1.03	1.72	3.77	15.24	10.57	1.03
FISP6	1.85	1.93	1.03	1.72	3.77	15.24	10.57	1.03
FISPIN	1.85	1.93	1.03	1.72	3.77	15.25	10.57	1.03
INVENT	1.84	1.93	1.03	1.72	3.77	15.24	10.57	1.03
KORIGEN	1.84	1.93	1.03	1.72	3.77	15.24	10.56	1.03
MECCYCO	1.84	1.93	1.03	1.72	3.77	15.24	10.57	1.03
PEPIN	1.84	1.93	1.03	1.72	3.77	15.24	10.57	1.03
ORIGEN-S	1.84	1.93	1.03	1.72	3.77	15.24	10.57	1.03

Code	$^{136}\text{I}$	$^{136m}\text{I}$	$^{137}\text{I}$	$^{138}\text{I}$	$^{139}\text{I}$	$^{137}\text{Xe}$	$^{139}\text{Xe}$	$^{140}\text{Xe}$	$^{140}\text{Cs}$
AFPA	3.46	3.29	8.76	8.99	1.96	1.27	10.86	14.67	6.82
CINDER10	3.51	3.30	8.77	9.00	1.96	1.28	10.86	14.68	6.83
DCHAIN	3.51	3.30	8.77	9.00	1.96	1.27	10.86	14.68	6.83
FISP6	3.51	3.30	8.77	9.00	1.96	1.27	10.86	14.68	6.83
FISPIN	3.51	3.30	8.77	9.00	1.96	1.28	10.86	14.68	6.83
INVENT	3.51	3.30	8.77	8.99	1.96	1.28	10.86	14.68	6.83
KORIGEN	3.51	3.30	8.76	8.99	1.96	1.27	10.87	14.69	6.84
MECCYCO	3.51	3.30	8.76	9.00	1.96	1.28	10.86	14.69	6.83
PEPIN	3.51	3.30	8.77	9.00	1.96	1.27	10.86	14.68	6.83
ORIGEN-S	3.51	3.30	8.77	9.00	1.96	1.27	10.86	14.68	6.83

Table 10: Fission Product Contribution as a Percentage of the Total Decay Heat for a  $^{235}\text{U}$  Fission Pulse After  $10^6$  Seconds

Code	$^{131m}\text{Te}$	$^{132}\text{Te}$	$^{131}\text{I}$	$^{132}\text{I}$	$^{133}\text{I}$	$^{135}\text{I}$	$^{135}\text{Xe}$	$^{140}\text{Ba}$	$^{140}\text{La}$
AFFA	2.23	2.72	1.18	23.20	25.47	18.69	18.32	1.81	4.10
CINDER10	2.21	2.70	1.19	23.05	25.31	18.56	18.19	1.80	4.08
DCHAIN	2.23	2.72	1.19	23.20	25.47	18.69	18.32	1.81	4.10
FISP6	2.23	2.72	1.19	23.20	25.47	18.68	18.31	1.81	4.10
FISPIN	2.23	2.72	1.19	23.20	25.47	18.69	18.32	1.81	4.10
INVENT	2.23	2.72	1.19	23.20	25.46	18.69	18.31	1.81	4.10
KORIGEN	2.22	2.75	1.19	23.49	25.36	18.61	18.19	1.81	4.09
MECCYCO	2.23	2.72	1.19	23.20	25.47	18.69	18.31	1.81	4.10
PEPIN	2.23	2.72	1.19	23.20	25.47	18.69	18.32	1.81	4.10
ORIGEN-S	2.23	2.72	1.19	23.21	25.47	18.70	18.29	1.82	4.10

Table 11: Fission Product Contribution as a Percentage of the Total Decay Heat for a  $^{235}\text{U}$  Fission Pulse After  $10^9$  Seconds

Code	$^{137}\text{Cs}$	$^{137m}\text{Ba}$
AFFA	22.91	77.09
CINDER10	22.92	77.08
DCHAIN	22.91	77.09
FISP6	22.91	77.09
FISPIN	22.92	77.08
INVENT	22.91	77.09
KORIGEN	22.92	77.08
MECCYCO	22.91	77.09
PEPIN	22.91	77.09
ORIGEN-S	22.91	77.07

## 5.2 Extended $^{235}\text{U}$ Irradiation and Decay

The second numerical benchmark in the NEA code comparison involved calculating the fission product decay heating for an extended irradiation ( $3 \times 10^7$  seconds) of pure  $^{235}\text{U}$  followed by cooling for times up to  $10^{13}$  s. The decay and fission product yield data were the same as for the fission pulse benchmark, and additional one-group capture cross-section data were provided. The problem specified a fixed flux of  $5 \times 10^{13}$  n/(cm<sup>2</sup>·s), a constant fission rate of  $1.25 \times 10^{15}$  fissions/s, and assumed no depletion of  $^{235}\text{U}$  takes place.

To ensure that  $^{235}\text{U}$  is not significantly depleted during irradiation, the fission cross section was reduced to  $10^{-3}$  barns, to ensure that the product of the fission cross section  $\sigma_f$ , flux  $\phi$ , and irradiation time  $t$ , does not exceed a value of about  $10^{-6}$ . The initial  $^{235}\text{U}$  content was adjusted to give the specified fission rate.

The results of the total, beta, and gamma decay heat are presented in Tables 12–14. The principal fission product contributors are compared in Tables 15–16. The ORIGEN-S results are seen to be in good agreement with the other codes, although a much larger variance between code results is observed than for the decay-only problem. The CINDER code in particular shows large deviations from the other codes. The total decay heat results of the AFPA, CINDER-10, FISP6, INVENT, KORIGEN, and ORIGEN-S are graphed in Figure 1. All other code results (except CINDER) lie within the range of these codes. The ORIGEN-S results are well within the range of calculated values of the other codes. The deviation in the results is typically about 0.2%, but increases to about 1% at  $10^5$  and  $10^7$  s cooling time. The ORIGEN-S results are slightly higher (0.3%) than the average above  $10^{10}$  s, showing the same trend as the KORIGEN code in this time range. The ORIGEN-S results are within 0.2% of the average for all times below  $10^{10}$  s.

The irradiation benchmark identified a dependence of the ORIGEN-S results to the time step intervals used during irradiation. This dependence was also identified in the ORIGEN-S and KORIGEN codes used in the original benchmark, and noted in the summary report [15]. Both codes use similar numerical methods (KORIGEN is based on ORIGEN2). While theoretically the results are not dependent on time subdivision, numerical approximations used in the codes do introduce a dependence.

An approximation is introduced during solution of the exponential matrix, when the code must remove short-lived isotopes from the matrix to prevent numerical instabilities. The code solves the matrix without these isotopes, and then solves for the removed isotopes using the Bateman equations. The criteria for removing an isotope is based on the machine precision, the nuclide half-life and the time step of the interval. Therefore varying the time subdivisions used in the calculation will change which isotopes are removed from the matrix. In removing a short-lived isotope  $B$  in the chain  $A \rightarrow B \rightarrow C$ , the code adjusts the matrix to ensure the correct prediction of isotope  $C$  in the matrix calculation. However, the Bateman solution of isotope  $B$  assumes a constant rate of production from  $A$ . While in most cases the method produces good results, as demonstrated in the first (burst irradiation) benchmark, the approximation can lead to a dependence in depleted inventories of several percent. In the second (irradiation) benchmark case, ORIGEN-S overpredicts

Table 12: Total Decay Heat Results in MeV/s/fission for a  $^{235}\text{U}$  Irradiation Case Given at Cooling Times from 1 to  $10^{13}$  Seconds

Code	Cooling Time (s)						
	1	10	$10^2$	$10^3$	$10^4$	$10^5$	$10^6$
AFPA	3.821+15	3.514+15	2.601+15	1.730+15	8.229+14	4.830+14	1.870+14
CINDER10	3.827+15	3.519+15	2.606+15	1.730+15	8.275+14	4.872+14	1.873+14
CINDER	3.800+15	3.493+15	2.582+15	1.710+15	8.123+14	4.771+14	1.863+14
DCHAIN	3.823+15	3.515+15	2.601+15	1.726+15	8.231+14	4.834+14	1.871+14
FISP6	3.822+15	3.515+15	2.602+15	1.726+15	8.236+14	4.837+14	1.873+14
FISPIN	3.821+15	3.514+15	2.601+15	1.726+15	8.230+14	4.833+14	1.871+14
INVENT	3.832+15	3.524+15	2.609+15	1.732+15	8.277+14	4.864+14	1.877+14
KORIGEN	3.824+15	3.517+15	2.604+15	1.729+15	8.256+14	4.849+14	1.872+14
MECCYCO	3.821+15	3.514+15	2.600+15	1.726+15	8.230+14	4.833+14	1.870+14
PEPIN	3.822+15	3.515+15	2.601+15	1.726+15	8.231+14	4.834+14	1.871+14
ORIGEN-S	3.821+15	3.514+15	2.601+15	1.726+15	8.235+14	4.832+14	1.871+14

Code	Cooling Time (s)						
	$10^7$	$10^8$	$10^9$	$10^{10}$	$10^{11}$	$10^{12}$	$10^{13}$
AFPA	5.101+12	2.492+12	6.531+11	8.981+8	2.796+5	2.772+5	2.544+5
CINDER10	5.104+12	2.493+12	6.531+11	8.982+8	2.797+5	2.773+5	2.545+5
CINDER	5.156+12	2.501+12	6.415+11	8.833+8	2.701+5	2.678+5	2.458+5
DCHAIN	5.103+12	2.493+12	6.531+11	8.981+8	2.795+5	2.771+5	2.543+5
FISP6	5.102+12	2.492+12	6.530+11	8.984+8	2.796+5	2.772+5	2.543+5
FISPIN	5.102+12	2.492+12	6.531+11	8.981+8	2.796+5	2.772+5	2.543+5
INVENT	5.130+12	2.503+12	6.543+11	9.011+8	2.793+5	2.769+5	2.540+5
KORIGEN	5.165+12	2.517+12	6.532+11	8.982+8	2.801+5	2.777+5	2.548+5
MECCYCO	5.103+12	2.493+12	6.531+11	8.981+8	2.796+5	2.773+5	2.544+5
PEPIN	5.104+12	2.493+12	6.531+11	8.981+8	2.795+5	2.771+5	2.543+5
ORIGEN-S	5.114+12	2.497+12	6.532+11	8.983+8	2.807+5	2.783+5	2.554+5

Table 13: Beta Decay Heat Results in MeV/s/fission for a  $^{235}\text{U}$  Irradiation Case Given at Cooling Times from 1 to  $10^{13}$  Seconds

Code	Cooling Time (s)						
	1	10	$10^2$	$10^3$	$10^4$	$10^5$	$10^6$
AFPA	1.675+15	1.491+15	1.004+15	5.625+14	2.274+14	1.281+14	4.707+13
CINDER10	1.680+15	1.495+15	1.009+15	5.656+14	2.319+14	1.321+14	4.728+13
CINDER	1.666+15	1.482+15	9.971+14	5.561+14	2.242+14	1.263+14	4.700+13
DCHAIN	1.676+15	1.491+15	1.004+15	5.612+14	2.274+14	1.282+14	4.709+13
FISP6	1.675+15	1.491+15	1.004+15	5.612+14	2.275+14	1.282+14	4.711+13
FISPIN	1.675+15	1.491+15	1.004+15	5.611+14	2.274+14	1.282+14	4.710+13
INVENT	1.679+15	1.494+15	1.006+15	5.627+14	2.284+14	1.288+14	4.722+13
KORIGEN	1.676+15	1.491+15	1.005+15	5.617+14	2.279+14	1.285+14	4.710+13
MECCYCO	1.675+15	1.491+15	1.004+15	5.610+14	2.273+14	1.281+14	4.709+13
PEPIN	1.676+15	1.491+15	1.004+15	5.612+14	2.274+14	1.282+14	4.709+13
ORIGEN-S	1.674+15	1.490+15	1.004+15	5.608+14	2.276+14	1.282+14	4.710+13

Code	Cooling Time (s)						
	$10^7$	$10^8$	$10^9$	$10^{10}$	$10^{11}$	$10^{12}$	$10^{13}$
AFPA	8.483+11	5.010+11	1.985+11	2.732+8	2.796+5	2.772+5	2.544+5
CINDER10	8.487+11	5.011+11	1.985+11	2.732+8	2.797+5	2.773+5	2.545+5
CINDER	8.511+11	4.993+11	1.961+11	2.702+8	2.701+5	2.678+5	2.458+5
DCHAIN	8.485+11	5.010+11	1.985+11	2.732+8	2.795+5	2.771+5	2.543+5
FISP6	8.484+11	5.009+11	1.985+11	2.733+8	2.796+5	2.772+5	2.543+5
FISPIN	8.484+11	5.010+11	1.985+11	2.732+8	2.796+5	2.772+5	2.543+5
INVENT	8.518+11	5.025+11	1.988+11	2.740+8	2.793+5	2.769+5	2.540+5
KORIGEN	8.543+11	5.032+11	1.985+11	2.731+8	2.801+5	2.777+5	2.548+5
MECCYCO	8.485+11	5.010+11	1.985+11	2.731+8	2.796+5	2.773+5	2.544+5
PEPIN	8.486+11	5.011+11	1.985+11	2.732+8	2.795+5	2.772+5	2.543+5
ORIGEN-S	8.497+11	5.016+11	1.984+11	2.732+8	2.807+5	2.783+5	2.554+5

Table 14: Gamma Decay Heat Results in MeV/s/fission for a  $^{235}\text{U}$  Irradiation Case Given at Cooling Times from 1 to  $10^{13}$  Seconds

Code	Cooling Time (s)						
	1	10	$10^2$	$10^3$	$10^4$	$10^5$	$10^6$
AFPA	2.146+15	2.024+15	1.597+15	1.168+15	5.956+14	3.549+14	1.399+14
CINDER10	2.147+15	2.024+15	1.597+15	1.165+15	5.957+14	3.551+14	1.400+14
CINDER	2.133+15	2.011+15	1.585+15	1.154+15	5.881+14	3.507+14	1.393+14
DCHAIN	2.147+15	2.024+15	1.597+15	1.165+15	5.957+14	3.552+14	1.400+14
FISP6	2.147+15	2.024+15	1.598+15	1.165+15	5.961+14	3.555+14	1.402+14
FISPIN	2.146+15	2.023+15	1.597+15	1.165+15	5.956+14	3.551+14	1.400+14
INVENT	2.153+15	2.030+15	1.602+15	1.169+15	5.993+14	3.576+14	1.404+14
KORIGEN	2.148+15	2.026+15	1.599+15	1.167+15	5.976+14	3.564+14	1.400+14
MECCYCO	2.146+15	2.024+15	1.596+15	1.165+15	5.955+14	3.551+14	1.400+14
PEPIN	2.147+15	2.024+15	1.597+15	1.165+15	5.957+14	3.552+14	1.400+14
ORIGEN-S	2.147+15	2.024+15	1.597+15	1.165+15	5.958+14	3.550+14	1.400+14

Code	Cooling Time (s)						
	$10^7$	$10^8$	$10^9$	$10^{10}$	$10^{11}$	$10^{12}$	$10^{13}$
AFPA	4.253+12	1.991+12	4.546+11	6.250+8	3.323-4	2.406-4	8.910-6
CINDER10	4.255+12	1.992+12	4.546+11	6.250+8	3.345-4	2.406-4	8.909-6
CINDER	4.305+12	2.002+12	4.454+11	6.131+8	3.345-4	2.406-4	8.914-6
DCHAIN	4.254+12	1.992+12	4.546+11	6.250+8	3.346-4	2.406-4	8.909-6
FISP6	4.253+12	1.991+12	4.546+11	6.252+8	—	—	—
FISPIN	4.253+12	1.991+12	4.546+11	6.250+8	3.345-4	2.406-4	8.909-6
INVENT	4.278+12	2.001+12	4.545+11	6.270+8	—	—	—
KORIGEN	4.310+12	2.013+12	4.546+11	6.250+8	3.351-4	2.410-4	8.923-6
MECCYCO	4.254+12	1.991+12	4.546+11	6.250+8	3.345-4	—	—
PEPIN	4.255+12	1.992+12	4.546+11	6.250+8	3.346-4	2.406-4	8.910-6
ORIGEN-S	4.265+12	1.996+12	4.547+11	6.251+8	3.344-4	2.405-4	8.908-6

Table 15: Fission Product Contribution as a Percentage of the Total Decay Heat for a  $^{235}\text{U}$  Irradiation Case After  $10^4$  Seconds

Code	$^{132}\text{Te}$	$^{133m}\text{Te}$	$^{131}\text{I}$	$^{132}\text{I}$	$^{133}\text{I}$	$^{134}\text{I}$	$^{135}\text{I}$
AFPA	2.10	1.05	2.18	17.79	9.62	10.08	13.46
CINDER10	2.09	1.04	2.17	17.70	9.57	10.02	13.38
CINDER	2.13	1.06	2.20	18.03	9.27	10.21	13.50
DCHAIN	2.10	1.05	2.18	17.80	9.62	10.08	13.46
FISP6	2.10	1.05	2.17	17.78	9.61	10.07	13.45
FISPIN	2.10	1.05	2.18	17.79	9.62	10.08	13.46
INVENT	2.09	1.04	2.16	17.73	9.58	10.04	13.40
KORIGEN	2.09	1.04	2.17	17.74	9.59	10.05	13.41
MECCYCO	2.10	1.05	2.17	17.79	9.62	10.08	13.46
PEPIN	2.10	1.05	2.18	17.80	9.62	10.08	13.46
ORIGEN-S	2.10	1.05	2.18	17.83	9.60	10.07	13.45

Code	$^{133}\text{Xe}$	$^{135}\text{Xe}$	$^{138}\text{Cs}$	$^{139}\text{Ba}$	$^{140}\text{Ba}$	$^{140}\text{La}$
AFPA	1.83	1.81	1.84	2.61	4.65	27.17
CINDER10	1.82	1.80	1.83	2.60	4.62	27.02
CINDER	1.85	1.72	1.85	2.64	4.71	27.16
DCHAIN	1.83	1.81	1.84	2.61	4.65	27.16
FISP6	1.82	1.83	1.84	2.61	4.65	27.15
FISPIN	1.83	1.81	1.84	2.61	4.65	27.18
INVENT	1.82	1.81	1.84	2.60	4.63	27.43
KORIGEN	1.82	1.81	1.84	2.61	4.63	27.39
MECCYCO	1.83	1.81	1.84	2.61	4.65	27.17
PEPIN	1.83	1.81	1.84	2.61	4.65	27.16
ORIGEN-S	1.83	1.81	1.84	2.61	4.65	27.15

Table 16: Fission Product Contribution as a Percentage of the Total Decay Heat for a  $^{235}\text{U}$  Irradiation Case After  $10^8$  Seconds

Code	$^{134}\text{Cs}$	$^{137}\text{Cs}$	$^{137m}\text{Ba}$
AFPA	49.36	11.60	39.04
CINDER10	49.38	11.60	39.02
CINDER	50.44	11.45	38.11
DCHAIN	49.37	11.60	39.03
FISP6	49.36	11.60	39.04
FISPIN	49.36	11.60	39.04
INVENT	49.50	11.57	38.93
KORIGEN	49.85	11.50	38.66
MECCYCO	49.36	11.60	39.03
PEPIN	49.38	11.60	39.02
ORIGEN-S	49.46	11.58	38.97

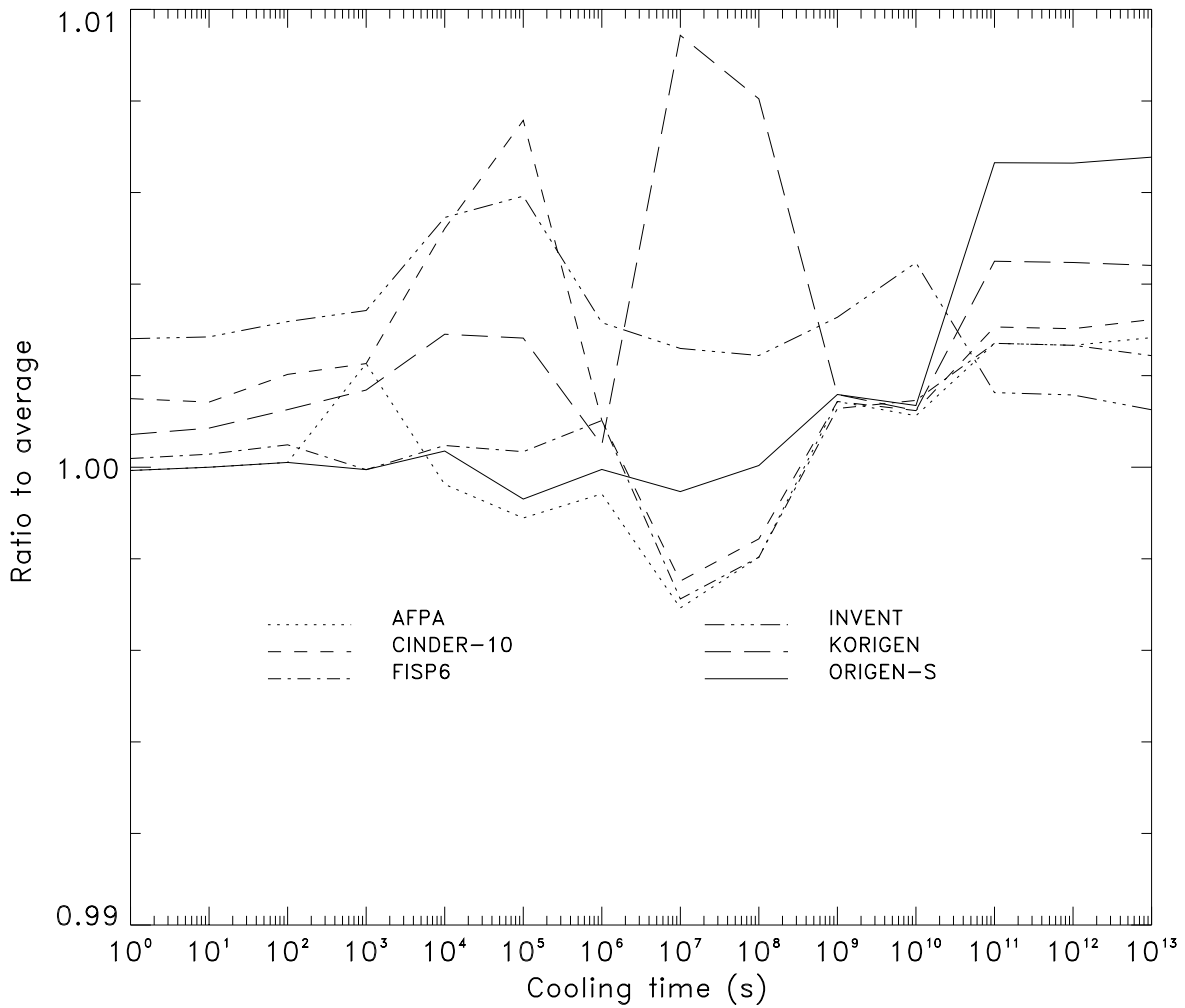


Figure 1: Intercomparison of Total Decay Heat Predictions for the Extended <sup>235</sup>U Irradiation NEA Numerical Benchmark Problem. The results are expressed as the ratio of each code result to the average of all codes.

the concentration of  $^{134}\text{Cs}$  by about 2% when less than 10 time intervals are used during irradiation. This results in an overprediction in the beta (and total) decay heat between  $10^7$  and  $10^8$  s where  $^{134}\text{Cs}$  contributes about half of the total heat. This dependence was reduced by increasing the number of intervals.

A time-step dependence in the total heat predicted by ORIGEN-S was also noted at cooling times greater than  $10^{10}$  s, due to a sensitivity in the calculated  $^{137}\text{Cs}$  inventory. Increasing the number of time intervals during irradiation above about 10 resulted in an overprediction in the total heat between  $10^{11}$  and  $10^{13}$  s of about 2%. A more detailed discussion of the Bateman approximation, its affects, and the selection of time step intervals for calculations can be found in the ORIGEN-S manual [1].

In general, at least ten time intervals should be used for a typical irradiation simulation. For decay periods, a general “rule of three” is recommended, whereby a given time intervals should be no greater than three times that of the previous interval (e.g., 1, 3, 9, 27, ...). For any application, the effect of the time step intervals on the results should be investigated by doubling, or more, the number of intervals to determine the condition for computing acceptable accuracies [1].

### 5.3 Summary of Results

The results of ORIGEN-S have been compared to those from ten codes using both similar and numerically independent methods. All codes used an identical nuclear data base for the calculations, allowing an evaluation of the code methods.

In a burst fission benchmark, the ORIGEN-S results have been demonstrated to yield results that are within 0.1% of the average of all codes, which is within the numerical accuracy of the ORIGEN-S code methods associated with the solution of the matrix exponential equations. In the second benchmark, that involved simulating irradiation and decay, a larger variance was observed between the codes used in the study. The ORIGEN-S results are in good agreement with the code averages, within 0.2% below  $10^{10}$  s cooling time, and are slightly higher (0.7%) than other code results above  $10^{11}$  s. The ORIGEN-S results were found to be somewhat dependent on the time-step intervals to model the irradiation, due to approximations introduced by the numerical methods. The magnitude of this sensitivity on the results was found to be less than 2% for all cooling times studied.

The purpose of the NEA benchmark was to compare international codes used in decay heat calculations using a common nuclear data base in order to provide a valid comparison of solution methods used by the various codes. The results presented in this comparison reflect the subset of nuclear data used in the study, and as a result do not represent realistic decay heating values.

## 6 USED-FUEL NUCLIDE INVENTORY BENCHMARK STUDIES

The ORIGEN-S code was benchmarked against experimental measurements of used fuel isotopic inventories for three CANDU reactor designs including NPD, Bruce, and Pickering reactors. The NPD and Bruce experimental data are limited to uranium and plutonium mass and isotopic ratio measurements, while the Pickering fuel bundle measurements include fission product and transuranic nuclide inventory measurements. Also included are comparisons against measured inventories from a Pressurized Water Reactor (PWR) assembly which include a number of nuclides not available in the CANDU reactor fuel studies. The PWR measurements were also used as the basis for an international code comparison carried out by the Nuclear Energy Agency (NEA), providing a numerical benchmark for several nuclides without experimental data.

All of the ORIGEN-S inventory calculations were performed with cross-section libraries created specifically for the benchmark problems, using a power history that reflected the actual history of the assemblies used in the studies as closely as possible.

### 6.1 NPD Reactor Fuel Study

#### 6.1.1 Description of the Benchmark

Measurements of the uranium and plutonium inventories for the Canadian Nuclear Power Demonstration Reactor (NPD) in Rolphton, Ontario, have been published [18]. NPD fuel consists of a 19-element bundle with natural uranium. Measurements were made on fuel bundle 1016, six months after discharge with a scheduled burnup of about 6200 MWd/MgU. The bundle resided within a single channel over its lifetime in the reactor. The measurements consist of total plutonium and uranium mass and isotopic ratios for the central, middle, and outer concentric fuel element rings on the bundle.

The samples were obtained by removing a one inch section from each of the 19 fuel elements. The 12 outer pin sections were combined to give a representative sample of the outer region, the 6 middle pin sections were combined to represent the middle region, and the single central pin sample provided the central pin data. Chemical analyses were performed to determine uranium and plutonium mass, while mass spectrometry was used to determine the isotopic ratios. The results of the chemical and mass analyses included the Pu/U atom ratio,  $^{235}\text{U}/^{238}\text{U}$  atom ratio, and the atom ratios of  $^{239}\text{Pu}$ ,  $^{240}\text{Pu}$ ,  $^{241}\text{Pu}$ , and  $^{242}\text{Pu}$  to total Pu.

The specifications used in the WIMS-AECL reactor lattice model and the ORIGEN-S depletion analysis are listed in Table 17. The fuel and lattice specifications are based on those given with the published data [18].

Table 17: Specifications for the NPD Fuel Inventory Calculations

Fuel material	Natural UO <sub>2</sub>
Initial uranium compositions (weight percent)	
<sup>234</sup> U	0.0054
<sup>235</sup> U	0.7110
<sup>238</sup> U	99.2836
Fuel density	10.47 g/cm <sup>3</sup>
Number of fuel pins	19
Element radius	0.7144 cm
Inner fuel ring radius (6)	1.6561 cm
Outer fuel ring radius (12)	3.1993 cm
Cladding material	Zircaloy
Cladding radius	0.7626 cm
Pressure tube	Zircaloy
Inner radius	4.140 cm
Outer radius	4.572 cm
Calandria tube	Aluminum
Inner radius	5.080 cm
Outer radius	5.208 cm
Coolant	D <sub>2</sub> O
Atom purity	99.722 %
Density	0.863 g/cm <sup>3</sup>
Moderator	D <sub>2</sub> O
Atom purity	99.722 %
Temperature	311 K
Fuel channel square pitch	26.035 cm
Approximate burnup	6200 MWd/MgU
Equivalent full power days	620.55
Cluster average exit <sup>235</sup> U/ <sup>238</sup> U ratio	0.2849
Cooling time in days	182

### 6.1.2 Results

The indicator of burnup for the calculations was the  $^{235}\text{U}/^{238}\text{U}$  ratio. All calculations correspond to the irradiation at which the experimental cluster average  $^{235}\text{U}/^{238}\text{U}$  ratio in Table 17 equals the calculated  $^{235}\text{U}/^{238}\text{U}$  cluster average ratio. The ORIGEN-S calculations were performed with a constant bundle power level of 9.365 kW/kgU over the irradiation period. This power level resulted in the experimental  $^{235}\text{U}/^{238}\text{U}$  ratio at exit from the reactor. The ORIGEN-S depletion calculation was performed using seven cycles over an effective time at full power of 620.55 days. At each cycle during the irradiation a complete recalculation of the flux spectrum is made using WIMS-AECL, which is subsequently used to collapse multigroup reaction cross sections for use in the ORIGEN-S depletion analysis. The bundle cooling time was 182 days at the time of the measurements.

The calculated isotopic ratios are compared to experiment in Table 18. In addition to the ORIGEN-S results, the results from WIMS-AECL [5, 6] and ORIGEN2 [11] are also included for comparison. Both of these codes are routinely used in the Canadian nuclear industry for inventory predictions. The WIMS-AECL results were obtained using the ENDF/B-V library, while the ORIGEN2 results were obtained using the fixed CANDU library based on the Gentilly-2 reactor design. Note that all calculations report a  $^{235}\text{U}/^{238}\text{U}$  ratio of 0.2849 since this was the parameter used to normalize all code calculations.

Table 18: Measured and Calculated Atom Ratios for NPD Fuel Study

Atom Ratio	Measured	Calculated					
		ORIGEN-S		WIMS-AECL		ORIGEN2	
$^{235}\text{U}/^{238}\text{U}$	$2.849\text{-}3 \pm 0.3\%$	2.849-3	(1.00) <sup>†</sup>	2.849-3	(1.00)	2.849-3	(1.00)
Pu/U	$3.13\text{-}3 \pm 0.7\%$	3.17-3	(1.01)	3.189-2	(1.02)	3.552-3	(1.13)
$^{239}\text{Pu}/\text{Pu}$	$7.334\text{-}1 \pm 0.1\%$	7.364-1	(1.00)	7.355-1	(1.00)	7.264-1	(0.99)
$^{240}\text{Pu}/\text{Pu}$	$2.204\text{-}1 \pm 0.3\%$	2.165-1	(0.98)	2.160-1	(0.98)	2.245-1	(1.02)
$^{241}\text{Pu}/\text{Pu}$	$3.815\text{-}2 \pm 0.2\%$	3.872-2	(1.01)	3.958-2	(1.03)	4.065-2	(1.07)
$^{242}\text{Pu}/\text{Pu}$	$8.12\text{-}3 \pm 0.3\%$	7.587-3	(0.93)	8.183-3	(1.01)	7.750-3	(0.95)

<sup>†</sup> Values in parentheses are the ratios of calculated to measured results.

The WIMS-AECL calculations were performed using spatially-dependent burnup, whereby the fuel compositions in each fuel ring were allowed to vary independently. The inventories at exit burnup were subsequently combined to form bundle average compositions, which was the basis for the comparison. In contrast, the ORIGEN codes use point depletion which is spatially independent.

The ORIGEN-S results show good agreement with the measured ratios. The total plutonium production is within about 1% of the measurement, while individual plutonium atom ratios are generally within about 2%, with the exception of  $^{242}\text{Pu}$  which was underpredicted by about 6%. The WIMS-AECL results are also seen to be in good agreement with the measurements, with calculated ratios being generally within several percent of the experimental values. The ORIGEN2

results for the plutonium atom percentages are also in good agreement, although the total amount of plutonium predicted by ORIGEN2 is overpredicted by 13%.

## 6.2 Bruce-A Reactor Fuel Study

### 6.2.1 Description of the Benchmark

The second set of actinide isotopic measurements on CANDU fuel used in the validation study were obtained from unpublished experimental data from the Thorium Fuel Reprocessing Experiment Program carried out at AECL in 1982 [19]. The isotopic analyses were made on fuel bundle F21037C from the Bruce-A Nuclear Generating Station. The Bruce reactor fuel bundles have 37 fuel pins, consisting of a central pin surrounded by three concentric rings of 6, 12, and 18 fuel pins, respectively.

Like the NPD reactor fuel measurements, fuel assays were taken from several fuel pins at different radial positions within the bundle. These measurements were combined to generate average cluster inventories for use in the benchmark.

The most accurate experimental data available from the fuel pin assays were the uranium and plutonium atom ratios, measured primarily using mass spectrometry, and this data was selected for the present study. The data for  $^{238}\text{Pu}$  are based on alpha-spectrometric counting.

The measured atom ratios for the individual fuel pins from Bruce bundle F21037C are listed in Table 19, with the derived cluster averaged values, since this data has not been published elsewhere. The cluster averages were derived by weighting the individual fuel pin results. The measured inventories are listed for each fuel ring. The outermost fuel ring corresponds to a batch consisting of 9 even-numbered elements, the middle fuel ring to 6 even-numbered elements, and the inner fuel ring to 3 even-numbered elements. These results therefore provide isotopic data representative of 36 of the 37 elements in the bundle. The central fuel pin was not analyzed and was assumed to have the same composition as the innermost fuel ring.

A detailed irradiation history was available for the bundle and was applied to all calculations. The fuel specifications and irradiation history used in the ORIGEN-S calculations are listed in Table 20 and 21.

### 6.2.2 Results

The Bruce-A study used the measured  $^{235}\text{U}/\text{U}$  atom ratio as the indicator for burnup. The ORIGEN-S depletion calculations were performed using seven cycles. The irradiation time of each cycle was selected to closely match the bundle irradiation history, and included the major operational down times.

Table 19: Experimental Fuel Analysis Results for Bruce-A Bundle F21037C  
Atom Percent

Isotope	Outer Ring	Middle Ring	Inner Ring	Average
$^{235}\text{U}$	$0.174 \pm 0.009$	$0.237 \pm 0.008$	$0.272 \pm 0.006$	$0.213 \pm 0.005$
$^{236}\text{U}$	$0.087 \pm 0.005$	$0.075 \pm 0.011$	$0.073 \pm 0.007$	$0.080 \pm 0.005$
$^{238}\text{U}$	$99.739 \pm 0.106$	$99.689 \pm 0.015$	$99.655 \pm 0.014$	$99.707 \pm 0.052$
$^{239}\text{Pu}$	$62.97 \pm 0.39$	$67.60 \pm 0.68$	$70.11 \pm 0.18$	$65.82 \pm 0.29$
$^{240}\text{Pu}$	$29.03 \pm 0.56$	$26.58 \pm 0.51$	$24.93 \pm 0.11$	$27.46 \pm 0.32$
$^{241}\text{Pu}$	$5.70 \pm 0.28$	$4.46 \pm 0.11$	$3.93 \pm 0.18$	$4.96 \pm 0.15$
$^{242}\text{Pu}$	$2.30 \pm 0.17$	$1.37 \pm 0.12$	$1.03 \pm 0.07$	$1.76 \pm 0.09$

The experimental results (reduced to cluster average values) are compared to the calculations of ORIGEN-S, WIMS-AECL and ORIGEN2 in Table 22. The ORIGEN-S results are seen to lie within the experimental uncertainty for all quantities measured. The WIMS-AECL and ORIGEN2 results are also in good agreement with experiment for most isotopes, although several isotopes are outside the uncertainty in the measurements.

### 6.3 Pickering-A Reactor Fuel Study

#### 6.3.1 Description of the Benchmark

An extensive fuel inventory assay was performed on a single outer element of Pickering-A non-CANLUB fuel bundle 19558C [20, 21]. These measurements were made in order to provide a data base against which to benchmark the computational codes and nuclear data used to predict used fuel inventories for the Waste Management Program at AECL in its concept assessment of deep geological disposal of used CANDU fuel in plutonic rock of the Canadian Precambrian Shield. The measurements are the most comprehensive published to date for irradiated CANDU reactor fuel.

The analysis was performed on a single outer fuel element (number 7) of bundle 19558C. This bundle type has 28 Zircaloy-4 clad elements containing natural uranium oxide pellets. During its in-reactor life, bundle 19558C resided at a single channel position and, as a result, its irradiation history is well characterized. The bundle received a relatively uniform axial neutron flux as verified by high-resolution axial gamma scans of 5 of the 28 elements [21]. The outer elements were irradiated at a linear power of approximately 40 kW/m, and reached a burnup at discharge of about 9208 MWd/MgU (221 MWh/kgU) based on a  $^{235}\text{U}$  to  $^{238}\text{U}$  ratio determined from chemical analyses and reactor physics calculations. This value of the outer element burnup is in good agreement with other estimates [20], and was used in the present calculations. Details of the power history are given elsewhere [21].

Table 20: Material and Lattice Specifications for the Bruce-A Fuel Inventory Calculations

Fuel material	Natural UO <sub>2</sub>
Initial uranium compositions (weight percent)	
<sup>234</sup> U	0.0054
<sup>235</sup> U	0.7110
<sup>238</sup> U	99.2836
Fuel density	10.6 g/cm <sup>3</sup>
Fuel temperature	1155 K
Element radius	0.6075 cm
Number of fuel pins	37
Inner fuel ring radius (6)	1.4885 cm
Middle fuel ring radius (12)	2.8755 cm
Outer fuel ring radius (18)	4.3305 cm
Cladding material	Zircaloy
Cladding radius	0.6540 cm
Pressure tube	Zr-Nb2.5%
Inner radius	5.1689 cm
Outer radius	5.6032 cm
Calandria tube	Zircaloy
Inner radius	6.4478 cm
Outer radius	6.5875 cm
Coolant	D <sub>2</sub> O
Atom purity	99.75 %
Density	0.8360 g/cm <sup>3</sup>
Temperature	549 K
Moderator	D <sub>2</sub> O
Atom purity	99.91 %
Density	1.0829 g/cm <sup>3</sup>
Temperature	346 K
Fuel channel square pitch	28.575 cm
Approximate burnup	7800 MWd/MgU
Cluster average exit <sup>235</sup> U/U ratio	0.213
Cooling time in days	5590

Table 21: Specifications for the Bruce-A Bundle F21037C Bundle Irradiation History

Operating Cycle	Power (kW/kgU)	Irradiation (days)	Cooling (days)
1	1.040	31.63	0.0
2	30.10	13.00	10.0
3	30.21	43.25	55.3
4	30.30	49.75	9.0
5	30.30	50.33	15.0
6	30.30	103.00	3.0
7	0.870	117.25	5590.0

Table 22: Measured and Calculated Atom Percents for Bruce-A Fuel Inventory Study

Isotope	Measured	Calculated					
		ORIGEN-S		WIMS-AECL		ORIGEN2	
<sup>235</sup> U	0.213 ± 2%	0.2121	(1.00) <sup>†</sup>	0.2130	(1.00)	0.2131	(1.00)
<sup>236</sup> U	0.080 ± 6%	0.0784	(0.98)	0.0783	(0.98)	0.0777	(0.97)
<sup>238</sup> U	99.707 ± 0.05%	99.705	(1.00)	99.708	(1.00)	99.705	(1.00)
<sup>239</sup> Pu	65.82 ± 1%	65.218	(0.99)	65.474	(0.99)	67.738	(1.03)
<sup>240</sup> Pu	27.46 ± 1%	27.798	(1.01)	27.323	(1.00)	26.152	(0.95)
<sup>241</sup> Pu	4.96 ± 3%	5.109	(1.03)	5.197	(1.05)	4.607	(0.93)
<sup>242</sup> Pu	1.76 ± 5%	1.757	(1.00)	1.895	(1.08)	1.410	(0.80)

<sup>†</sup> Values in parentheses are the ratios of calculated to measured results.

The fuel inventory assays were performed on three samples taken from the central region of the outer element. An attempt was made to capture the fission gases in the element gap and off-gases that evolved during dissolution of the fuel samples. The fuel cladding and undissolved residues were also analyzed. Details of the chemical separation processing, and analyses using mass spectrometry, alpha and gamma spectrometry, and liquid scintillation counting have been previously published [21]. Results are reported for uranium and plutonium isotope fractions, and activities for three transuranic nuclides and ten fission product radionuclides.

The irradiation history of the element was modeled in six irradiation time steps, with the major reactor down times over the history represented. The fuel specifications and irradiation history used in the calculations are listed in Tables 23 and 24.

The benchmark calculations for the Pickering-A outer element nuclide inventories required required some special modeling in order to accurately represent the just outer element environment, rather than the bundle average environment normally simulated. The code system will provide cross sections and the neutron flux for any material region in the WIMS-AECL model, therefore allowing ORIGEN-S to calculate the outer element inventories. However, the time-dependent fuel compositions of the inner fuel element rings, required for the WIMS-AECL analysis, are not provided by ORIGEN-S. These were precalculated at the appropriate time intervals using the burnup capability in WIMS-AECL, and added to the outer element composition as calculated by ORIGEN-S.

The oxygen in the fuel, the zirconium cladding, the coolant and the moderator were included in the ORIGEN-S model in order to obtain an accurate value of the recoverable energy per fission. Inclusion of this material is required to account for the energy release due to neutron capture in the light elements outside the fuel region, which accounts for a small fraction of the assembly power. Details of the effects of light elements are provided in the ORIGEN-S manual [1].

### 6.3.2 Results

The calculated results are compared to the measured actinide and fission product inventories in Tables 25 and 26, respectively. The ratios (C/E) of the calculated (C) to experimental (E) quantities are also given. Results from ORIGEN2 are not presented since the libraries contain bundle-averaged cross sections which are not representative of the outer fuel elements used in the benchmark.

The calculated atom fractions for the uranium and plutonium isotopes are in excellent agreement with the measured values (Table 25). The ORIGEN-S values are within the range of the analytical errors for all nuclides, with the exception of  $^{238}\text{Pu}$  which is about 10% low, although still within two standard deviations of the experimental uncertainty. These results indicate that the code and nuclear data are accurately representing uranium depletion and plutonium production.

Table 23: Specifications for the Pickering-A Fuel Inventory Calculations

Fuel material	Natural UO <sub>2</sub>
Initial uranium compositions (weight percent)	
<sup>234</sup> U	0.0054
<sup>235</sup> U	0.7110
<sup>238</sup> U	99.2836
Fuel density	10.6 g/cm <sup>3</sup>
Fuel temperature	1003 K
Element radius	0.7120 cm
Number of fuel pins	28
Inner fuel ring radius (4)	1.175 cm
Middle fuel ring radius (8)	2.685 cm
Outer fuel ring radius (16)	4.229 cm
Cladding material	Zircaloy-4
Cladding radius	0.7605 cm
Pressure tube	Zr-Nb2.5%
Inner radius	5.1815 cm
Outer radius	5.6965 cm
Calandria tube	Zircaloy
Inner radius	6.5405 cm
Outer radius	6.6955 cm
Coolant	D <sub>2</sub> O
Atom purity	99.75 %
Density	0.8445 g/cm <sup>3</sup>
Temperature	545 K
Moderator	D <sub>2</sub> O
Atom purity	99.91 %
Density	1.0838 g/cm <sup>3</sup>
Temperature	336 K
Fuel channel square pitch	28.575 cm
Exit outer element burnup (measured)	221 MWh/kgU
Cooling time in days	1162

Table 24: Specifications for the Pickering-A Outer Fuel Element Irradiation History

Operating Cycle	Power (kW/kgU)	Irradiation (days)	Cooling (days)
1	31.4	31.33	3.25
2	28.9	15.38	5.61
3	31.1	66.67	0.0
4	29.5	66.67	9.0
5	28.7	64.55	15.0
6	26.7	70.78	1162.0

Table 25: Measured and Calculated U and Pu Inventories in the Pickering-A Fuel Study

Isotope	Atom Percent		C/E
	Measured	Calculated	
U-234	0.0035 ± 55%	0.0044	1.26
U-235	0.1680 ± 2.4%	0.1691	1.01
U-236	0.0820 ± 3.7%	0.0833	1.02
U-238	99.7465 ± 0.01%	99.758	1.00
Pu-238	0.14 ± 5.6%	0.125	0.89
Pu-239	64.91 ± 2.5%	64.77	1.00
Pu-240	29.45 ± 3.7%	29.60	1.01
Pu-241	3.24 ± 9.1%	3.34	1.03
Pu-242	2.27 ± 6.7%	2.28	1.00
Pu/U (g) (x10 <sup>2</sup> )	0.4235 ± 2.0%	0.427	1.01

Table 26: Measured and Calculated Isotopic Activities in the Pickering-A Fuel Study

Isotope	Activity (Bq/kgU)		C/E
	Measured	Calculated	
H-3	2.07(+9) <sup>†</sup> ± 7%	2.23(+9)	1.08
Sr-90	4.86(+11) ± 4%	5.03(+11)	1.03
Tc-99	1.08(+8) ± 10%	1.50(+8)	1.39
Ru-106	8.72(+7) ± 5%	2.53(+8)	2.89
Sb-125	2.20(+9) ± 18%	2.56(+9)	1.16
I-129	2.44(+5)	3.62(+5)	1.48
Cs-134	4.16(+9) ± 7%	4.07(+9)	0.98
Cs-137	8.05(+11) ± 5%	7.88(+11)	0.98
Eu-154	8.14(+9) ± 5%	1.27(+10)	1.11
Eu-155	3.35(+9) ± 8%	3.81(+9)	0.93
Np-237	9.99(+5) ± 20%	8.99(+5)	0.90
Am-241	1.86(+10) ± 20%	1.89(+10)	1.02
Cm-244	7.12(+8) ± 15%	8.03(+8)	1.04

<sup>†</sup> Read as 2.07 x 10<sup>9</sup>

A comparison of calculated and measured transuranic and fission product nuclide activity is listed in Table 26. The measured activities of the transuranic isotopes  $^{237}\text{Np}$ ,  $^{241}\text{Am}$ , and  $^{244}\text{Cm}$  are well within the range of the analytical errors, although these errors are larger than those for the uranium and plutonium isotopes. The accurate prediction of  $^{244}\text{Cm}$  is particularly important to neutron shielding of used fuel at intermediate cooling times, due to its major contribution to the neutron source from spontaneous fission. The results indicate that ORIGEN-S is accurately predicting these inventories in used CANDU fuel.

The tritium in the fuel arises primarily from fission as a tertiary fission product. The predicted tritium inventory is about 8% higher than measured, which is just outside of the estimated measurement uncertainty of  $\pm 7\%$ . The cesium and strontium inventories are determined to be well within the analytical errors of the measurements for these isotopes of about  $\pm 5\%$ . The calculated  $^{125}\text{Sb}$  inventory is also within the experimental uncertainty of  $\pm 18\%$ .

The predicted  $^{154}\text{Eu}$  inventory is within about 10% of measurement, which is outside of the estimated  $\pm 5\%$  measurement uncertainty. It is important to note that earlier calculations using pre-ENDF/B-VI cross sections were in error by over 50%. The inventory of  $^{155}\text{Eu}$ , previously overpredicted by 14% using ENDF/B-IV data, is now within the experimental uncertainty using ENDF/B-VI cross sections.

The relatively large discrepancies observed for  $^{99}\text{Tc}$  and  $^{106}\text{Ru}$  are attributed to significant quantities of these nuclides remaining in the undissolved residues after recovery. The errors are likely attributable to the poor counting geometries used in analyzing these residues. The discrepancy in the  $^{129}\text{I}$  inventory is attributed to difficulties in capturing the iodine off-gases during recovery. A detailed review of the analytical measurements and associated uncertainties has been published earlier [21].

## 6.4 NEA Benchmark on PWR Isotopic Prediction

### 6.4.1 Description of the Benchmark

The Nuclear Energy Agency (NEA) Nuclear Science Committee (NSC) adopted one of a series of experiments designed to characterize irradiated fuel from light water reactors, as a benchmark for validating isotopic predictions by depletion codes [17]. This specific isotopic prediction benchmark was one part of a larger program carried out by the NEA/NSC to benchmark codes for burnup credit in criticality analyses.

The experimental nuclide inventory measurements were performed at the Materials Characterization Center (MCC) at Pacific Northwest Laboratories (PNL) as part of the United States Department of Energy Office of Civilian Radioactive Waste Management Program [22]. The used fuel in these experiments was designated as Approved Testing Material (ATM). The fuel material characterized at PNL was from Assembly D047 of the Calvert Cliffs Nuclear Power Plant (Unit

1), a pressurized water reactor (PWR), and designated ATM-104. The fuel assembly (D047) is a standard 14 x 14 assembly manufactured by Combustion Engineering, with 176 uranium oxide fuel rods. The fuel achieved a moderately high burnup of about 42 MWd/kgU. A detailed description of the assembly and the results of the experimental fuel characterization have been previously published [22].

The fuel, reactor lattice, and operating history specifications used in the depletion calculations are based on those provided in the NEA/NSC benchmark problem specifications [17]. The actual specifications of the assembly have been simplified to a simple pin cell for calculational purposes, preserving the fuel-to-moderator ratio equivalent to that in the two-dimensional fuel assembly. The specifications used in the calculations are listed in Table 27.

The irradiation history of the fuel was specified in four operating cycles, with reactor down times between cycles. The specific operating power and boron concentration in the coolant were varied for each cycle. The operating history corresponding to the low burnup (27.35 MWd/kgU) fuel sample 104-MKP109-LL is listed in Table 28. The benchmark specified history parameters for three used fuel samples, corresponding to exit burnup values of 27.35, 37.12 and 44.34 MWd/kgU. In the present calculations, only the 27.35 MWd/kgU burnup sample was used in the benchmark. The quoted burnup values are determined from measured data.

#### 6.4.2 Results

Chemical and radiochemical assays are available on the ATM-104 fuel pins for a comprehensive number of actinide and fission product isotopes. A detailed description of the radiochemical analysis procedures used to characterize the nuclide inventories of the fuel samples has been published [22]. Burnup was determined using measured  $^{148}\text{Nd}$  content, with a quoted uncertainty of about  $\pm 2.5\%$ .

The NEA/NSC benchmark [17] presents calculated results for an additional ten fission products, providing a numerical benchmark of these nuclides using other codes and data bases. Calculations contributed to the international benchmark include results from the codes LWR-WIMS (AEA Winfrith and Belgonucleaire), Apollo (CEA France), CASMO-3G (CSN Spain), SRAC and ORIGEN (JAERI), OREST (Germany), ORIGEN2 (NUPEC/INS), WIMS-AECL (AECL), and two submissions using the SAS2 sequence of SCALE (ORNL).

The present ORIGEN-S calculated results are compared in Table 29 with reference results presented in the NEA/NSC benchmark. The reference results are based on experimental measurements where the data was available, and the average of the calculated contributions when experimental data was not available. These are indicated as either E or C in the table, respectively.

The uranium and plutonium inventories are generally within several percent (the standard deviation in the measurements) of the measured values. The exceptions are  $^{234}\text{U}$  and  $^{238}\text{Pu}$ . The calculated  $^{238}\text{Pu}$  inventory is within 4% of the average value of all calculated values submitted in the calculational benchmark. It is worth noting that all WIMS calculations (including WIMS-

Table 27: Specifications for the ATM-104 PWR Fuel Inventory Calculations

Fuel material	3.038 wt% enriched UO <sub>2</sub>
Initial fuel compositions (atoms/(b·cm))	
<sup>234</sup> U	6.15165(-6) <sup>†</sup>
<sup>235</sup> U	6.89220(-4)
<sup>236</sup> U	3.16265(-6)
<sup>238</sup> U	2.17104(-2)
<sup>12</sup> C	9.13357(-6)
<sup>14</sup> N	1.04072(-5)
O	4.48178(-2)
Fuel density	10.045 g/cm <sup>3</sup>
Fuel diameter	0.9563 cm
Fuel temperature	841 K
Element pitch	1.5586 cm
Cladding material	Zircaloy-2
Cladding temperature	620 K
Cladding inside diameter	0.9860 cm
Cladding outside diameter	1.1180 cm
Coolant density	0.7569 g/cm <sup>3</sup>
Coolant temperature	558 K
Initial boron concentration	331 ppm
Exit burnup	27.35 MWd/kgU
Cooling time in days	1870

<sup>†</sup> Read as 6.15165 x 10<sup>-6</sup>.

Table 28: Specifications for the ATM-104 Assembly Irradiation History

Operating Cycle	Power (kW/kgU)	Irradiation (days)	Cooling (days)	Coolant Boron (Fraction of Initial)
1	17.24	306.0	71.0	1.000
2	19.43	381.7	83.1	1.419
3	17.04	466.0	85.0	1.523
4	14.57	461.1	1870	1.488

Table 29: Comparison of Calculated and Reference PWR Fuel Inventories

Isotope	Ref. Type <sup>‡</sup>	g/kg UO <sub>2</sub>		C/E
		Reference	Calculated	
U-234	E	1.600(-1)* ± 1.6%	1.758(-1)	1.09
U-235	E	8.470 ± 1.6%	8.114	0.96
U-236	E	3.140 ± 1.6%	3.282	1.05
U-238	E	8.425(+2) ± 1.6%	8.372(+2)	0.99
Pu-238	E	1.012(-1) ± 1.6%	8.165(-2)	0.81
Pu-239	E	4.264 ± 1.6%	4.271	1.00
Pu-240	E	1.719 ± 1.6%	1.700	0.99
Pu-241	E	6.812(-1) ± 1.6%	6.777(-1)	0.99
Pu-242	E	2.886(-1) ± 1.6%	2.948(-1)	1.02
Np-237 <sup>†</sup>	E	1.89(-4) ± 1.9%	1.696(-4)	0.90
Am-241 <sup>†</sup>	E	8.56(-1) ± 4.9%	8.279(-1)	0.97
Se-79 <sup>†</sup>	E	4.55(-5) ± 4.9%	4.950(-4)	10.8
Sr-90 <sup>†</sup>	E	4.59(+1) ± 5.7%	4.984(+1)	1.09
Mo-95	C	5.515(-1)	5.691(-1)	1.03
Tc-99 <sup>†</sup>	E	9.59(-3) ± 3.9%	1.011(-2)	1.05
Rh-103	C	3.462(-1)	3.491(-1)	1.01
Sn-126 <sup>†</sup>	E	1.25(-4) ± 10.2%	3.773(-4)	3.02
Cs-133	C	8.332(-1)	8.630(-1)	1.04
Cs-135 <sup>†</sup>	E	4.16(-4) ± 14%	4.308(-4)	1.04
Cs-137 <sup>†</sup>	E	6.71(+1) ± 3.5%	6.811(+1)	1.02
Nd-143	C	5.864(-1)	6.166(-1)	1.05
Nd-145	C	5.037(-1)	5.102(-1)	1.01
Sm-147	C	1.770(-1)	1.879(-1)	1.06
Sm-149	C	2.079(-3)	1.970(-3)	0.95
Sm-150	C	1.938(-1)	2.033(-1)	1.05
Sm-151	C	1.035(-2)	9.925(-3)	0.94
Sm-152	C	9.344(-2)	9.951(-2)	1.06
Eu-153	C	7.515(-2)	7.795(-2)	1.04
Gd-155	C	4.241(-3)	1.945(-3)	0.46

<sup>‡</sup> Indicates either experimental (E) or calculated (C) reference value.

\* Read as 1.600 x 10<sup>-1</sup>.

<sup>†</sup> These values are in units of Ci/kg UO<sub>2</sub>.

AECL) significantly underpredicted  $^{238}\text{Pu}$  by about a factor of two due to missing alpha decay chain information for  $^{244}\text{Cm}$ .

Neptunium, americium, and the fission product inventories are generally within about 5% of the measurements, or calculated inventories based on the average of the different code contributions. In most cases the present calculations agree to within 10% of the reference values quoted. The largest deviations are for  $^{79}\text{Se}$  and  $^{126}\text{Sn}$ , which are overpredicted by about a factor of ten and three, respectively. These discrepancies were also observed in ORIGEN2 calculations cited in the ATM-104 study [22], and their cause is unresolved.

A large factor of two discrepancy is observed for  $^{155}\text{Gd}$  that is not seen in most other calculated results. This is due to the use of ENDF/B-VI cross sections for the Eu isotopes in the ORIGEN-S calculations. Calculations repeated using pre-ENDF/B-VI  $^{154}\text{Eu}$  and  $^{155}\text{Eu}$  cross sections yielded similar results to the other codes, which also used for the most part older evaluations. The differences are due to large changes in the new evaluations [23] which yield significantly better Eu and Gd nuclide inventory predictions [10, 9].

The calculational model used in the benchmark is a simplification of assembly D047, and does not include the details of the control rod guide tubes, end fittings, or spacer grids. In addition, the low burnup sample 104-MKP109-LL was obtained from the bottom portion of rod MKP109, where leakage effects may be significant. The approximations in the model are the likely cause of the actinide discrepancies observed. This is supported by the close agreement of the present calculations with those reported in the NEA/NSC calculational benchmark results.

## 7 ANSI/ANS-5.1 DECAY HEAT CALCULATIONAL BENCHMARK

A calculational benchmark was performed that compares the results of ORIGEN-S against the current American National Standards Institute Standard ANSI/ANS-5.1-1979 (reaffirmed in 1985) for decay heat predictions [16]. The calculations were performed using a standard CANDU reactor 37-element fuel bundle model with nominal power rating and several irradiation times to represent low, middle, and high burnup fuel. Decay heat was compared over a range of cooling times from 1 to  $3 \times 10^9$  seconds (about 100 years).

The methods used in implementing the ANS-5.1-1979 decay heat standard are also described.

### 7.1 Description of the Benchmark

Three burnup values representing low (505 GJ/kgU), mid-range (685 GJ/kgU), and high (1045 GJ/kgU) CANDU fuel burnup were selected for ORIGEN-S and ANS-5.1 decay heat calculations. A constant power of 34.664 kW/kgU was applied in each of the three cases for an irradiation time required to reach the desired burnup, with no down times (zero power) during the irradiation. The

model specifications are those of a Bruce-A CANDU 37-element fuel bundle (see specifications in Table 20).

The ANS-5.1 Standard for decay heat states that it is limited to decay times up to  $10^9$  s (about 30~years). This benchmark has extended the comparison to longer cooling times and demonstrates that the standard compares favorably with the ORIGEN-S calculations up to at least  $3 \times 10^9$  seconds (100 years) after discharge for typical CANDU reactor fuel.

The principal quantity compared in this study is the total decay heat from fission products. Decay heating from activated light element (e.g., cladding) generally contributes less than about 1% to the total heating, and was not considered here. Heating from actinide decay becomes dominant at cooling times exceeding  $10^8$  s, but is a relatively small fraction of the total decay heat for CANDU fuel at shorter times. The ANS-5.1 Standard was developed primarily for predicting fission product decay heat, although expressions are presented for calculating actinide decay heating from  $^{239}\text{U}$  and  $^{239}\text{Np}$ , the dominant actinides for cooling times less than  $10^6$  s (12 days). The ANS-5.1 Standard representation of actinide decay heating was not used in this study. It has been calculated explicitly in the ORIGEN-S calculations as a means of assessing the impact of neglecting actinide heating when using the standard for calculating decay heat for CANDU reactor fuel.

## 7.2 Implementation of the ANS-5.1-1979 Standard

The ANSI/ANS-5.1-1979 Standard for decay heat provides data describing the recoverable energy release rates (decay heat power) due to fission products from thermal fission of  $^{235}\text{U}$  and  $^{239}\text{Pu}$ , and fast fission of  $^{238}\text{U}$  for cooling times up to  $10^9$  s. The ANS Standard values and uncertainties for  $^{235}\text{U}$  and  $^{239}\text{Pu}$  fission are based on statistical evaluation of available experimental data, and summation calculations using ENDF/B-IV nuclear data. The data for  $^{238}\text{U}$  is based on summation calculations due to a lack of experimental data.

The ANS Standard describes the fission product decay heat from a single fission event as a sum of 23 exponential contributions. For a single fission from nuclide  $k$ , the decay heat power (MeV/s) at a time  $t$  after the fission event is given by:

$$f_k(t) = \sum_{i=1}^{23} \alpha_{ki} e^{-\lambda_{ki} t}$$

where  $\alpha_{ki}$  and  $\lambda_{ki}$  are parameters given in the standard. This expression, when integrated with respect to the fission time  $T$  for a constant fission rate of unity, yields the expression:

$$F_k(t, T) = \int_{-T}^0 f_k(t - t') dt' = \sum_{i=1}^{23} \frac{\alpha_{ki}}{\lambda_{ki}} e^{-\lambda_{ki} t} [1 - e^{\lambda_{ki} T}]$$

**Table 30: CANDU Reactor Fuel Fission Fractions**

Burnup (MWh/kgU)	Fission Fractions <sup>†</sup>		
	<sup>235</sup> U	<sup>238</sup> U	<sup>239</sup> Pu
8.285	0.95	0.05	0.00
33.479	0.90	0.05	0.05
72.840	0.73	0.05	0.22
112.070	0.57	0.05	0.38
151.237	0.46	0.05	0.49
190.384	0.37	0.06	0.57
229.529	0.30	0.06	0.64
268.682	0.23	0.07	0.70
307.856	0.20	0.07	0.73
347.037	0.15	0.07	0.78

† Fractions rounded to two decimal places.

where  $F_k(t, T)$  is the decay heat power of nuclide  $k$  at a time  $t$  following unit fission rate for time  $T$ . The implementation of the ANS-5.1-1979 Standard used in the present calculations is based on FORTRAN-77 subroutines adopted from previous work on transient analysis studies [24]. This implementation expresses the fission rate of nuclide  $k$  in terms of the fraction  $a_k$  of the total recoverable fission power that comes from that nuclide. The fission rate for a given nuclide  $R_{fk}$  can then be expressed in terms of the total fission rate  $R_f$  by the relation  $R_{fk} = a_k R_f$ .

The expressions assume a constant operating power (fission rate) during irradiation, and a constant value of the recoverable energy per fission  $Q_k$  for each nuclide. The present analysis subdivided the irradiation history of the fuel assemblies into equal time intervals of ten days each. The time-dependent total recoverable energy  $Q$  for each interval was determined using values calculated by ORIGEN-S. Fission fractions for <sup>235</sup>U, <sup>238</sup>U, and <sup>239</sup>Pu at each interval were calculated using the WIMS-AECL lattice code with the ENDF/B-V cross-section library. Table 30 lists the fission fractions for a range of fuel burnup for a standard CANDU reactor irradiation. A cubic spline was fit to the data so that the fission fractions for each nuclide at any given time interval during the irradiation could be determined.

The ANS-5.1-1979 Standard equations are based on the decay heat following a single fission event, and therefore do not account for the effect of neutron capture in fission products during extended irradiations which will alter the fission product distribution. This generally acts to increase the decay heat due to neutron capture by stable fission products such as <sup>133</sup>Cs. To take these effects into account, the Standard uses an expression for a correction factor  $G(t, T)$  that is applied to  $F(t, T)$ . For cooling times less than  $10^4$  s, the correction factor is on the order of several percent.

For longer cooling times (between  $10^4$  and  $10^9$  s) the ANS Standard provides tabulated values for an upper bound on the correction factor,  $G_{max}(t)$ . These upper values are based specifically on Light Water Reactor (LWR) conditions: a) cross-sections averaged for a typical LWR spectrum, b)

constant power for four years, c) a thermal neutron flux of about  $2 \times 10^{14}$  n/(cm<sup>2</sup>·s), and d) <sup>235</sup>U thermal fission. For irradiation times and flux levels lower than these,  $G_{max}(t)$  will overestimate the capture correction. A graph of  $G_{max}(t)$  versus cooling time is shown in Figure 2. The correction is small below about  $10^4$  s, but increases to over 50% at  $10^8$  s cooling time.

The  $G_{max}(t)$  factor is expected to be highly conservative if used for CANDU reactor decay heat predictions on the basis of the much lower fuel burnup achieved in CANDU fuel relative to LWR fuel. While the thermal neutron flux is comparable between CANDU reactor and LWR fuel, the effective full power residence time of fuel bundles in CANDU reactors is typically about one quarter of the time used in the determination of  $G_{max}(t)$  for LWR applications. For the present study, the ORIGEN-S results were compared to the ANS-5.1-1979 Standard predictions with and without the  $G_{max}(t)$  factor applied, providing upper and lower bounding values.

### 7.3 Results

The results of the ANS-5.1-1979 Standard and ORIGEN-S predictions of fission product decay heat for CANDU reactor fuel irradiated to low (505 GJ/kgU), mid-range (685 GJ/kgU), and high (1045 GJ/kgU) burnup, are compared in Figures 3–5, respectively, for cooling times from 1 to over  $10^9$  s. The ANS Standard results are graphed with and without the correction for neutron capture in fission products.

The ORIGEN-S results for all three CANDU reactor cases compare very favorably with the ANS-5.1 predictions without any correction for neutron capture, confirming that the  $G_{max}(t)$  factor is highly conservative when applied to typical CANDU reactor fuel. When the  $G_{max}(t)$  correction for neutron capture in fission products is applied to the ANS-5.1 Standard values they exceed the ORIGEN-S results up to the  $10^9$  s range of application of the standard.

The ORIGEN-S and ANS-5.1 Standard (without corrections) results are within about  $\pm 3\%$  up to a cooling time of 1 year ( $3 \times 10^7$  s) for the high burnup (1045 GJ/kgU) case, and up to about three years ( $10^8$  s) for the two lower burnup cases. A maximum difference of 13% occurs for the high burnup case near  $10^8$  s, where the  $G_{max}(t)$  values are largest (see Figure 2). The  $1 \sigma$  uncertainty in the ANS Standard results (neglecting the effect of neutron capture) is nuclide dependent, but is typically about 5% at cooling times greater than a few seconds [16].

When the neutron capture correction is applied, the ANS-5.1 Standard results dramatically over-predict the fission product decay heat, by several percent at short cooling times, to about 50% at  $10^8$  s. The present results suggest that values of  $G(t, T)$  for CANDU reactor fuel decay heat predictions are near unity for most decay times less than  $10^9$  s. Values greater than unity occur over limited cooling times between  $10^8$  and  $3 \times 10^8$  s, and will not exceed a value of about 1.1 for mid-range burnup fuel. In all cases, the ORIGEN-S results were within the envelope of the ANS-5.1 Standard results.

Additional calculations were performed to assess the impact of actinide decay heating, which is not

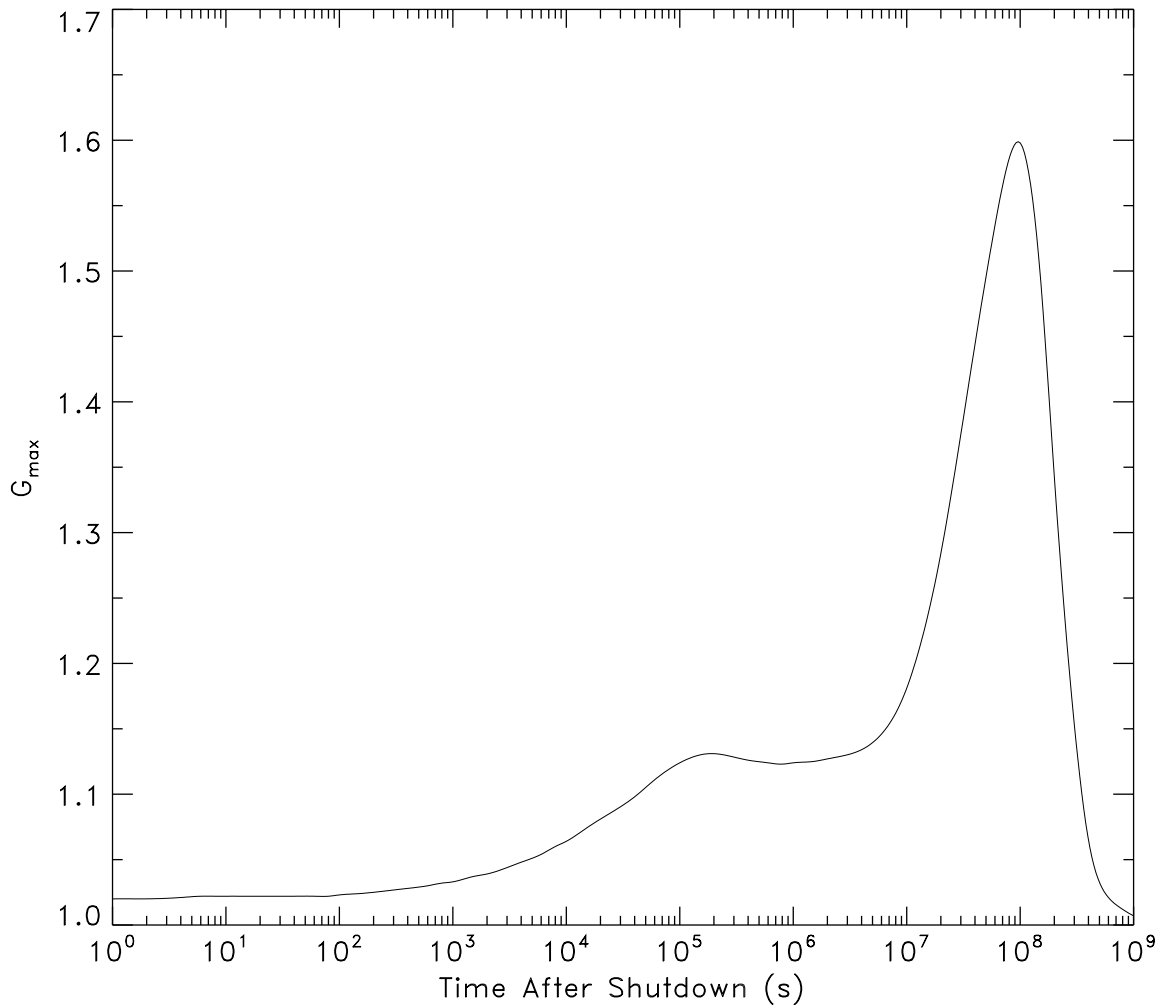


Figure 2: The Maximum Correction Factor for Neutron Capture in Fission Products  $G_{max}(t)$  as a Function of Cooling Time Since Irradiation as Prescribed by the ANSI/ANS-5.1-1979 Decay Heat Standard. The factors are based on conservative irradiation history parameters for LWR fuel.

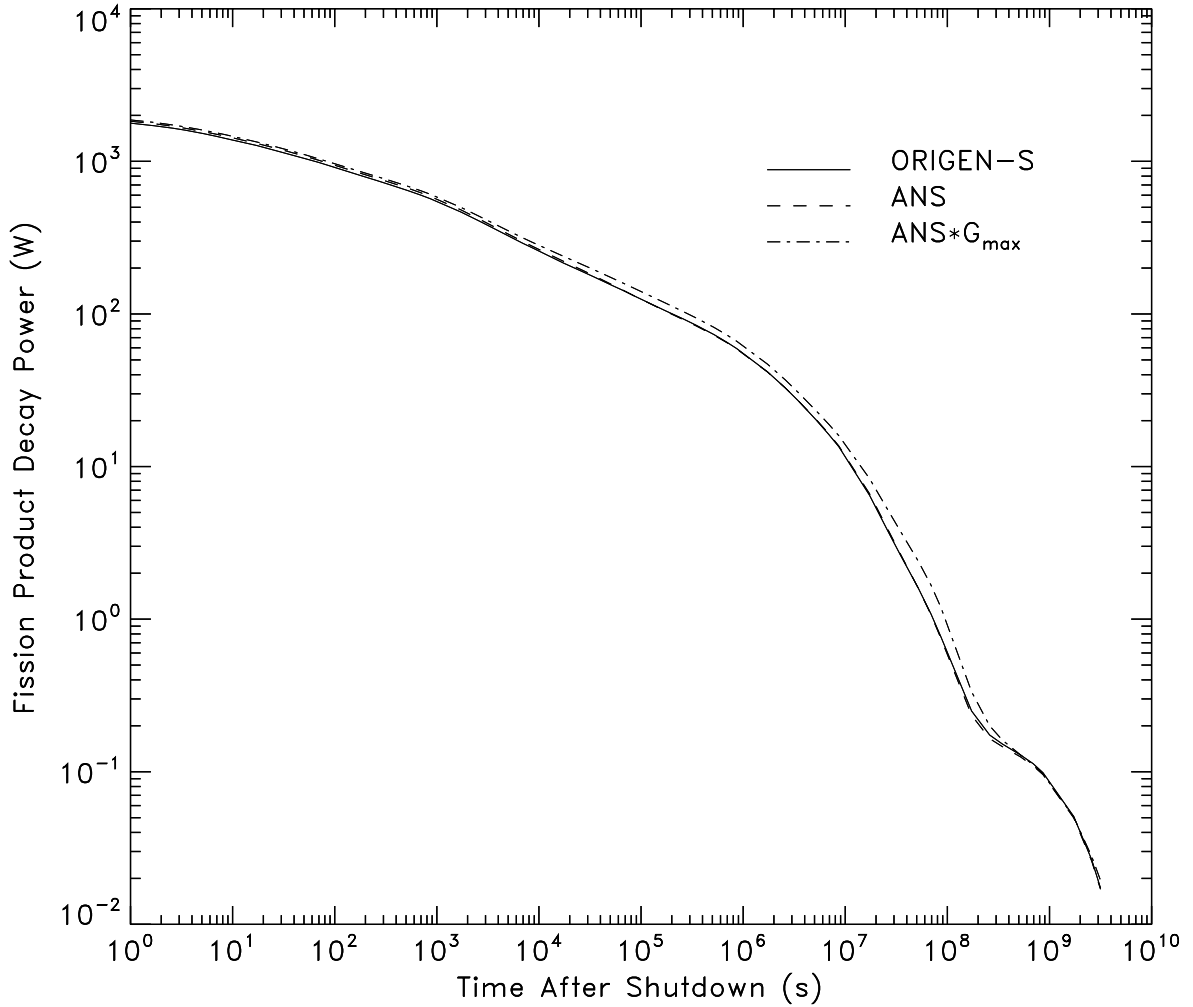


Figure 3: Comparison of Fission Product Decay Heat Predictions by ORIGIN-S and the ANS-5.1-1979 Standard for CANDU Reactor Fuel with a Low Burnup of 505 GJ/kgU. The ANS Standard curves correspond to values obtained with and without the correction factor for neutron capture in fission products.

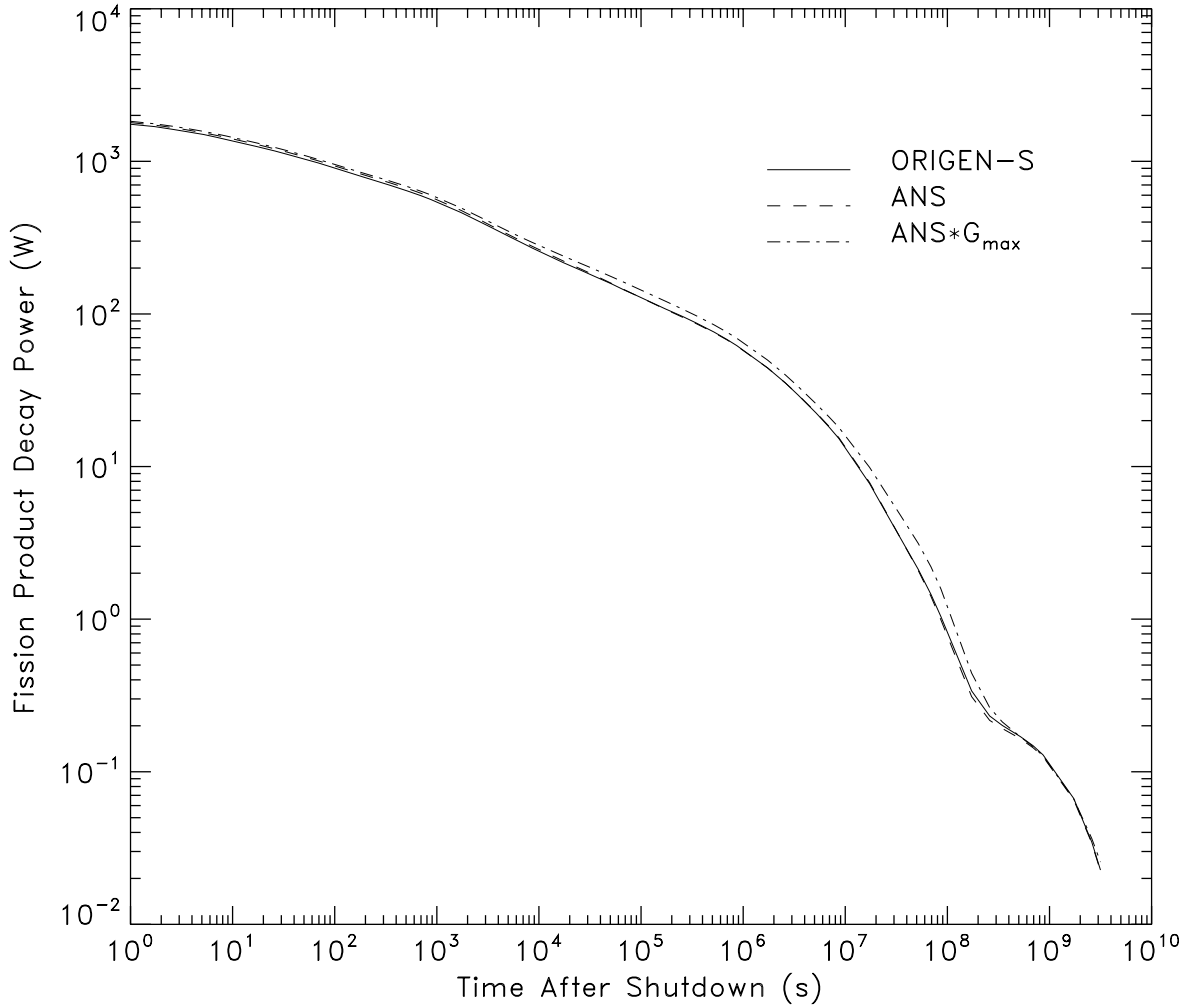


Figure 4: Comparison of Fission Product Decay Heat Predictions by ORIGIN-S and the ANS-5.1-1979 Standard for CANDU Reactor Fuel with a Mid-Range Burnup of 685 GJ/kgU. The ANS Standard curves correspond to values obtained with and without the correction factor for neutron capture in fission products.

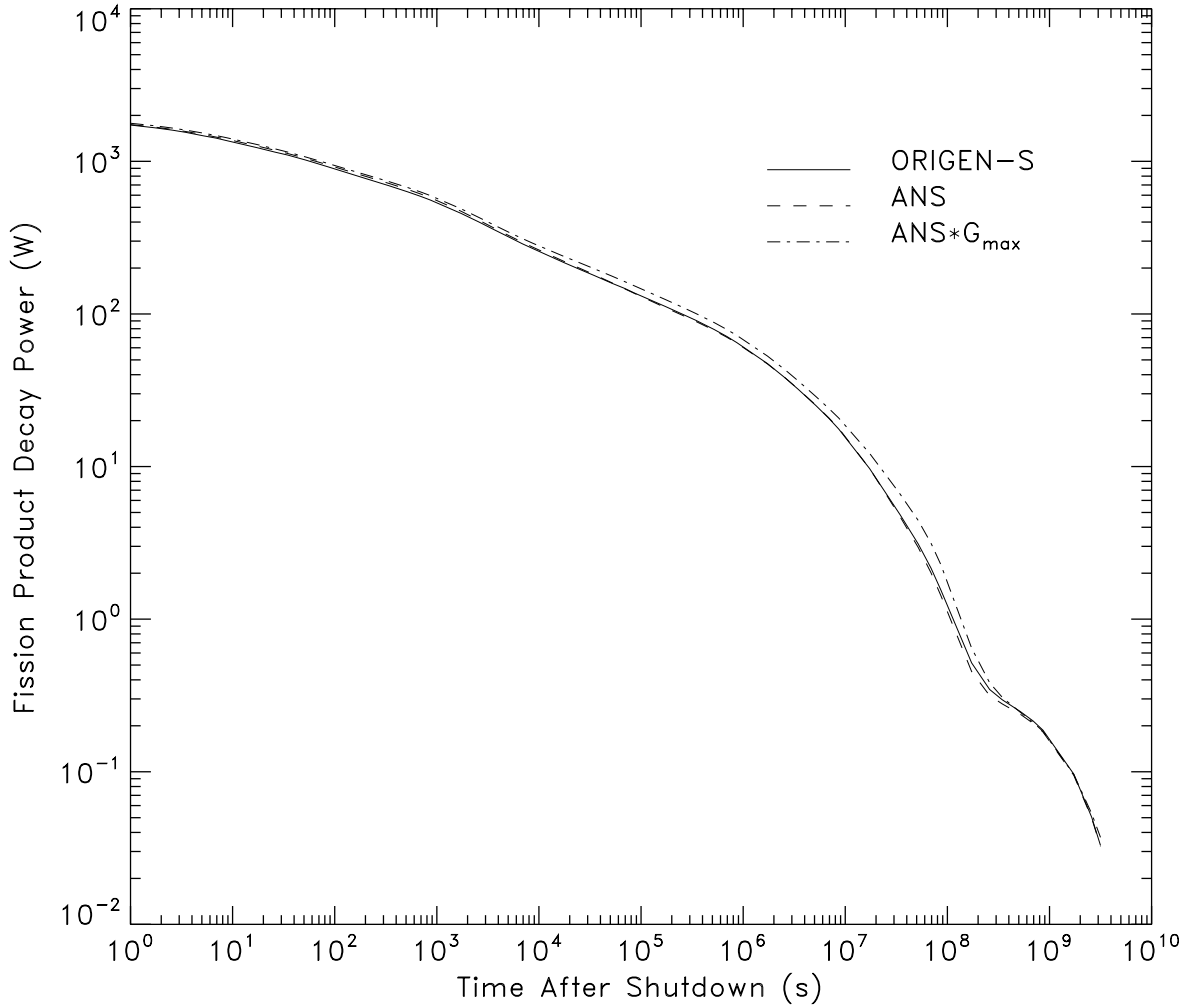


Figure 5: Comparison of Fission Product Decay Heat Predictions by ORIGEN-S and the ANS-5.1-1979 Standard for CANDU Reactor Fuel with a High Burnup of 1045 GJ/kgU. The ANS Standard curves correspond to values obtained with and without the correction factor for neutron capture in fission products.

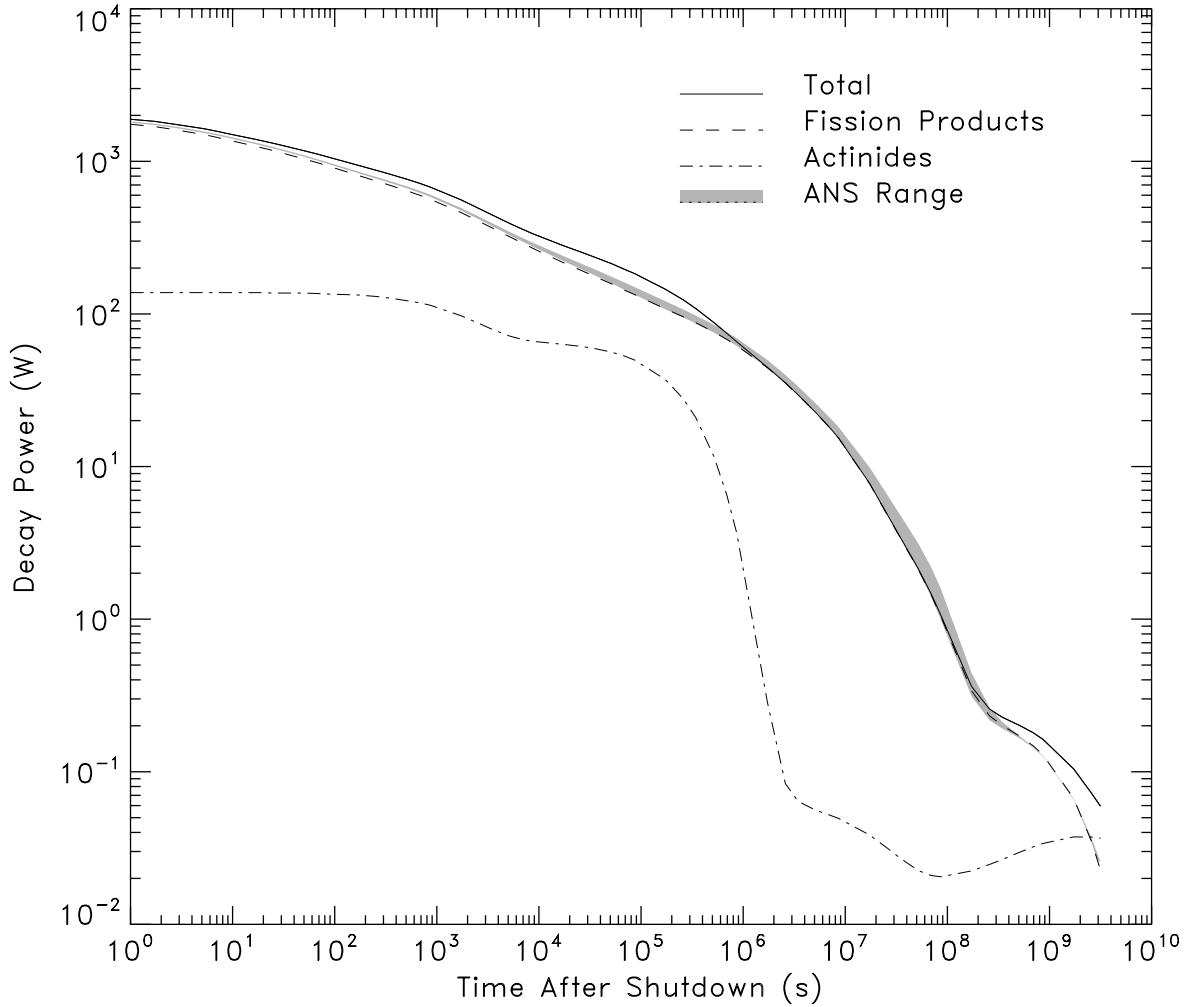


Figure 6: Comparison of Fission Product, Actinide, and Total Decay Heat Predictions by ORIGEN-S with the ANS-5.1-1979 Standard for 685 GJ/kgU Burnup CANDU Reactor Fuel. The ANS Standard results are indicated by the shaded area, and represent the range of values obtained with and without applying the  $G_{max}(t)$  correction factor for neutron capture in fission products.

treated rigorously by the ANS-5.1 Standard. Figure 6 compares the fission product, actinide, and total decay heat power calculated by ORIGEN-S against the ANS Standard results with and without the neutron capture correction (represented as the shaded area in the figure) for a CANDU reactor fuel burnup of 685 GJ/kgU. The ANS Standard curves do not include the actinide contribution.

The figure shows that actinide heating is an important component of the total heating at times less than  $10^6$  s and times greater than about  $10^8$  s. Below  $10^4$  s actinide decay heat contributes up to about 10% of the total, and increases to over 25% at  $10^5$  s. Between  $10^6$  and  $10^8$  s their contribution is negligible. Above  $10^9$  s actinide heating is the dominant term. These results indicate that the ANS-5.1 Standard results must be corrected for actinide heating at certain cooling times.

An analysis of the principal fission product contributors to the decay heat indicates that for cooling times between about one and three years the dominant nuclides are  $^{144}\text{Pr}$  and  $^{106}\text{Rh}$ . For longer times (to a maximum of 100 years) the dominant nuclides are  $^{90}\text{Y}$ ,  $^{90}\text{Sr}$ ,  $^{137m}\text{Ba}$ , and  $^{137}\text{Cs}$ . For shorter cooling times in the order of hours to days, heating is dominated by a large number of nuclides including  $^{140}\text{La}$  and number of iodine isotopes. A similar analysis of the principal actinides showed that in the first 200 s the dominant contributors are  $^{239}\text{U}$  (50.4%) and its daughter  $^{239}\text{Np}$  (48.6%).  $^{239}\text{Np}$  then becomes the dominant heat source (99%) at 8000 s and then rapidly declines. Above 1000 days ( $9 \times 10^7$  s)  $^{241}\text{Am}$ , produced from beta-decay of  $^{241}\text{Pu}$ , becomes the major actinide source, and it dominates the total decay heat after about 50 years.

In summary, the ORIGEN-S results have been shown to be in good agreement with those of the ANSI/ANS-5.1-1979 Decay Heat Standard for a range of CANDU fuel burnup. The ANS Standard provides a good benchmark against which to compare code predictions, particularly for cooling times less than about  $10^5$  s where the standard is based largely on experimental measurements, and the correction factor for neutron capture is relatively small. Above  $10^5$  s the standard relies heavily on summation calculations and may require use of a problem-dependent correction factor for neutron capture, and is therefore less of an independent benchmark. Definitive testing of the code and nuclear data however, particularly for CANDU reactor fuel, requires decay heat measurements for benchmarking.

## 8 DOUGLAS POINT CANDU FUEL DECAY HEAT STUDY

Decay heat measurements performed by Ontario Hydro using Douglas Point CANDU reactor fuel bundles [25] are compared here against the calculated results of ORIGEN-S, and those of ANSI/ANS-5.1-1979 [16], the American National Standard for decay heat power. The experimental program to measure the decay heat for irradiated CANDU fuel was initiated in 1976 with the primary objective of establishing a data base against which the accuracy of present and future methods of decay heat prediction could be assessed. The program involved experimental measurements on seventeen irradiated bundles with cooling times ranging from 47 days to 5.5 years. This section compares the results of the ORIGEN-S calculations and the ANS-5.1-1979 Standard against the measured data. The methods used in implementing the ANS-5.1 Standard are described earlier in Section 7.2.

## 8.1 Description of the Douglas Point Fuel Measurements

The decay heat measurements from each bundle were obtained using a flow-calorimetric technique which measured the temperature change of water before and after it flowed past the bundle. The rise in the water temperature  $\Delta T$  is related to the magnitude of the heat source  $Q$  by  $Q = \rho \cdot C_p \cdot \dot{m} \cdot \Delta t$ , where  $\rho$  is the density of the heat transfer medium (water),  $C_p$  is the heat capacity of water, and  $\dot{m}$  is the mass flow rate across the heat source.

A calibration curve for the calorimeter was created by using an electrically powered simulation fuel bundle. The calibration curve was used to correct each measurement for heat transfer losses and flow effects in the calorimeter. The combined uncertainty in the measurements, assuming error sources are not correlated, was estimated to be  $\pm 3\%$ .

Additional correction factors were required to account for gamma radiation leakage from the flow calorimeter. The decay heat measured by the calorimeter will be lower than the actual total decay heat since a fraction of the energy associated with gamma decay will escape with the emitted photons. Since the calculated parameter was total bundle decay heat, either the calculations or the measurement had to be adjusted to normalize the quantity compared in the benchmark. In this study, the measurements were corrected for gamma leakage, and the quantity used in all comparisons was total decay heat.

The gamma escape factors were calculated and reported in the original report [25] based on 1-D radiation transport calculations using the ANISN code [28], and have been used in the present study. The treatment of gamma energy leakage is described in the following section.

In an attempt to reduce the uncertainty in the power histories of the Douglas Point reactor fuel, irradiated fuel bundles which had resided in a single fuel channel over their lifetime in the reactor were selected where possible. The irradiation history of each fuel bundle used in the study is listed in Table 31. The histories were obtained from the fuel scheduling code SORO [26] in conjunction with the daily log of the Douglas Point reactor power.

A recent analysis of the SORO code [27] which compared computed bundle burnup with chemical assay-determined burnup, indicates that SORO overpredicts bundle average burnup at burnups less than about 200 MWh/kgU and underpredicts when the burnup exceeds this amount. The errors do not exceed about 4% for typical CANDU reactor exit burnup fuel. Correlations between experimentally determined burnup and SORO calculated burnup can be used to adjust calculated burnup using a linear regression relationship [27]. The last column in Table 31 shows corrected bundle powers which were used in all calculations. These were calculated by taking the final uncorrected (SORO) bundle burnup and applying the linear regression fit to get a corrected burnup. The ratio of the corrected to the uncorrected exit burnup was then applied to the bundle power over its entire irradiation history.

Table 31: Douglas Point Fuel Bundle Irradiation Histories

Bundle Identification Irradiation Period	Irradiation (days)	Bundle Power (kW)	Burnup (MWh/kgU)	Corrected Power (kW)
G1606	62	326.9	35.9	331.6
Aug 29/75 - Aug 18/76	37	0	35.9	0
Cooling Time (days): 49	24	176.4	43.4	178.9
	24	364.6	58.9	369.8
	6	0	58.9	0
	55	327.5	90.8	332.2
	6	0	90.8	0
	62	388.8	133.5	394.4
	30	369.9	153.1	375.2
	49	305.3	179.6	309.7
H0206	246	226.8	98.8	230.9
Feb 26/75 - Aug 18/76	37	0	98.8	0
Cooling Time (days): 47	24	103.5	103.2	105.4
	24	162.3	110.1	165.2
	6	0	110.1	0
	55	235.5	134.8	239.7
	6	0	134.8	0
	62	246.8	161.9	251.2
	79	230.1	194.1	234.2
E0906	94	352.0	58.6	357.1
Oct 13/74 - Aug 20/75	12	0	58.6	0
Cooling Time (days): 410	35	350.0	80.3	355.1
	56	368.0	116.8	373.4
	31	315.1	134.1	319.7
	30	346.3	152.5	351.4
	31	313.3	169.7	317.9
	20	335.9	180.8	340.8
F1206	112	403.3	80.0	410.7
Sep 26/74 - Aug 1/75	12	0	80.0	0
Cooling Time (days): 428	35	379.1	103.5	368.1
	56	366.0	139.8	372.8
	31	340.6	158.5	346.9
	30	380.2	178.7	387.2
	31	318.7	196.2	324.6

Table 31: (continued) Douglas Point Fuel Bundle Irradiation Histories

Bundle Identification Irradiation Period	Irradiation (days)	Bundle Power (kW)	Burnup (MWh/kgU)	Corrected Power (kW)
N0806	49	320.3	27.8	326.0
Nov 12/73 - Aug 1/75	31	151.2	36.1	153.9
Cooling Time (days): 426	59	303.3	67.8	308.7
	74	127.4	84.5	129.7
	31	0	84.5	0
	24	221.1	95.9	225.1
	163	339.8	194.0	345.9
	12	0	194.0	0
	183	294.6	289.5	299.9
R1706	49	159.0	13.8	162.0
Nov 12/73 - Oct 21/75	31	85.6	18.5	87.2
Cooling Time (days): 345	59	175.1	36.8	178.4
	74	78.6	47.1	80.1
	31	0	47.1	0
	187	206.7	115.6	210.5
	12	0	115.6	0
	154	195.0	168.8	198.6
	111	141.4	196.6	144.0
T0906	106	157.7	29.6	161.2
Nov 6/74 - Feb 23/76	103	125.0	52.2	127.8
Cooling Time (days): 224	33	0	52.2	0
	196	186.4	116.9	190.6
	13	0	116.9	0
	273	165.0	196.7	168.7
	37	0	196.7	0
	78	132.5	215.0	135.5
B1106	162	252.3	72.4	257.0
Feb 1/74 - Feb 13/75	11	0	72.4	0
Cooling Time (days): 596	9	175.6	75.2	178.9
	88	0	75.2	0
	229	130.4	128.1	132.8
	33	0	128.1	0
	184	195.4	191.8	199.1
	13	0	191.8	0
	15	207.0	197.3	210.9

Table 31: (continued) Douglas Point Fuel Bundle Irradiation Histories.

Bundle Identification Irradiation Period	Irradiation (days)	Bundle Power (kW)	Burnup (MWh/kgU)	Corrected Power (kW)
R1206	40	220.2	15.6	223.9
Feb 24/72 - Aug 15/74	270	0	15.6	0
Cooling Time (days): 776	214	256.7	112.9	261.0
	88	0	112.9	0
	65	231.9	139.6	235.8
	31	105.6	145.4	107.4
	135	143.4	179.7	145.8
	33	0	179.7	0
	29	186.9	189.13	190.0
G1706	165	272.1	80.0	276.4
Oct 18/71 - Nov 12/73	273	0	80.0	0
Cooling Time (days): 1048	76	292.3	119.4	296.9
	7	0	119.4	0
	106	287.6	173.4	292.1
	16	0	173.4	0
	9	250.9	177.4	254.9
	88	0	177.4	0
	15	293.6	185.2	298.2
L1006	38	433.8	29.2	448.0
Jun 28/71 - Feb 28/74	76	0	29.2	0
Cooling Time (days): 943	166	340.1	129.2	351.3
	270	0	129.2	0
	214	285.7	237.5	295.1
	88	0	237.5	0
	65	279.7	269.7	288.9
	31	122.0	276.4	126.0
	28	219.8	287.3	227.0
H0906	105	395.2	73.5	407.9
Apr 22/71 - Nov 12/73	76	0	73.5	0
Cooling Time (days): 1050	166	314.6	166.0	324.7
	270	0	166.0	0
	192	294.1	266.0	303.5
	13	0	266.0	0
	9	282.3	270.5	291.4
	88	0	270.5	0
	17	338.7	280.7	349.6

Table 31: (continued) Douglas Point Fuel Bundle Irradiation Histories

Bundle Identification Irradiation Period	Irradiation (days)	Bundle Power (kW)	Burnup (MWh/kgU)	Corrected Power (kW)
K0707	135	363.8	87.0	377.2
Mar 20/71 - Mar 7/74	76	0	87.0	0
Cooling Time (days): 936	166	319.4	180.9	331.1
	270	0	180.9	0
	214	259.9	279.4	269.5
	88	0	279.4	0
	65	278.8	311.5	289.0
	31	120.2	318.1	124.6
	35	172.6	328.8	178.9
5622	102	259.9	46.6	269.6
Jul 10/69 - Dec 14/71	31	0	46.6	0
Cooling Time (days): 1749	161	229.0	111.9	237.5
	165	244.0	183.2	253.1
	41	0	183.2	0
	258	270.0	306.4	280.0
	76	0	306.4	0
	53	282.3	333.9	292.8
5112	124	22.8	5.0	23.4
Nov 1/68 - Feb 29/72	127	0	5.0	0
Cooling Time (days): 1680	355	22.6	19.2	23.2
	103	243.4	63.6	249.8
	41	0	63.6	0
	258	249.5	177.6	256.0
	76	0	177.6	0
	132	249.8	236.0	256.3
4821	230	26.0	10.6	27.0
May 15/67 -Mar 25/71	181	169.1	64.8	175.4
Cooling Time (days): 2014	243	187.3	145.4	194.3
	127	0	145.4	0
	113	152.4	175.9	158.1
	181	159.1	226.9	165.0
	165	206.3	287.2	214.0
	41	0	287.2	0
	120	223.1	334.6	231.4

Table 31: (concluded) Douglas Point Fuel Bundle Irradiation Histories

Bundle Identification Irradiation Period	Irradiation (days)	Bundle Power (kW)	Burnup (MWh/kgU)	Corrected Power (kW)
4640	230	7.6	3.1	7.8
May 15/67 - Sep 22/70	151	59.4	19.0	60.9
Cooling Time (days): 2200	50	0	19.0	0
	227	127.8	70.4	131.0
	127	0	70.4	0
	105	200.6	107.5	205.5
	31	0	107.5	0
	161	208.7	167.0	213.8
	144	236.3	227.3	242.1

## 8.2 Gamma Energy Leakage

The measured results were adjusted for gamma leakage from the calorimeter. The path lengths of alpha and beta particles in the calorimeter system are such that virtually all of their energy will produce measurable heat within the calorimeter. On the other hand, a substantial amount of the emitted gamma radiation will penetrate the calorimeter walls and be absorbed outside the calorimeter. The gamma leakage fractions were calculated previously with the discrete ordinates radiation transport code ANISN [28] using an model of the calorimeter to determine the amount of gamma radiation which escaped as a function of photon energy. The gamma energy spectrum is dependent on cooling time, and the gamma leakage factors will therefore be somewhat bundle dependent.

The gamma leakage factors for each fuel bundle were taken from the original report [25]. The determination of the total correction to the decay heating also requires the fraction of the total decay heat that is due to gamma decay. This fraction was determined from the present ORIGEN-S calculations.

Table 32 lists the measured (calibrated) decay heat, the calculated fraction of the total gamma energy escaping the calorimeter [25], the calculated fraction of the total decay heat attributed to gamma decay processes from ORIGEN-S, and the final measured decay heat corrected for gamma leakage. The net correction factor for each bundle was calculated as  $1/(1 - \epsilon_{gam}\epsilon_{esc})$  where  $\epsilon_{gam}$  and  $\epsilon_{esc}$  are the gamma heat fraction and the gamma escape fraction respectively. The uncertainty in the gamma leakage correction is estimated at  $\pm 1\%$ , leading to an overall uncertainty of the corrected decay heat measurements of less than  $\pm 4\%$  [25]. The uncertainty in the irradiation history and exit burnup is estimated to be  $\pm 5\%$ .

Table 32: Summary of Measured Decay Heat Data and Correction Factors

Bundle	Cooling (days)	$\epsilon_{esc}$	$\epsilon_{gam}$	Decay Heat (watts)	
				Measured	Corrected*
G1606	49	0.189	0.504	231.3	255.6
H0206	47	0.191	0.490	186.6	205.9
T0906	224	0.178	0.246	51.3	53.6
R1706	345	0.179	0.190	35.1	36.3
E0906	410	0.178	0.178	38.7	40.0
N0806	426	0.182	0.185	50.3	52.1
F1206	428	0.178	0.173	40.8	42.1
B1106	596	0.181	0.175	20.1	20.8
R1206	776	0.181	0.193	14.9	15.4
L1006	943	0.182	0.247	17.0	17.8
K0707	936	0.183	0.266	18.1	19.0
G1706	1048	0.182	0.229	9.5	9.9
H0906	1050	0.182	0.264	14.0	14.7
5112	1680	0.180	0.315	5.6	5.9
5622	1749	0.181	0.351	9.5	10.1
4821	2014	0.181	0.369	8.2	8.8
4640	2200	0.184	0.343	5.6	6.0

\* Total decay heat corrected for gamma energy losses.

### 8.3 Calculations using the ANSI/ANS-5.1-1979 Standard

The ANS-5.1-1979 Standard calculations of the Douglas Point fuel decay heat were performed using the same methodology used in the decay heat calculational benchmark (see Section 7.2). The irradiation times were subdivided according to those listed in Table 31, and average values of the fission fractions, and recoverable energy per fission were estimated as before.

Table 33 presents the ANS-5.1 Standard decay heat results for the seventeen bundles. The results with and without the neutron capture correction factor  $G_{max}(t)$  are presented for comparison, and represent upper and lower bounds on the ANS-5.1 Standard results. Note that the actinide decay heat contribution over the cooling times of the measurements is negligible, and the results from ANS-5.1 therefore do not require any correction for their omission (see Figure 6). The correction factor for neutron capture however is significant for the cooling times of interest, ranging from about a 10 to 60% correction.

### 8.4 Calculations using the ORIGEN-S Code

Separate calculations were performed using ORIGEN-S with cross-section libraries generated that reflected the specific power and irradiation history of each fuel bundle. The irradiation time steps and corrected bundle powers in Table 31 were used for each calculation. The results of the ORIGEN-S analyses for each bundle are given in Table 34. The table lists the total and the gamma component of the decay heat (used to determine the correction factors for the measurements), and the final exit burnup of the fuel.

### 8.5 Summary of Douglas Point Fuel Decay Heat Study

The results of the measured decay heat and calculated decay heat using the ORIGEN-S code and ANS-5.1-1979 Standard are summarized in Table 35. The ANS-5.1 Standard results given in the table do not include the neutron capture correction. The data are shown in Figure 7, with the ANS-5.1 Standard results shown as the shaded area representing the range with and without the conservative neutron capture correction for LWR fuel.

The figure displays the decay heat results as a function of bundle cooling time. However, not all bundles had similar exit burnup values, and as a result the decay heat curve is not a smooth one. The cooling times of some bundle were also shifted (in the figure only) to avoid overlapping the results of bundles with very similar cooling times.

Table 33: ANS-5.1 Decay Heat Standard Results for Douglas Point Fuel

Bundle	Cooling (days)	$G_{max}(t)$	ANS-5.1 Decay Heat (watts)	
			Unadjusted	$G_{max}(t)$ Adjusted
G1606	49	1.135	284.3	322.7
H0206	47	1.134	217.5	246.7
E0906	410	1.415	39.8	56.3
F1206	428	1.425	41.0	58.4
N0806	426	1.424	50.2	71.5
R1706	345	1.373	37.5	51.4
T0906	224	1.278	51.8	66.2
B1106	596	1.502	20.4	30.6
R1206	776	1.557	13.7	21.3
G1706	1048	1.597	8.79	14.0
L1006	943	1.588	15.6	24.8
H0906	1050	1.597	12.5	19.9
K0707	936	1.587	16.7	26.4
5622	1749	1.495	7.92	11.8
5112	1680	1.512	6.17	9.32
4821	2014	1.421	6.66	9.46
4640	2200	1.371	4.50	6.17

Table 34: Decay Heat for Douglas Point Fuel Calculated using ORIGEN-S

Bundle	Cooling (days)	Burnup (MWh/kgU)	Decay Heat (watts)	
			Gamma	Total
G1606	49	182.2	142.2	282.2
H0206	47	195.8	104.3	212.9
E0906	410	184.6	7.2	40.7
F1206	428	199.8	7.3	42.4
N0806	426	292.6	9.9	53.6
R1706	345	200.2	7.4	39.2
T0906	224	220.0	13.1	53.5
B1106	596	199.1	3.8	21.8
R1206	776	192.5	2.9	15.0
G1706	1048	187.6	2.2	9.8
L1006	943	296.7	4.4	18.0
H0906	1050	289.7	3.8	14.4
K0707	936	344.2	5.2	19.7
5622	1749	345.8	3.4	9.6
5112	1680	242.3	2.3	6.8
4821	2014	347.1	3.0	7.4
4640	2200	233.1	1.8	4.8

Table 35: Summary of Douglas Point Fuel Measured and Calculated Decay Heat

Bundle	Cooling (days)	Decay Heat (watts)			C/E <sup>†</sup>	
		Measured	ANS-5.1	ORIGEN-S	ANS-5.1	ORIGEN-S
G1606	49	255.6	284.3	282.2	1.11	1.10
H0206	47	205.9	217.5	212.9	1.06	1.03
E0906	410	40.0	39.8	40.7	1.00	1.02
F1206	428	42.1	41.0	42.4	0.97	1.01
N0806	426	52.1	50.2	53.6	0.96	1.03
R1706	345	36.3	37.5	39.2	1.03	1.08
T0906	224	53.6	51.8	53.5	0.97	1.00
B1106	596	20.8	20.4	21.8	0.98	1.05
R1206	776	15.4	13.7	15.0	0.89	0.97
G1706	1048	9.9	8.79	9.8	0.89	0.99
L1006	943	17.8	15.6	18.0	0.88	1.01
H0906	1050	14.7	12.5	14.4	0.85	0.98
K0707	936	19.0	16.7	19.7	0.88	1.04
5622	1749	10.1	7.92	9.6	0.78	0.95
5112	1680	5.9	6.17	6.8	1.05	1.15
4821	2014	8.8	6.66	7.4	0.76	0.84
4640	2200	6.0	4.50	4.8	0.75	0.80

<sup>†</sup> Ratio of calculated to measured values.

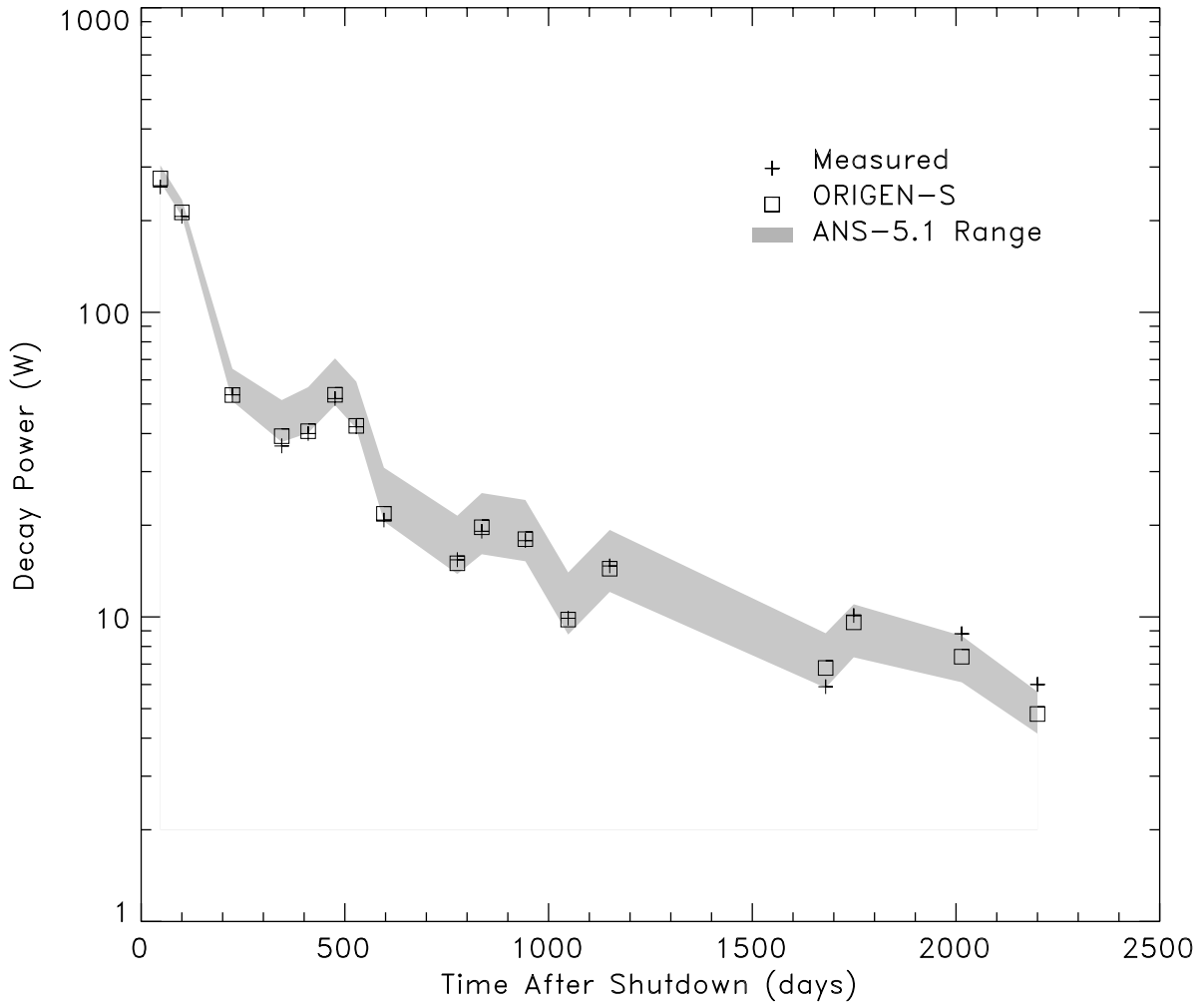


Figure 7: Comparison of the Measured and Calculated Decay Heat from Douglas Point Reactor Fuel. The calculations include the ORIGEN-S code and the ANS-5.1-1979 decay heat standard. The ANS Standard results are shown as the shaded area, representing the range with and without the conservative correction factor to account for neutron capture in fission products. Note that the curve is not smooth as a result of the different exit burnup of the bundles used in the study.

As expected the ANS-5.1 Standard accurately predicts the decay heat at the shorter cooling time where the neutron capture correction is small, and tends to underestimate the decay heat at the longer cooling times. The affect of not accounting for neutron capture in CANDU fuel is estimated to be about 10% based on the ANS-5.1 Standard calculational benchmark. The results are overestimated by approximately 20 to 40% throughout when the  $G_{max}(t)$  correction factor is applied.

The ORIGEN-S results fall within a range of -3% to +8% of the measurements if the last three bundles with the longest cooling times are excluded. Two of these bundles (5112 and 4640) were identified in the original report [25] as having questionable irradiation history parameters, however, no further information was available. Excluding the two questionable bundles, the standard error of the ORIGEN-S results is  $\pm 6\%$ , with an average calculated to measured ratio of 1.004. This is within the overall combined uncertainty of the experiment and irradiation history parameters of  $\pm 7\%$ . If a third bundle 4821 is removed from the data, the average calculated to measured ratio becomes  $1.016 \pm 3.5\%$ .

## 9 $^{235}\text{U}$ AND $^{239}\text{Pu}$ FISSION PRODUCT ENERGY RELEASE BENCHMARK

Fission product energy release rates following thermal neutron fission of  $^{235}\text{U}$  and  $^{239}\text{Pu}$  have been measured and reported for times after irradiation between 2 and 14000 s (4 hours) [29, 30]. The experiments involved short irradiations of fissile material in the Oak Ridge Research Reactor (ORR) of between 1 and 100 s. The published data includes the total energy release rates (decay heat) from both beta and gamma decay. The primary objective of the original experiments was to reduce the uncertainty in the short term fission product energy release rate for application to loss-of-coolant accident (LOCA) analyses.

This benchmark compares the ORIGEN-S code results with the measured energy releases following short irradiations of  $^{235}\text{U}$  and  $^{239}\text{Pu}$ , providing additional validation of the ORIGEN-S methods and nuclear data base for the fission product isotopes important to short-term decay heating. The study provides a more rigorous benchmark of the nuclear data by interrogating individually the beta and gamma decay components. In addition, the benchmark provides an opportunity to verify the numerical methods of the integral option of ORIGEN-S since all measurements are reported as integral energy release (MeV) over the specified counting times of the experiment.

### 9.1 Description of the ORR Experiments

Samples of enriched  $^{235}\text{U}$  and  $^{239}\text{Pu}$  of mass between 1 to 10  $\mu\text{g}$  were irradiated between 1 and 100 s at a constant thermal neutron flux of approximately  $3 \times 10^{13} \text{ n}/(\text{cm}^2 \cdot \text{s})$ . The gamma and beta spectral data  $N(E_\gamma)$  and  $N(E_\beta)$  from decay emissions were collected separately for cooling times from 2 to 14000 seconds. Gamma measurements were performed using a NaI detector, while beta spectra were obtained using an NE-110 detector. The beta and gamma spectra were subsequently

unfolded to provide spectral distributions that were integrated over energy to provide total energy integrals as a function of time after irradiation. Corrections were made to the integral data to account for fission-product gas loss.

## 9.2 $^{235}\text{U}$ Results

The ORIGEN-S calculations were performed using irradiation times and fissile material sample sizes that closely matched those used in the experiments. Following irradiation, the integral option of ORIGEN-S was used to obtain integral heating over the time intervals used in the experiments. The option provides integral results for all time dependent quantities for fission products only. The beta decay heat was obtained from the difference of the total and gamma decay heat calculated by ORIGEN-S. All calculations were normalized to one fission for comparison with the experimental data.

The calculated beta and gamma energy release with time after fission is compared to experiment in Tables 36 and 37, respectively. The present calculations are in good agreement with experiment, with differences ranging from -7% to +10% for the beta energy release data and -14% to +6% for the gamma energy release data. This is significantly better than earlier summation calculations [29] which had differences exceeding 25%.

The integral  $^{235}\text{U}$  energy release results can also be expressed in terms of the energy release rate  $f(t)$  in units of MeV/s/fission after an instantaneous fission pulse by dividing the integral energy release by the counting time. The effective time  $t$  after a fission pulse is estimated to be  $t = t_{wait} + \frac{1}{2}(t_{irrad} + t_{count})$ . The calculated and measured integral results, expressed in terms of the heating rate at time  $t$  after an effective fission pulse, are graphed in Figures 8 and 9. The ordinate in the figures is the product of the average heating rate  $f(t)$  and the effective time after fission  $t$ , which allowed comparisons with previously calculated results [29].

## 9.3 $^{239}\text{Pu}$ Results

The ORIGEN-S results of integral energy release following  $^{239}\text{Pu}$  fission for beta and gamma decay are listed in Tables 38 and 39. The differences between calculation and experiment never exceed 9% for all cooling times. Earlier summation calculations using the CINDER code yielded differences of up to 34% at short cooling times, which was attributed to the use of largely ENDF/B-IV fission yield and nuclear decay data. The present calculations clearly demonstrate the improvement obtained with the ENDF/B-V (fission yields) and ENDF/B-VI (decay data) used in the present ORIGEN-S calculations. The results are also graphed in Figures 10 and 11, as effective energy release following a fission pulse.

Table 36:  $^{235}\text{U}$  Beta-ray Energy Release

Irradiation Time (s)	Waiting Time (s)	Counting Time (s)	Beta Energy Release (MeV/fission)		Ratio (E/C)
			Experiment (E)	Calculated (C)	
$1.0 \pm 0.1$	$1.7 \pm 0.1$	1	$0.2410 \pm 0.020$	0.2558	0.94
	2.7	1	$0.1940 \pm 0.012$	0.2057	0.94
	3.7	1	$0.1610 \pm 0.009$	0.1713	0.94
	4.7	2	$0.2540 \pm 0.012$	0.2721	0.93
	6.7	3	$0.2820 \pm 0.013$	0.2957	0.95
	9.7	5	$0.3050 \pm 0.014$	0.3282	0.93
	14.7	5	$0.2060 \pm 0.009$	0.2198	0.94
	19.7	5	$0.1550 \pm 0.007$	0.1613	0.96
	24.7	10	$0.2230 \pm 0.009$	0.2291	0.97
	34.7	10	$0.1590 \pm 0.007$	0.1631	0.97
	44.7	15	$0.1750 \pm 0.007$	0.1810	0.97
	59.7	15	$0.1310 \pm 0.005$	0.1388	0.94
	75.0	15	$0.1042 \pm 0.0040$	0.1079	0.97
	90.0	20	$0.1094 \pm 0.0042$	0.1146	0.95
	10.0	10.7	6	$0.2460 \pm 0.012$	0.2566
16.7		8	$0.2180 \pm 0.011$	0.2281	0.96
24.7		10	$0.1920 \pm 0.009$	0.1967	0.98
34.7		10	$0.1420 \pm 0.006$	0.1461	0.97
44.7		10	$0.1140 \pm 0.005$	0.1162	0.98
54.7		20	$0.1740 \pm 0.008$	0.1803	0.97
75.0		20	$0.1290 \pm 0.006$	0.1318	0.98
95.0		20	$0.0971 \pm 0.0038$	0.1031	0.94
115.0		40	$0.1470 \pm 0.006$	0.1534	0.96
155.0		60	$0.1540 \pm 0.006$	0.1569	0.98
215.0		80	$0.1350 \pm 0.005$	0.1423	0.95
295.0		100	$0.1220 \pm 0.005$	0.1258	0.97
395.0		200	$0.1700 \pm 0.006$	0.1723	0.99
595.0		200	$0.1260 \pm 0.005$	0.1209	1.04
100.0		70.0	40	$0.1680 \pm 0.007$	0.1622
	110.0	60	$0.1660 \pm 0.007$	0.1617	1.03
	170.0	80	$0.1480 \pm 0.006$	0.1443	1.03
	250.0	100	$0.1290 \pm 0.005$	0.1266	1.02
	350.0	200	$0.1780 \pm 0.007$	0.1726	1.03
	550.0	200	$0.1280 \pm 0.005$	0.1208	1.06
	750.0	400	$0.1830 \pm 0.006$	0.1692	1.08
	1150.0	400	$0.1280 \pm 0.005$	0.1182	1.08
	1550.0	400	$0.0961 \pm 0.0031$	0.0891	1.08
	1950.0	500	$0.0930 \pm 0.0030$	0.0853	1.09
	2450.0	500	$0.0703 \pm 0.0023$	0.0658	1.07
	2950.0	1000	$0.1020 \pm 0.0037$	0.0954	1.07
	3950.0	2000	$0.1230 \pm 0.005$	0.1165	1.06
	5950.0	4000	$0.1290 \pm 0.008$	0.1243	1.04
	9950.0	4000	$0.0792 \pm 0.0054$	0.0743	1.07

Table 37:  $^{235}\text{U}$  Gamma-ray Energy Release

Irradiation Time (s)	Waiting Time (s)	Counting Time (s)	Gamma Energy Release (MeV/fission)		Ratio (E/C)
			Experiment (E)	Calculated (C)	
$1.0 \pm 0.1$	$1.7 \pm 0.1$	1	$0.1880 \pm 0.010$	0.1800	1.04
	2.7	1	$0.1460 \pm 0.007$	0.1420	1.03
	3.7	1	$0.1190 \pm 0.005$	0.1174	1.01
	4.7	2	$0.1880 \pm 0.008$	0.1865	1.01
	6.7	3	$0.2100 \pm 0.008$	0.2064	1.02
	9.7	5	$0.2480 \pm 0.008$	0.2415	1.03
	14.7	5	$0.1820 \pm 0.006$	0.1750	1.04
	19.7	5	$0.1430 \pm 0.005$	0.1383	1.03
	24.7	10	$0.2230 \pm 0.007$	0.2141	1.04
	34.7	10	$0.1700 \pm 0.005$	0.1647	1.03
	44.7	15	$0.1990 \pm 0.006$	0.1928	1.03
	59.7	15	$0.1540 \pm 0.005$	0.1535	1.00
	75.0	15	$0.1240 \pm 0.004$	0.1218	1.02
	90.0	20	$0.1310 \pm 0.004$	0.1315	1.00
10.0	10.7	6	$0.2160 \pm 0.007$	0.2055	1.05
	16.7	8	$0.2110 \pm 0.007$	0.2014	1.05
	24.7	10	$0.1980 \pm 0.006$	0.1904	1.04
	34.7	10	$0.1560 \pm 0.005$	0.1506	1.04
	44.7	10	$0.1270 \pm 0.004$	0.1245	1.02
	54.7	20	$0.1970 \pm 0.006$	0.1993	0.99
	75.0	20	$0.1490 \pm 0.004$	0.1495	1.00
	95.0	20	$0.1170 \pm 0.004$	0.1189	0.98
	115.0	40	$0.1750 \pm 0.005$	0.1789	0.98
	155.0	60	$0.1770 \pm 0.005$	0.1836	0.96
	215.0	80	$0.1580 \pm 0.005$	0.1650	0.96
	295.0	100	$0.1370 \pm 0.004$	0.1444	0.95
	395.0	200	$0.1860 \pm 0.006$	0.1979	0.94
	595.0	200	$0.1320 \pm 0.005$	0.1409	0.94
100.0	70.0	40	$0.1820 \pm 0.008$	0.1880	0.97
	110.0	60	$0.1810 \pm 0.008$	0.1889	0.96
	170.0	80	$0.1570 \pm 0.007$	0.1675	0.94
	250.0	100	$0.1340 \pm 0.006$	0.1454	0.92
	350.0	200	$0.1800 \pm 0.007$	0.1981	0.91
	550.0	200	$0.1250 \pm 0.005$	0.1408	0.89
	750.0	400	$0.1770 \pm 0.007$	0.2016	0.88
	1150.0	400	$0.1260 \pm 0.005$	0.1449	0.87
	1550.0	400	$0.0970 \pm 0.0040$	0.1122	0.86
	1950.0	500	$0.0953 \pm 0.0041$	0.1108	0.86
	2450.0	500	$0.0772 \pm 0.0036$	0.0886	0.87
	2950.0	1000	$0.1170 \pm 0.006$	0.1350	0.87
	3950.0	2000	$0.1570 \pm 0.010$	0.1776	0.88
	5950.0	4000	$0.1870 \pm 0.015$	0.1972	0.95
9950.0	4000	$0.1140 \pm 0.013$	0.1089	1.05	

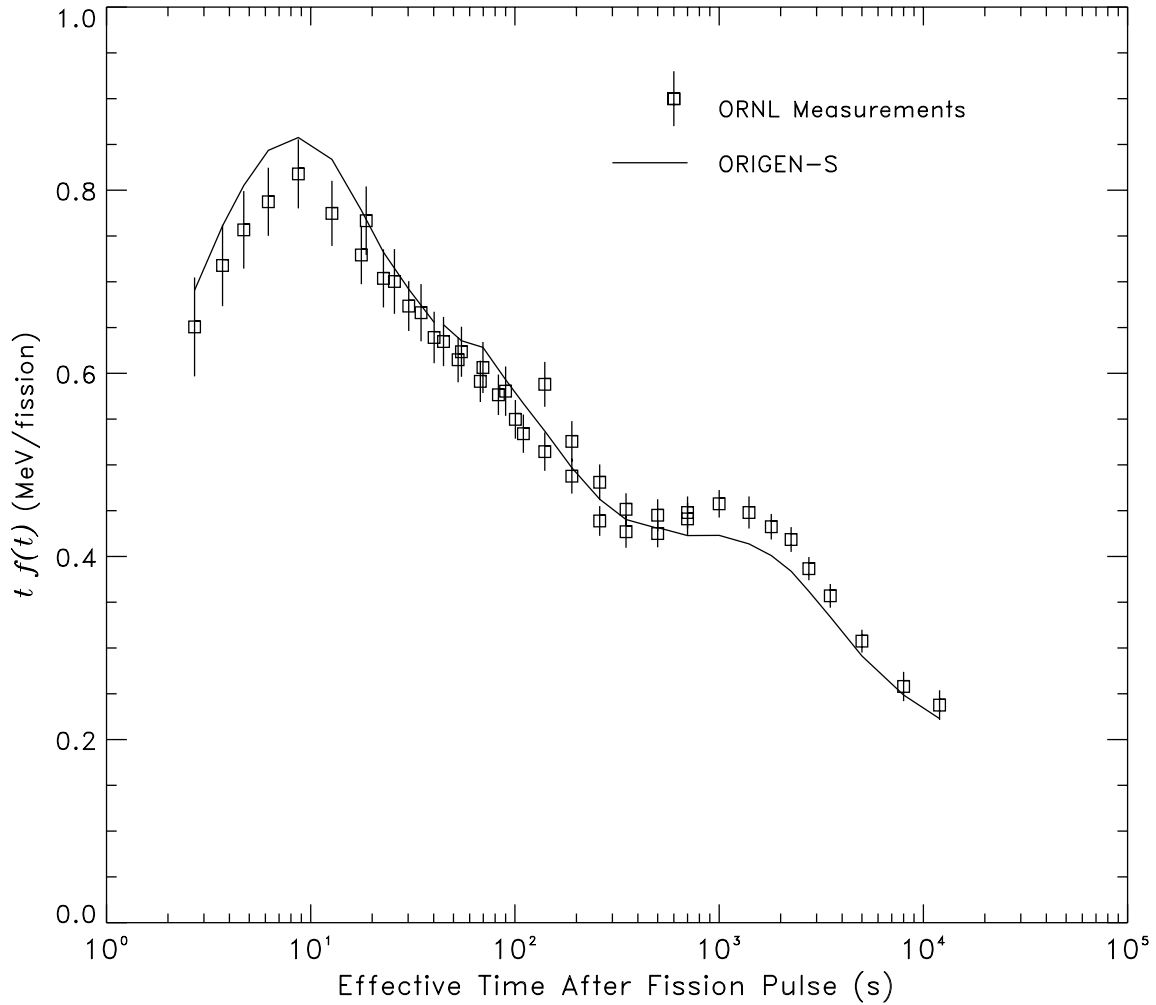


Figure 8: Comparison of the Measured and Calculated Beta Energy Release Rates Following a Fission Pulse of  $^{235}\text{U}$ . The data is derived from the tabulated integral measured and calculated data. The Y-values represent the product of the effective time  $t$  after a fission pulse (s) and the energy release rate  $f(t)$  (MeV/fission/s). The open squares represent the ORNL measurements and the solid line is the result calculated with ORIGEN-S and the ENDF/B-VI decay library.

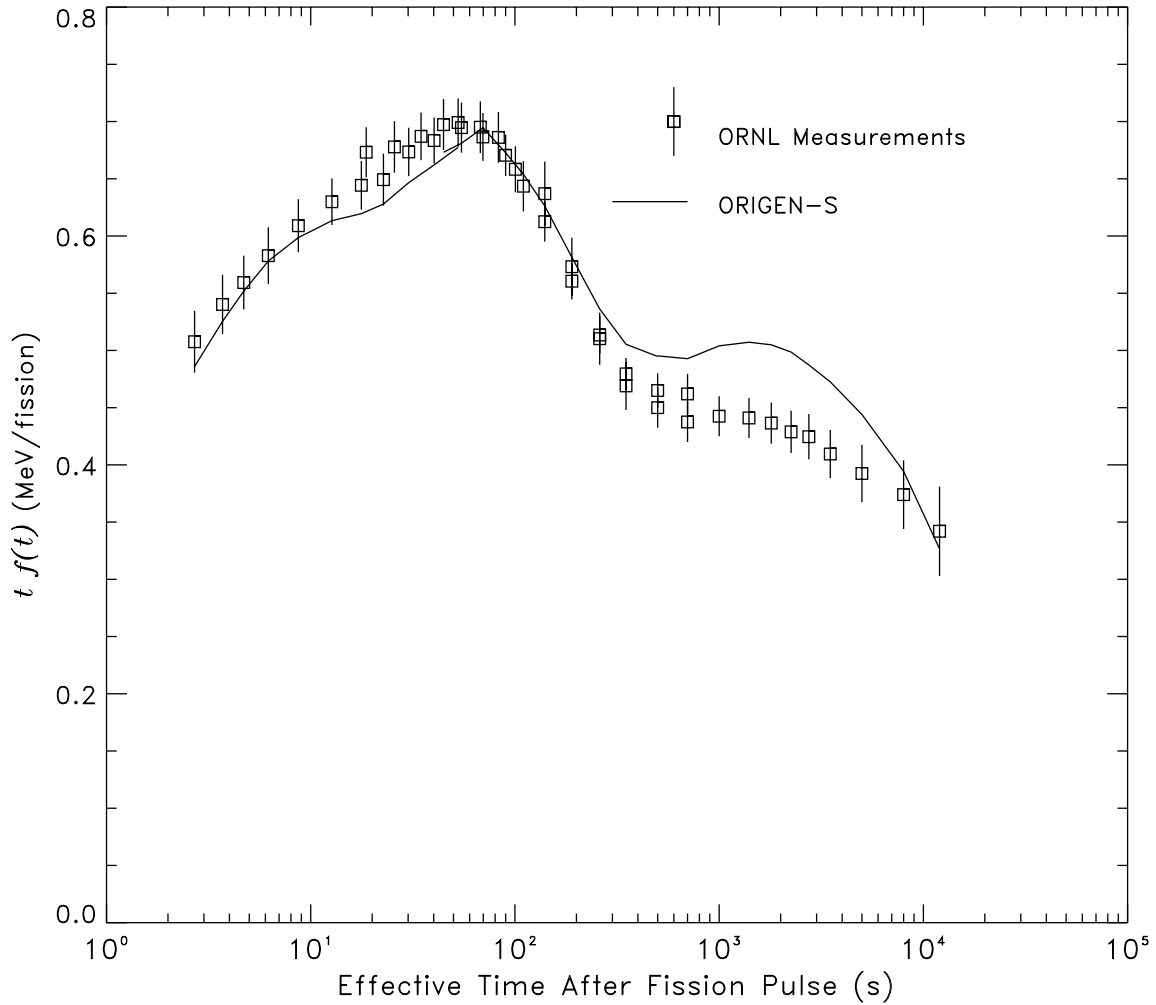


Figure 9: Comparison of the Measured and Calculated Gamma Energy Release Rates Following a Fission Pulse of  $^{235}\text{U}$ . The data is derived from the tabulated integral measured and calculated data. The Y-values represent the product of the effective time  $t$  after a fission pulse (s) and the energy release rate  $f(t)$  (MeV/fission/s). The open squares represent the ORNL measurements and the solid line is the result calculated with ORIGEN-S and the ENDF/B-VI decay library.

Table 38:  $^{239}\text{Pu}$  Beta-ray Energy Release

Irradiation Time (s)	Waiting Time (s)	Counting Time (s)	Beta Energy Release (MeV/fission)		Ratio (E/C)
			Experiment (E)	Calculated (C)	
$1.0 \pm 0.1$	$1.7 \pm 0.1$	1	$0.1811 \pm 0.0091$	0.1850	0.98
	2.7	1	$0.1470 \pm 0.0072$	0.1485	0.99
	3.7	1	$0.1211 \pm 0.0058$	0.1233	0.98
	4.7	2	$0.1945 \pm 0.0090$	0.1957	0.99
	6.7	3	$0.2152 \pm 0.0098$	0.2143	1.00
	9.7	5	$0.2438 \pm 0.0108$	0.2435	1.00
	14.7	5	$0.1680 \pm 0.0074$	0.1683	1.00
	19.7	5	$0.1288 \pm 0.0056$	0.1269	1.02
	24.7	10	$0.1905 \pm 0.0081$	0.1859	1.02
	34.7	10	$0.1406 \pm 0.0060$	0.1362	1.03
	44.7	15	$0.1580 \pm 0.0067$	0.1548	1.02
	59.7	15	$0.1208 \pm 0.0052$	0.1190	1.02
	75.0	15	$0.0980 \pm 0.0043$	0.0975	1.01
	90.0	20	$0.1062 \pm 0.0046$	0.1025	1.04
	110.0	20	$0.0849 \pm 0.0037$	0.0827	1.03
5.0	17.7	5	$0.1258 \pm 0.0056$	0.1276	0.99
	22.7	10	$0.1852 \pm 0.0077$	0.1865	0.99
	32.7	10	$0.1363 \pm 0.0055$	0.1366	1.00
	42.7	15	$0.1545 \pm 0.0060$	0.1550	1.00
	57.7	15	$0.1185 \pm 0.0045$	0.1191	0.99
	72.7	15	$0.0949 \pm 0.0036$	0.0975	0.97
	88.0	20	$0.1028 \pm 0.0039$	0.1025	1.00
	108.0	20	$0.0827 \pm 0.0031$	0.0828	1.00
	128.0	40	$0.1279 \pm 0.0048$	0.1276	1.00
	168.0	60	$0.1366 \pm 0.0051$	0.1362	1.00
	228.0	70	$0.1157 \pm 0.0044$	0.1145	1.01
	298.0	100	$0.1210 \pm 0.0046$	0.1206	1.00
	398.0	200	$0.1703 \pm 0.0065$	0.1677	1.02
	598.0	200	$0.1225 \pm 0.0048$	0.1190	1.03
	798.0	400	$0.1741 \pm 0.0067$	0.1669	1.04
100.0	250.0	100	$0.1218 \pm 0.0044$	0.1216	1.00
	350.0	200	$0.1706 \pm 0.0061$	0.1683	1.01
	550.0	200	$0.1232 \pm 0.0045$	0.1192	1.03
	750.0	400	$0.1766 \pm 0.0064$	0.1669	1.06
	1150.0	400	$0.1228 \pm 0.0044$	0.1151	1.07
	1550.0	400	$0.0922 \pm 0.0034$	0.0853	1.08
	1950.0	500	$0.0867 \pm 0.0032$	0.0803	1.08
	2450.0	500	$0.0653 \pm 0.0024$	0.0609	1.07
	2950.0	1000	$0.0917 \pm 0.0034$	0.0862	1.06
	3950.0	2000	$0.1071 \pm 0.0042$	0.1009	1.06
	5950.0	2000	$0.0631 \pm 0.0028$	0.0594	1.06
	7950.0	2000	$0.0439 \pm 0.0022$	0.0413	1.06
9950.0	4000	$0.0617 \pm 0.0033$	0.0574	1.08	

Table 39:  $^{239}\text{Pu}$  Gamma-ray Energy Release

Irradiation Time (s)	Waiting Time (s)	Counting Time (s)	Gamma Energy Release (MeV/fission)		Ratio (E/C)
			Experiment (E)	Calculated (C)	
$1.0 \pm 0.1$	$1.7 \pm 0.1$	1	$0.1348 \pm 0.0083$	0.1270	1.06
	2.7	1	$0.1046 \pm 0.0055$	0.1015	1.03
	3.7	1	$0.0866 \pm 0.0041$	0.0845	1.02
	4.7	2	$0.1382 \pm 0.0060$	0.1355	1.02
	6.7	3	$0.1540 \pm 0.0057$	0.1520	1.01
	9.7	5	$0.1852 \pm 0.0064$	0.1814	1.02
	14.7	5	$0.1365 \pm 0.0047$	0.1342	1.02
	19.7	5	$0.1096 \pm 0.0036$	0.1078	1.02
	24.7	10	$0.1717 \pm 0.0055$	0.1697	1.01
	34.7	10	$0.1324 \pm 0.0042$	0.1328	1.00
	44.7	15	$0.1561 \pm 0.0050$	0.1574	0.99
	59.7	15	$0.1219 \pm 0.0039$	0.1241	0.98
	75.0	15	$0.0988 \pm 0.0032$	0.1028	0.96
	90.0	20	$0.1058 \pm 0.0035$	0.1087	0.97
	110.0	20	$0.0846 \pm 0.0028$	0.0880	0.96
	5.0	17.7	5	$0.1088 \pm 0.0054$	0.1082
22.7		10	$0.1703 \pm 0.0071$	0.1701	1.00
32.7		10	$0.1328 \pm 0.0048$	0.1330	1.00
42.7		15	$0.1555 \pm 0.0052$	0.1576	0.99
57.7		15	$0.1212 \pm 0.0038$	0.1242	0.98
72.7		15	$0.0979 \pm 0.0029$	0.1029	0.95
88.0		20	$0.1052 \pm 0.0031$	0.1088	0.97
108.0		20	$0.0848 \pm 0.0024$	0.0880	0.96
128.0		40	$0.1295 \pm 0.0036$	0.1352	0.96
168.0		60	$0.1379 \pm 0.0038$	0.1432	0.96
228.0		70	$0.1167 \pm 0.0032$	0.1196	0.98
298.0		100	$0.1256 \pm 0.0034$	0.1260	1.00
398.0		200	$0.1810 \pm 0.0049$	0.1787	1.01
598.0		200	$0.1351 \pm 0.0037$	0.1309	1.03
798.0	400	$0.1974 \pm 0.0057$	0.1913	1.03	
100.0	250.0	100	$0.1276 \pm 0.0039$	0.1272	1.00
	350.0	200	$0.1828 \pm 0.0054$	0.1792	1.02
	550.0	200	$0.1352 \pm 0.0039$	0.1311	1.03
	750.0	400	$0.1989 \pm 0.0058$	0.1913	1.04
	1150.0	400	$0.1439 \pm 0.0042$	0.1384	1.04
	1550.0	400	$0.1114 \pm 0.0033$	0.1069	1.04
	1950.0	500	$0.1091 \pm 0.0034$	0.1048	1.04
	2450.0	500	$0.0862 \pm 0.0028$	0.0831	1.04
	2950.0	1000	$0.1290 \pm 0.0044$	0.1245	1.04
	3950.0	2000	$0.1661 \pm 0.0062$	0.1585	1.05
	5950.0	2000	$0.0985 \pm 0.0045$	0.0989	1.00
	7950.0	2000	$0.0679 \pm 0.0035$	0.0686	0.99
	9950.0	4000	$0.0874 \pm 0.0052$	0.0898	0.97

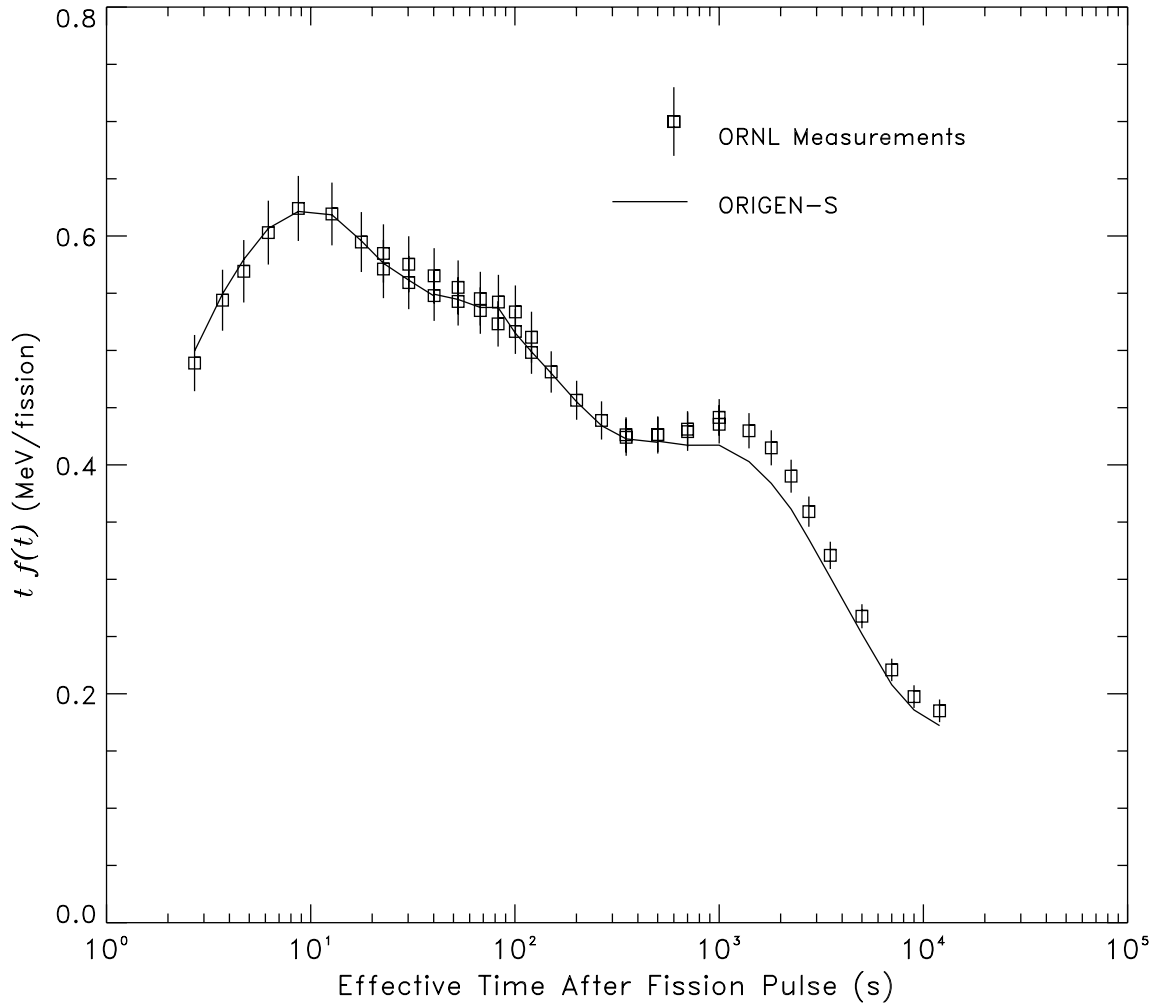


Figure 10: Comparison of the Measured and Calculated Beta Energy Release Rates Following a Fission Pulse of  $^{239}\text{Pu}$ . The data is derived from the tabulated integral measured and calculated data. The Y-values represent the product of the effective time  $t$  after a fission pulse (s) and the energy release rate  $f(t)$  (MeV/fission/s). The open squares represent the ORNL measurements and the solid line is the result calculated with ORIGEN-S and the ENDF/B-VI decay library.

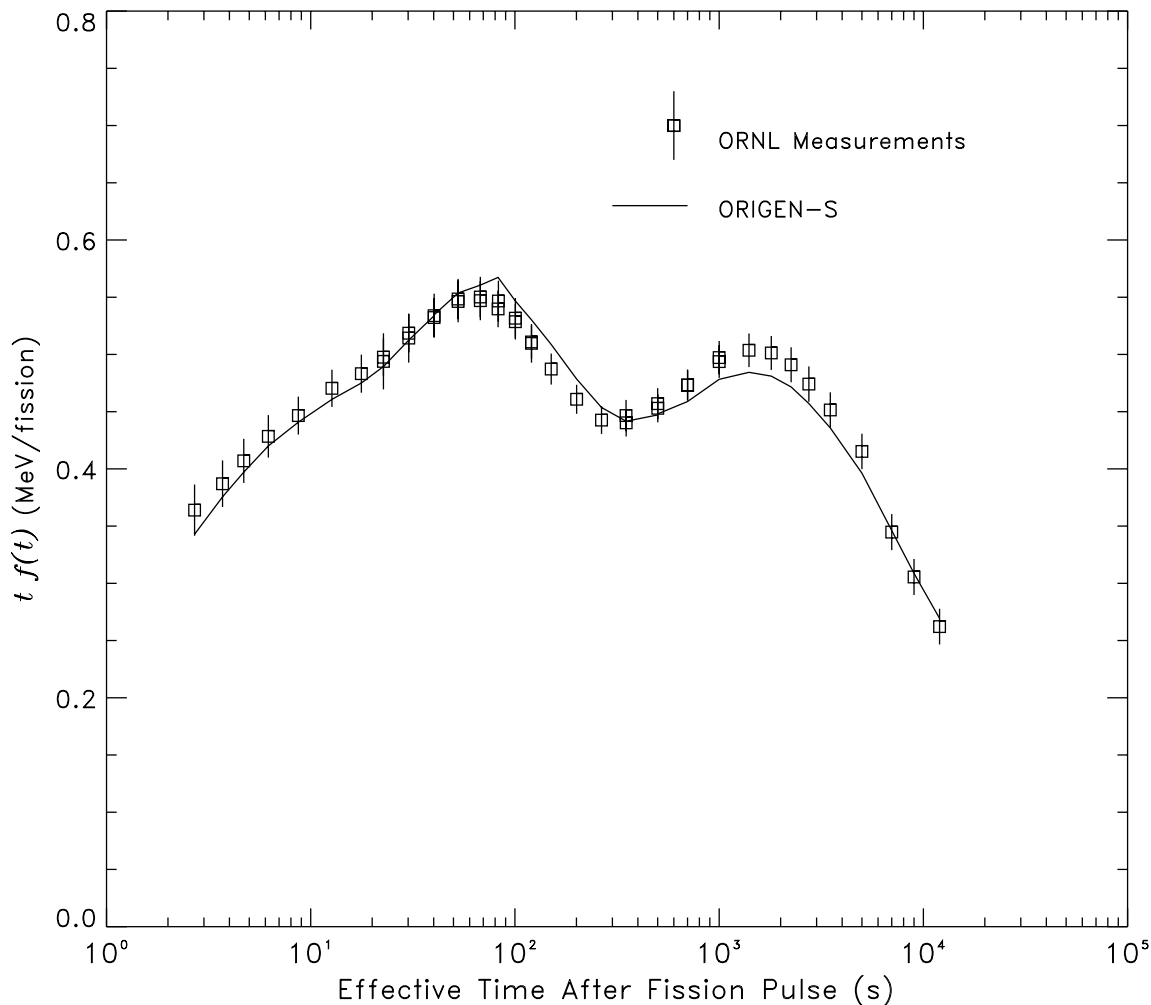


Figure 11: Comparison of the Measured and Calculated Gamma Energy Release Rates Following a Fission Pulse of  $^{239}\text{Pu}$ . The data is derived from the tabulated integral measured and calculated data. The Y-values represent the product of the effective time  $t$  after a fission pulse (s) and the energy release rate  $f(t)$  (MeV/fission/s). The open squares represent the ORNL measurements and the solid line is the result calculated with ORIGEN-S and the ENDF/B-VI decay library.

## 9.4 Summary of the Energy Release Studies

The experimental benchmark of the ORIGEN-S code and nuclear data libraries against the beta and gamma energy release measurements performed at Oak Ridge National Laboratory [29, 30], demonstrates that the code is predicting both components of fission product decay heat to within generally 10% for times ranging from 2 to 14000 s. This time range is particularly important to accident (LOCA) analyses, where 50% of the total decay energy is released within about the first 100 seconds. The fission product decay heat calculated with the present ENDF/B-VI-based data libraries yielded significantly improved results compared to previously published results using ENDF/B-IV-based data, particularly at the short cooling times important to LOCA analyses.

As observed from Figures 8–11, the  $^{239}\text{Pu}$  results are in better agreement than the  $^{235}\text{U}$  results. The largest discrepancy for  $^{235}\text{U}$  occurs between  $10^3$  and  $10^4$  s after fission, where the gamma heating component is overestimated by about 15% and the beta component is underestimated by about 10%. The calculated total energy release rate over the range of measurements is within 5% of the measurements. The largest discrepancy in the  $^{239}\text{Pu}$  results occurs in the same time period, with the ORIGEN-S calculations underpredicting all components of the energy release by typically 5%.

The study has provided a benchmark of the fission product yield, decay, and energy release data used in the ORIGEN-S nuclear data libraries for the short-lived fission product isotopes important to decay heat calculations. The study has also provided a valuable verification of the numerical methods used in the integral option of the code.

## 10 RADIATION SOURCE SPECTRA BENCHMARK

There is very little benchmark quality experimental data available for use in validating radiation source term data bases. Measurements on irradiated fuel assemblies are invariably made with a shielded source configuration due to the high source intensity. Measurements on shielded sources include the uncertainties in the shielding calculation which are inseparable from those in the calculated source spectra. In addition, shielded configurations provide a measure of the spectrum accuracy over a limited energy range which is dependent on the shield thickness and material.

A number of calculational comparisons of the source spectra predicted by different codes and data bases have been performed [13, 14]. A comparison of solutions to these problems suffers from the drawback that there are no definitive values to which the predicted spectra can be compared.

The Nuclear Energy Agency (NEA) Reactor Physics Committee (CRP) initiated an international code comparison for shielding problems in 1985. The committee recognized the limitations of doing code-only comparisons, and included with a series of theoretical problems, an experimental benchmark based on measurements on the French TN12 flask containing 12 irradiated PWR fuel assemblies, performed by the French Energy Commission CEA and Transnucléaire of France. The benchmark provided neutron and gamma dose rate measurements on the exterior of the TN12 flask.

The TN12 flask benchmark [31] has two parts: 1) detailed comparisons of the neutron and gamma source spectra used in each of the calculations submitted, and 2) a comparison of calculated and measured dose rates on the flask exterior performed using the calculated spectra. The comparison of the calculated dose rates with measurements provides a benchmark of the source spectra accuracy calculated in the first part, over the limited energy range of importance to the dose rate results. The present study used the published source spectra, validated by the dose rate measurements, as a benchmark for the ORIGEN-S code and source term data base. A separate shielding analysis of the TN12 flask using the present calculated sources was not undertaken since the spectra used in the benchmark have been shown to yield accurate dose rate predictions. The radiation source terms associated with activation of the assembly end fittings and structural materials were not considered.

The calculated source spectra in the NEACRP benchmark included submissions using FISPIN (U.K.), Apollo (France) and several versions of ORIGEN (U.S.A., Italy, The Netherlands, Belgium, and Germany).

## 10.1 Gamma Source Spectra

The gamma source benchmark involved a comparison of calculated spectra for a PWR fuel assembly, designated Assembly 5, at approximately mid-height of the active fuel, having an exit burnup of 19461 MWd/MgU [31]. The assembly used in the gamma ray benchmark has a 17 x 17 lattice arrangement with 264 fuel rods, 24 guide tubes, 1 instrument tube, and support grids. The initial  $^{235}\text{U}$  enrichment of Assembly 5 was 2.11%. Details of the fuel assembly and irradiation history are provided in the benchmark summary report [31]. The cooling time of Assembly 5 was 816 days.

The assembly was approximated in the present study using a simplified pin-cell model, neglecting the effects of the guide and instrument tubes. The lattice model and irradiation history specifications used in the calculations are listed in Tables 40 and 41 respectively. The irradiation history is for the mid-height of the active fuel of Assembly 5 which was the basis for the calculational comparisons, and not that of the entire fuel assembly.

The calculated gamma source spectra in units of MeV/s/MgU are compared in Table 42. The Belgium results are not included since they were derived by adjusting the results for the average assembly burnup rather than calculating mid-height values explicitly, and as a result they are significantly higher than the other reported results. The results are also graphed for comparison in Figure 12, with the source terms divided by the energy group width (MeV) to account for differences in the energy group structures used by the codes to report source spectra. The plotted results are limited to those from the FISPIN, Apollo, and ORIGEN-S codes, since all other results lie within the range of these codes. The results of the spectra calculated by Italy and the United States were both generated using ORIGEN-S calculations, and essentially overlie the present results.

Table 40: Specifications for PWR Assembly Gamma Benchmark Calculations

Fuel material	2.11 wt% enriched UO <sub>2</sub>
Fuel density	10.28 g/cm <sup>3</sup>
Fuel diameter	0.819 cm
Fuel temperature	1100 K
Element pitch	1.26 cm
Cladding material	Zircaloy-4
Cladding temperature	577 K
Cladding inside diameter	0.84 cm
Cladding outside diameter	0.95 cm
Coolant density	0.7569 g/cm <sup>3</sup>
Coolant temperature	550 K
Initial boron concentration	None specified
Exit burnup (Asmby 5 mid-height)	19461 MWd/MgU
Cooling time in days	816

Table 41: PWR Assembly Gamma Benchmark Irradiation History

Operating Cycle	Power (kW/kgU)	Irradiation (days)	Cooling (days)	Boron (fraction of initial)
1	35.04	20.0	0.0	1.0
2	35.04	40.0	0.0	1.0
3	35.04	60.0	0.0	1.0
4	35.04	80.0	26.0	1.0
5	47.35	64.0	5.0	1.0
6	47.35	199.0	816.0	1.0

Table 42: Calculated Gamma Source Spectra for Fuel Assembly 5 at Mid-Height with a Burnup of 19461 MWd/MgU. The energy boundaries (MeV) associated with each entry are the  $E_{max}$  value of the entry to the  $E_{max}$  value of the next entry with lower energy.

$E_{max}$ (MeV)	Gamma Spectra (MeV/s/MgU)							
	UK-1 <sup>†</sup>	UK-2 <sup>‡</sup>	Netherlands	Germany	Italy	France	USA	Canada <sup>§</sup>
4.00	2.73+11 <sup>†</sup>	1.70+11	1.68+11	1.81+08			3.37+11	3.55+11
3.50				3.62+11	3.40+11			
3.00	1.45+12	1.40+12	1.38+12	1.89+12	2.21+12	2.50+12	2.18+12	2.30+12
2.50	9.55+13	9.60+13	1.02+14	2.01+12	1.10+14		1.07+14	1.12+14
2.20				1.03+14		1.11+14		
2.00	6.92+12	6.80+12	6.40+12		2.09+13		2.06+13	2.17+13
1.80				1.42+14		1.94+14		
1.66	4.25+13	4.10+13	1.31+13				1.24+14	1.25+14
1.50			3.70+14		1.30+14			
1.44	1.56+14	1.20+14						
1.33			4.42+14	3.05+14	2.97+14		2.73+14	2.59+14
1.22	1.64+14	1.50+14				1.06+15		
1.00	1.86+14	1.40+14	1.32+14		6.26+14		6.04+14	5.81+14
0.80	3.90+15	3.10+15	7.37+14	4.35+15	2.62+15		2.57+15	2.58+15
0.70			2.24+15			2.90+15		
0.60	6.73+14	5.80+14	5.29+14		1.13+15		1.12+15	1.12+15
0.51			3.44+13			—		
0.40	1.40+12	1.10+12	1.14+12	1.04+15	1.48+14		1.45+14	1.56+14
0.30	3.03+12	2.30+12	—	—	1.37+14		1.34+14	1.40+14
0.20	9.65+13	9.50+13			3.22+14		3.15+14	3.28+14
0.10	9.02+12	—			1.68+14		1.66+14	1.73+14
0.05	2.92+12				2.04+14		2.07+14	2.10+14
0.02	1.16+09							
0.01	6.16+10				—		—	—
0.00	—							
Total	5.34+15	4.33+15	4.61+15	5.94+15	5.92+15	4.27+15	5.79+15	5.81+15

† UK-AEA Winfrith contribution.

‡ UK-BNFL contribution.

\* Read a 2.73 x 10<sup>11</sup>

§ Results of the present calculations using ORIGEN-S.

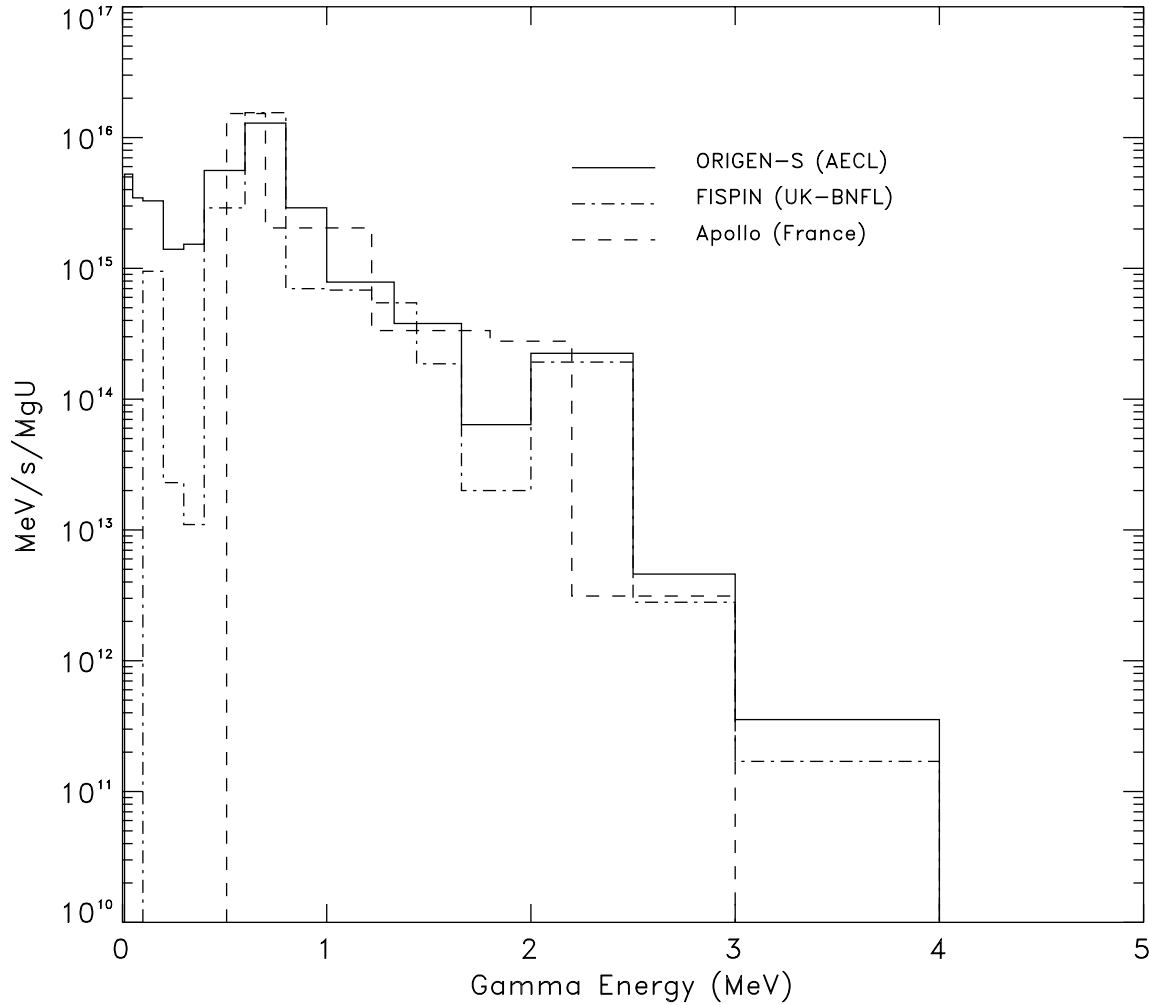


Figure 12: Comparison of the Gamma Energy Spectra Calculated by ORIGEN-S, France using the Apollo Code, and UK-BNFL using the FISPIN Code, for PWR Fuel Assembly 5 At Mid-Height. The results of other code contributions have been omitted since they either overlie or fall within the range of the plotted spectra.

The calculated gamma ray spectrum at mid-height of the active fuel Assembly 5 is in good agreement with the calculated published results. The present results closely parallel those of the United States, which were also generated using the ORIGEN-S code.

The largest discrepancies between the calculated spectra occur in the low energy region below about 400 keV. This is attributed to the inclusion of bremsstrahlung in some photon libraries. The ORIGEN-S photon library data includes bremsstrahlung based on a uranium oxide matrix. The region of importance to the subsequent flask shielding problem is between 2 and 2.5 MeV. All code results in this region are in good agreement, with a standard deviation in the calculated results of about  $\pm 10\%$ .

The dose rates outside the flask shielding at mid-height of the active fuel were calculated in the published benchmark using different codes, which included Monte Carlo, discrete ordinates, and point kernel methods. With the exception of a discrete ordinates contribution, the results are typically within 20% of the measured dose rate, with many results well within 10%. The benchmark provides indirect validation of the calculated gamma source spectra accuracy in the energy range above about 2 MeV, which is important in the shielding problem. In the energy range above about 500 keV, the present calculations have been demonstrated to be in good agreement with the results of other codes and data bases from international institutes.

## 10.2 Neutron Source Spectra

The neutron benchmark involved comparisons of the calculated spectra against those calculated in the NEACRP benchmark. The neutron spectra published in the benchmark summary [31] were used in shielding calculations to calculate the neutron dose rate on the exterior of the TN12 flask, which were compared to the measured dose rates. The majority of the dose rate results are in fair agreement with the measured values on the flask surface at fuel mid-height, with a standard deviation in the results of about  $\pm 20\%$ .

The neutron benchmark involved different fuel assemblies with higher burnup and initial enrichment than those used in the gamma benchmark. The calculational comparison was performed using data for the mid-height of the active fuel of Assembly 12, with a burnup of 38893 MWd/MgU. Initial fuel  $^{235}\text{U}$  enrichment was 3.13 wt%. The cooling time of the assembly was 647 days. A value of the flask  $k_{eff}$  of 0.15 is provided in the benchmark, giving a neutron multiplication factor of 1.176 which must be applied to account for source multiplication in shielding analyses. However, this factor was not required for the present comparisons.

The assembly was approximated in the present study using a simplified pin-cell model, neglecting the effects of the guide and instrument tubes. The specifications and irradiation history of the fuel assembly used in the neutron benchmark calculations is listed in Tables 43 and 44.

The results presented here include the neutron source terms (neutrons/s/MgU) for spontaneous fission events and  $(\alpha,n)$  reactions. The ORIGEN-S calculations performed for the present study

Table 43: Specifications for PWR Assembly used in Neutron Benchmark Calculations

Fuel material	3.13 wt% enriched UO <sub>2</sub>
Fuel density	10.28 g/cm <sup>3</sup>
Fuel diameter	0.819 cm
Fuel temperature	1100 K
Element pitch	1.26 cm
Cladding material	Zircaloy-4
Cladding temperature	577 K
Cladding inside diameter	0.84 cm
Cladding outside diameter	0.95 cm
Coolant density	0.7569 g/cm <sup>3</sup>
Coolant temperature	550 K
Initial boron concentration	None specified
Exit burnup (Asmby 5 mid-height)	38892.66 MWd/MgU
Cooling time in days	647

Table 44: PWR Assembly Irradiation History used in Neutron Benchmark

Operating Cycle	Power (kW/kgU)	Irradiation (days)	Cooling (days)	Boron (Fraction of Initial)
1	38.662	40.0	0.0	1.0
2	38.662	60.0	0.0	1.0
3	38.662	100.0	0.0	1.0
4	38.662	100.0	0.0	1.0
5	38.662	145.0	192.0	1.0
6	38.662	140.0	0.0	1.0
7	38.662	140.0	57.0	1.0
8	38.662	282.0	647.0	1.0

used an  $(\alpha,n)$  source based on a uranium oxide matrix. Comparisons of the principal actinide concentrations for those nuclides that dominate the neutron source at the cooling time of interest are also presented.

A code comparison of the spontaneous fission and  $(\alpha,n)$  neutron source strengths at mid-height of the active fuel region of Assembly 12 is presented in Table 45. No data were available for the contribution from the United States for this comparison, although it is noted that their results for other assemblies and fuel regions are in good agreement with the other codes. A comparison of the actinide concentrations that contribute significantly to the neutron source term of Assembly 12 is shown in Table 46.

The ORIGEN-S calculated spontaneous fission and  $(\alpha,n)$  reaction neutron source terms are in good agreement with the results of other codes and data libraries, as is the predicted actinide content for those nuclides contributing to the neutron source. A detailed comparison of the spectra for Assembly 12 was not available in the benchmark summary.

The results of the neutron shielding calculations using the source terms published in the benchmark at mid-height of the active fuel on the TN12 flask side are reported to be in good agreement with the measured neutron dose rates. The ratio of calculated to measured dose rate on the surface at mid-height generally lie between 0.8 and 1.2. Deviations in several contributed results which were larger than this are attributed to problems in the neutron transport aspects of the problem, and not in the source terms [31].

The agreement in the neutron source term predicted by ORIGEN-S in the present study with those calculated independently and validated through comparison of neutron dose rates through the TN12 flask, provides a validation benchmark of the ORIGEN-S code and neutron source term data in the code.

### 10.3 Summary of Source Term Studies

The gamma radiation source term and energy spectrum, and total neutron source terms from spontaneous fission and  $(\alpha,n)$  reactions, have been compared to independent code results for PWR fuel assemblies. The calculated results used to benchmark the present ORIGEN-S results have been indirectly validated by comparing calculated dose rates using the spectra against measured dose rates on a transport flask.

The results are in good agreement with the other calculations. However, the benchmark is limited in its ability to validate the source terms since the measured dose rates are sensitive to the spectrum in a narrow energy region, and additional benchmarking is recommended.

Table 45: Calculated Neutron Source Terms for Fuel Assembly 12 at Mid-Height with a Burnup of 38893 MWd/MgU

Country	Neutron Source (neutrons/s/MgU)	
	Spontaneous Fission	( $\alpha$ ,n) Reactions
UK-AEA Winfrith	6.17+8	1.37+7
Germany	7.09+8	3.42+7
Italy	6.42+8	1.54+7
France	7.56+8	1.59+7
Belgium	7.38+8	1.68+7
Canada	7.70+8	1.52+7

Table 46: Calculated Actinide Content for Fuel Assembly 12 at Mid-Height with a Burnup of 38893 MWd/MgU

Actinide	Actinide Content (atoms/MgU)						
	UK-1 <sup>†</sup>	UK-2 <sup>‡</sup>	Germany	Italy	USA	Belgium	Canada
<sup>238</sup> Pu	5.04+23	4.75+23	5.55+23	6.24+23	6.35+23	5.80+23	5.23+23
<sup>240</sup> Pu	6.66+24	6.66+24	7.10+24	6.14+24	6.08+24	6.45+24	6.88+24
<sup>242</sup> Pu	1.96+24	1.56+24	1.91+24	1.69+24	1.85+24	1.79+24	1.76+24
<sup>241</sup> Am	4.06+23	4.20+23	4.29+23	4.99+23	4.57+23	4.00+23	4.71+23
<sup>242</sup> Cm	3.49+21	2.84+21	3.38+21	3.49+21	3.18+21	3.30+21	3.26+21
<sup>244</sup> Cm	1.32+23	1.03+23	1.44+23	1.34+23	1.59+23	1.56+23	1.62+23
<sup>246</sup> Cm	9.59+20	6.59+20	1.18+21	9.97+20	1.29+21		1.33+21

<sup>†</sup> UK-AEA Winfrith contribution.

<sup>‡</sup> UK-BNFL contribution.

## 11 CONCLUSIONS

The ORIGEN-S code and its associated nuclear data libraries have been subjected to a broad spectrum of verification and validation benchmarks. The benchmark studies cover the major areas of code and nuclear data application: the prediction of 1) nuclide inventories 2) decay heat, and 3) neutron and gamma radiation source terms.

The numerical methods of ORIGEN-S were verified by comparisons against independent codes and methods using several studies. Two studies were cited involving comparisons of ORIGEN-S results with CINDER-2 results. The third, and most rigorous verification study, involved a numerical benchmark of ORIGEN-S against ten different international depletion codes, all using an identical nuclear data base. The results indicate that the ORIGEN-S methods are accurate, and produce results that are within the range of other code predictions.

The validation benchmarks were chosen to represent a broad class of problems to which the ORIGEN-S code is routinely applied by the Canadian nuclear industry. The benchmark studies include experimental measurements of nuclide inventories in irradiated CANDU reactor and PWR fuel, decay heat measurements on CANDU fuel, measurements of beta and gamma energy release following short irradiations, comparisons against the ANSI/ANS-5.1-1979 Standard for decay heat, and a comparison of neutron and gamma source terms and energy spectra against other validated code results. The ORIGEN-S results are generally within the uncertainties associated with the experiments or Standards, or within the range of independent code results.

The calculations presented in this report demonstrate that ORIGEN-S will accurately predict results over the wide range of applications covered by these studies. This report is intended to serve as a baseline verification and validation document for the ORIGEN-S code and nuclear data libraries, and meet the CSA N286.7 Standard requirements for software documentation.

## REFERENCES

- [1] O.W. Hermann and R.M. Westfall, "ORIGEN-S – SCALE System Module to Calculate Fuel Depletion, Actinide Transmutation, Fission Product Buildup and Decay, and Associated Radiation Source Terms", in SCALE: A Modular Code System for Performing Standardized Computer Analyses for Licensing Evaluations, NUREG/CR-0200, Rev. 4 (ORNL/NUREG/CSD-2/R4), Vol. II, Part I, (Draft November 1993).
- [2] Quality Assurance of Analytical, Scientific and Design Computer Programs for Nuclear Power Plants, Canadian Standards Association, Standard CAN/CSA-N286.7 (1994).
- [3] "SCALE: A Modular Code System for Performing Standardized Computer Analyses for Licensing Evaluations", NUREG/CR-0200, Rev. 4 (ORNL/NUREG/CSD-2/R4), Vols. I, II, and III (Draft November 1993).

- [4] S.M. Bowman, "Configuration Management Plan for the SCALE Code System", Nuclear Engineering Applications Section, Computing Applications Division report SCALE-CMP-001, Revision 4 (1994).
- [5] J.R. Askew, F.J. Fayers, and P.B. Kemshell, "A General Description of the Lattice Code WIMS", Journal of the British Nuclear Energy Society 5(4):564-585 (1966).
- [6] J. Griffiths, "WIMS-AECL Users Manual", Atomic Energy of Canada Ltd., Research Company, CANDU Owners Group, RC-1176, COG-94-52 (1994).
- [7] J.C. Ryman, "ORIGEN-S Data Libraries", in SCALE: A Modular Code System for Performing Standardized Computer Analyses for Licensing Evaluations, NUREG/CR-0200, Rev. 4 (ORNL/NUREG/CSD-2/R4), Vol. II, Part I, (Draft November 1993).
- [8] I.C. Gauld and K.A. Litwin, "SAS2W - A Coupled WIMS-AECL and ORIGEN-S Depletion Analysis System Based on SCALE", Atomic Energy of Canada Ltd. report, in preparation.
- [9] I.C. Gauld and K.A. Litwin, "Benchmarking of the Coupled WIMS/ORIGEN Code System Against the Pickering-A Bundle 19558C Fuel Element Assay", Atomic Energy of Canada Ltd. Research Company report RC-1218 (1994).
- [10] "Summary Record of the NSC Meeting on the Burnup Credit Criticality Benchmark", OECD Nuclear Energy Agency, Nuclear Science Committee, Oak Ridge National Laboratory, September 15-17 (1993).
- [11] A.G. Croff, "ORIGEN2 - A Revised and Updated Version of the Oak Ridge Isotope Generation and Depletion Code", Oak Ridge National Laboratory report ORNL-5621 (1980).
- [12] T.R. England, W.B. Wilson, and M.G. Stamatelatos, "Fission Product Data for Thermal Reactors, Part 2: User's Manual for EPRI-CINDER Code and Data", Electric Power Research Institute report EPRI NP-356, LA-6746-MS (1976).
- [13] O.W. Hermann, C.V. Parks, J.P. Renier, J.W. Roddy, R.C. Ashline, W.B. Wilson, and R.J. LaBauve, "Multicode Comparison of Selected Source-Term Computer Codes", Oak Ridge National Laboratory report ORNL/CSD/TM-251 (1989).
- [14] M.C. Brady, O.W. Hermann, and W.B. Wilson, "Comparison of Radiation Spectra from Selected Source-Term Codes", Oak Ridge National Laboratory report ORNL/CSD/M-259 (1989).
- [15] B. Duchemin and C. Nordborg, "Decay Heat Calculation - An International Nuclear Code Comparison", Nuclear Energy Agency report NEACRP-319 (1989).
- [16] American National Standard for Decay Heat Power in Light Water Reactors, ANSI/ANS-5.1-1979, American Nuclear Society, Lagrange Park, Illinois (1979).
- [17] "OECD Nuclear Energy Agency Burnup credit Criticality Benchmark - Phase I-B: Isotopic Prediction", NEA/NSC Draft report (1994).
- [18] J. Griffiths, M. Lounsbury and R.W. Durham, "Uranium and Plutonium Isotopes in NPD Fuel Bundle 1016", Atomic Energy of Canada Ltd. report AECL-2695 (1967).

- [19] Unpublished experimental data from measurements of Bruce Nuclear Generating Station fuel bundle F21037C performed by Atomic Energy of Canada Ltd., Whiteshell Laboratories (1982).
- [20] K.M. Wasywich and J.D. Chen, "Pre-Storage Data Package on the Irradiated Pickering-A Non-Canlub Fuel Bundle 19558C Stored in Dry Air at 150°C in a Concrete Canister at WNRE – Phase 1 on the Controlled Environment Experiment", unpublished report.
- [21] J.C. Tait, I.C. Gauld, and A.H. Kerr, "Validation of the ORIGEN-S Code for Predicting Radionuclide Inventories in Used CANDU Fuel", Atomic Energy of Canada Ltd. report AECL-10891, COG-93-346 (1994).
- [22] R.J. Guenther, D.E. Blahnik, U.P. Jenquin, J.E. Mendel, L.E. Thomas, and C.K. Thornhill, "Characterization of Spent Fuel Approved Testing Material — ATM-104", Pacific Northwest Laboratory report PNL-5109-104/UC-802 (1991).
- [23] R.Q. Wright, "Fission Product Evaluations for ENDF/B-VI", Presented in Transactions of the American Nuclear Society, Vol. 61, 1990 Annual Meeting, Nashville, Tennessee, June 10-14 (1990).
- [24] E.F. Talbot and R.J. Ellis, "Implementation of the ANS 1978 Standard for Decay Heat from Fission Products", unpublished report.
- [25] D.W. McKean and R.J. Fluke, "Decay Heat Generation in Irradiated CANDU Fuel After Prolonged Cooling — Calculation vs. Experiment", Ontario Hydro, unpublished report.
- [26] L. Wilk, "SORO Program Description, PARAGON Design Manual", Ontario Hydro, unpublished report.
- [27] M.R. Floyd and P. Sermer, "A Comparison of Soro-Computed Bundle Burnups with Chemical Measurements Performed at CRL/WL", Atomic Energy of Canada Ltd., Research Company, RC-1026 (1993).
- [28] W.W. Engle, Jr., "A User's Manual for ANISN: A One-Dimensional Discrete Ordinates Transport Code with Anisotropic Scattering", Oak Ridge Gaseous Diffusion Plant Computing Technology Center Report K-1693 (1967).
- [29] J.K. Dickens, T.A. Love, J.W. McConnell, J.F. Emery, K.J. Northcutt, R.W. Peelle, and H. Weaver, "Fission Product Energy Release for Times Following Thermal-Neutron Fission of  $^{235}\text{U}$  Between 2 and 14,000 Seconds", Oak Ridge National Laboratory report ORNL/NUREG-14 (1977).
- [30] J.K. Dickens, T.A. Love, J.W. McConnell, J.F. Emery, K.J. Northcutt, R.W. Peelle, and H. Weaver, "Fission Product Energy Release for Times Following Thermal-Neutron Fission of  $^{239}\text{Pu}$  Between 2 and 14,000 Seconds", Oak Ridge National Laboratory report ORNL/NUREG-34 (1978).
- [31] H.F. Locke, "Summary of the Results of the Comparison of Calculations and Measurements for the TN12 Flask Carried Out Under the NEACRP Intercomparison of Shielding Codes", NEACRP-L-339 (1992).

DISTRIBUTION LIST

AECL (Whiteshell):

R.F. Lidstone

I.C. Gauld (4)

A.G. Lee

G.B. Wilkin

AECL (Chalk River):

R.T. Jones

P.J. Laughton

AECL (Sheridan Park):

B. Rouben

K.M Aydogdu

C.R. Boss (2)

N. Gagnon

K. Tsang

Ontario Hydro:

D.W. McKean (2)

M.B. Gold

S. Hanna

L. Wilk

E. Tong

M. Zeya

C.A. Morrison

H. Roman

New Brunswick Power (Point Lepreau):

E. Young (2)

R.A. Gibb

Hydro Québec:

G. Hotte

R. Blagoueva

COG (OH-TCH 13A13):

J.S. Nathwani

**Notice:**

This report is not to be listed in abstract journals. If it is cited as a reference, the source from which copies may be obtained should be given as:

Scientific Document Distribution Office (SDDO)  
AECL  
Chalk River, Ontario  
Canada K0J 1J0

Fax: (613) 584-1745 Tel.: (613) 584-3311 ext. 4623

or

Reports Services (Station 71)  
AECL  
Pinawa, Manitoba  
Canada R0E 1L0

Fax: (204) 753-8490 Tel.: (204) 753-2311 ext. 2908